Université de Montréal

Ocular rigidity: A previously unexplored risk factor in the pathophysiology of open-angle glaucoma

Assessment using a novel OCT-based measurement method

By

Diane Noël Sayah

Department of Ophthalmology, Faculty of Medicine

Thesis submitted in partial fulfillment of the requirements of the degree of Doctorate (PhD)

in Vision Science, option Biology of Ocular Diseases

February 2020

Université de Montréal

Unité académique : Département d'Ophtalmologie, Faculté de Médecine

---

Cette thèse intitulée

La rigidité oculaire : Facteur de risque nouvellement considéré dans la physiopathologie du glaucome à angle ouvert

Investigation par l'entremise d'une nouvelle méthode de mesure basée sur l'imagerie par OCT

Présentée par

Diane Noël Sayah

A été évaluée par un jury composé des personnes suivantes

Langis Michaud
Président-rapporteur

Mark R Lesk
Directeur de recherche

Santiago Costantino
Codirecteur

Adriana Di Polo
Membre du jury

Cindy Hutnik
Examinateur externe

Résumé

Le glaucome est la première cause de cécité irréversible dans le monde. Bien que sa pathogenèse demeure encore nébuleuse, les propriétés biomécaniques de l'œil sembleraient jouer un rôle important dans le développement et la progression de cette maladie. Il est stipulé que la rigidité oculaire (RO) est altérée au travers les divers stades de la maladie et qu'elle serait le facteur le plus influent sur la réponse du nerf optique aux variations de la pression intraoculaire (PIO) au sein du glaucome. Pour permettre l'investigation du rôle de la RO dans le glaucome primaire à angle ouvert (GPAO), la capacité de quantifier la RO *in vivo* par l'entremise d'une méthode fiable et non-invasive est essentielle. Une telle méthode n'est disponible que depuis 2015. Basée sur l'équation de Friedenwald, cette approche combine l'imagerie par tomographie par cohérence optique (TCO) et la segmentation choroïdienne automatisée afin de mesurer le changement de volume choroïdien pulsatile (ΔV), ainsi que la tonométrie dynamique de contour Pascal pour mesurer le changement de pression pulsatile correspondant.

L'objectif de cette thèse est d'évaluer la validité de cette méthode, et d'en faire usage afin d'investiguer le rôle de la RO dans les maladies oculaires, particulièrement le GPAO. Plus spécifiquement, cette thèse vise à : 1) améliorer la méthode proposée et évaluer sa validité ainsi que sa répétabilité, 2) investiguer l'association entre la RO et le dommage neuro-rétinien chez les patients glaucomateux, et ceux atteints d'un syndrome de vasospasticité, 3) évaluer l'association entre la RO et les paramètres biomécaniques de la cornée, 4) évaluer l'association entre la RO et les pics de PIO survenant suite aux thérapies par injections intravitréennes (IIV), afin de les prédire et de les prévenir chez les patients à haut risque, et 5) confirmer que la RO est réduite dans les yeux myopes.

D'abord, nous avons amélioré le modèle mathématique de l'œil utilisé pour dériver ΔV en le rendant plus précis anatomiquement et en tenant compte de la choroïde périphérique. Nous avons démontré la validité et la bonne répétabilité de cette méthodologie. Puis, nous avons effectué la mesure des coefficients de RO sur un large éventail de sujets sains et glaucomateux en utilisant notre méthode non-invasive, et avons démontré, pour la première fois, qu'une RO

basse est corrélée aux dommages glaucomateux. Les corrélations observées étaient comparables à celles obtenues avec des facteurs de risque reconnus tels que la PIO maximale. Une forte corrélation entre la RO et les dommages neuro-rétiniens a été observée chez les patients vasospastiques, mais pas chez ceux atteints d'une maladie vasculaire ischémique. Cela pourrait potentiellement indiquer une plus grande susceptibilité au glaucome due à la biomécanique oculaire chez les patients vasospastiques. Bien que les paramètres biomécaniques cornéens aient été largement adoptés dans la pratique clinique en tant que substitut pour la RO, propriété biomécanique globale de l'œil, nous avons démontré une association limitée entre la RO et ces paramètres, offrant une nouvelle perspective sur la relation entre les propriétés biomécaniques cornéennes et globales de l'œil. Seule une faible corrélation entre le facteur de résistance cornéenne et la RO demeure après ajustement pour les facteurs de confusion dans le groupe des patients glaucomateux. Ensuite, nous avons présenté un modèle pour prédire l'amplitude des pics de PIO après IIV à partir de la mesure non-invasive de la RO. Ceci est particulièrement utile pour les patients à haut risque atteints de maladies rétiniennes exsudatives et de glaucome qui nécessiteraient des IIV thérapeutiques, et pourrait permettre aux cliniciens d'ajuster ou de personnaliser le traitement pour éviter toute perte de vision additionnelle. Enfin, nous avons étudié les différences de RO entre les yeux myopes et les non-myopes en utilisant cette technique, et avons démontré une RO inférieure dans la myopie axiale, facteur de risque du GPAO. Dans l'ensemble, ces résultats contribuent à l'avancement des connaissances sur la physiopathologie du GPAO. Le développement de notre méthode permettra non seulement de mieux explorer le rôle de la RO dans les maladies oculaires, mais contribuera également à élucider les mécanismes et développer de nouveaux traitements ciblant la RO pour contrer la déficience visuelle liée à ces maladies.

Mots-clés : Rigidité oculaire, Biomécanique oculaire, Choroïde, Sclère, Pression intraoculaire, Glaucome, Myopie, OCT, Pulsatilité, Mécanismes physiopathologiques.

Abstract

Glaucoma is the leading cause of irreversible blindness worldwide. While its pathogenesis is yet to be fully understood, the biomechanical properties of the eye are thought to be involved in the development and progression of this disease. Ocular rigidity (OR) is thought to be altered through disease processes and has been suggested to be the most influential factor on the optic nerve head's response to variations in intraocular pressure (IOP) in glaucoma. To further investigate the role of OR in open-angle glaucoma (OAG) and other ocular diseases such as myopia, the ability to quantify OR in living human eyes using a reliable and non-invasive method is essential. Such a method has only become available in 2015. Based on the Friedenwald equation, the method uses time-lapse optical coherence tomography (OCT) imaging and automated choroidal segmentation to measure the pulsatile choroidal volume change (ΔV), and Pascal dynamic contour tonometry to measure the corresponding pulsatile pressure change.

The purpose of this thesis work was to assess the validity of the methodology, then use it to investigate the role of OR in ocular diseases, particularly in OAG. More specifically, the objectives were: 1) To improve the extrapolation of ΔV and evaluate the method's validity and repeatability, 2) To investigate the association between OR and neuro-retinal damage in glaucomatous patients, as well as those with concomitant vasospasticity, 3) To evaluate the association between OR and corneal biomechanical parameters, 4) To assess the association between OR and IOP spikes following therapeutic intravitreal injections (IVIs), to predict and prevent them in high-risk patients, and 5) To confirm that OR is lower in myopia.

First, we improved the mathematical model of the eye used to derive ΔV by rendering it more anatomically accurate and accounting for the peripheral choroid. We also confirmed the validity and good repeatability of the method. We carried out the measurement of OR coefficients on a wide range of healthy and glaucomatous subjects using this non-invasive method, and were able to show, for the first time, that lower OR is correlated with more glaucomatous damage. The correlations observed were comparable to those obtained with recognized risk factors such as maximum IOP. A strong correlation between OR and neuro-retinal damage was found in patients

with concurrent vasospastic syndrome, but not in those with ischemic vascular disease. This could perhaps indicate a greater susceptibility to glaucoma due to ocular biomechanics in vasospastic patients. While corneal biomechanical parameters have been widely adopted in clinical practice as surrogate measurements for the eye's overall biomechanical properties represented by OR, we have shown a limited association between these parameters, bringing new insight unto the relationship between corneal and global biomechanical properties. Only a weak correlation between the corneal resistance factor and OR remained in glaucomatous eyes after adjusting for confounding factors. In addition, we presented a model to predict the magnitude of IOP spikes following IVIs from the non-invasive measurement of OR. This is particularly useful for high-risk patients with exudative retinal diseases and glaucoma that require therapeutic IVIs, and could provide the clinician an opportunity to adjust or customize treatment to prevent further vision loss. Finally, we investigated OR differences between non-myopic and myopic eyes using this technique, and demonstrated lower OR in axial myopia, a risk factor for OAG. Overall, these findings provide new insights unto the pathophysiology of glaucomatous optic neuropathy. The development of our method will permit further investigation of the role of OR in ocular diseases, contributing to elucidate mechanisms and provide novel management options to counter vision impairment caused by these diseases.

Keywords : Ocular rigidity, Ocular biomechanics, Choroid, Sclera, Intraocular pressure, Glaucoma, Myopia, OCT, Pulsatility, Pathophysiological mechanisms.

Table of Contents

List of Tables

List of Figures

List of Abbreviations

AC: Anterior chamber

ACD: Anterior chamber depth

AH: Aqueous humor

AL: Ocular axial length

AMD: Age-related macular degeneration

BF: Blood flow

BM: Bruch's membrane

BP: Blood pressure

CCT: Central corneal thickness

CH: Corneal hysteresis

CRA: Central retinal artery

CRF: Corneal resistance factor

CSI: Choroid-sclera interface

CT: Choroidal thickness

ΔCT: Pulsatile choroidal thickness change

DBP: Diastolic blood pressure

DCT: Dynamic contour tonometry

EDI: Enhanced depth imaging

ET-1: Endothelin-1

FAZ: Foveal avascular zone

GAT: Goldmann applanation tonometry

HTN: Hypertension

IOP: Intraocular pressure

IOPcc: corneal-compensated IOP

IOPg: Goldmann-correlated IOP

IVI: Intravitreal injection

LC: Lamina cribrosa

MD: Visual field mean defect

NCT: Non-contact tonometry

NTG: Normal-tension glaucoma

OAG: Open-angle glaucoma

OCT: Optical coherence tomography

OHT: Ocular hypertension

ONH: Optic nerve head

OPA: Ocular pulse amplitude

OPP: Ocular perfusion pressure

OR: Ocular rigidity

ORA: Ocular response analyzer

POAG: Primary open-angle glaucoma

PP: Perfusion pressure

PPS: Peripapillary sclera

PVD: Primary vascular dysregulation

R: Radius

RGC: Retinal ganglion cell

RNFL: Retinal nerve fiber layer

RPE: Retinal pigmented epithelium

RVI: Retina-vitreous interface

SBP: Systolic blood pressure

SPCA: Short posterior ciliary arteries

TM: Trabecular meshwork

Tmax: Maximum historic IOP

ΔV: Pulsatile ocular volume change

VF: Visual field

Vision is the art of discovery, like finding a treasure hidden in a field

Acknowledgements

This thesis work would not have been possible without the support of many.

First, I would like to thank my thesis directors, Dr Mark Lesk and Dr Santiago Costantino. I am truly grateful to have had the opportunity to work with you and to have you as mentors. Your help, availability and constant guidance are truly recognized and appreciated. Thank you for challenging me to learn and grow as a clinician-scientist.

Thank you to all members of the thesis evaluation committee, Dr Cindy Hutnik, Dr Adriana Di Polo, Dr Michaud, for taking the time to review my thesis and provide valuable suggestions.

I would like to thank the funding agencies, including the Fonds de Recherche du Québec – Santé (FRQS), the Ophthalmology Department of University of Montreal Research Fund (FROUM), and the Faculty of Graduate Studies of the University of Montreal for granting doctoral scholarship awards during my PhD studies.

To the members of the research laboratory at HMR, research is a team effort, and I couldn't have done it without you. To all my colleagues and collaborators at HMR, as well as to my colleagues at the University of Montreal and School of Optometry, you have made this journey memorable!

Finally, to my parents and siblings, you are partakers of this accomplishment. Your unwavering love and support have carried me through. Thank you!

Chapter 1 – Introduction

Glaucoma is the leading cause of irreversible blindness in the world (1). An insidious and unpredictable disease, glaucoma causes damage to the retinal ganglion cells (RGCs) that form the optic nerve and can remain asymptomatic until major irreversible visual loss has occurred. The clinical hallmark of this disease includes the progressive deformation and excavation of the tissues of the optic nerve head (2), as seen in Figure 1. Once detected, the disease's progression rate cannot be anticipated. Furthermore, the pathogenesis of open-angle glaucoma (OAG), the main form of glaucoma, is poorly understood.

While the development of OAG was traditionally attributed to elevated intraocular pressure (IOP), the susceptibility of individual eyes to glaucomatous damage is variable. Nearly half of OAG patients have IOP within the normal range (3), going up to almost 90% of patients in some populations (4). In contrast, most patients with elevated IOP do not develop glaucoma (5). This suggests that factors other than IOP must also underlie the susceptibility of the optic nerve head (ONH) to glaucomatous injury.

The realization that a given IOP can result in very different strains at the ONH in different eyes led to an entire field of research known as ocular biomechanics. Central to this theory is the fact that the retinal axons that unite at the ONH to form the optic nerve leave the eye through the lamina cribrosa. The lamina is the major load-bearing tissue of the ONH and is accepted as both a site of discontinuity and weakness in the corneoscleral shell of the eye and as the most likely site of damage to ONH axons (6-10). Two main hypotheses have been proposed to explain the development of glaucomatous optic neuropathy, namely the mechanical and vascular theories (11). The *mechanical theory* postulates that elevated mechanical stresses and strain lead to axonal damage and loss of retinal ganglion cells (12-14). The ONH's response to these biomechanical stimuli has been found to depend on eye-specific geometrical and material properties (Figure 2) (15). This is thought to determine an individual's predisposition to develop OAG.

There is mounting evidence that the stiffness of the sclera, major contributor to the rigidity of the corneoscleral shell, is an important risk factor in the development and progression of glaucomatous optic neuropathy, perhaps more so than IOP (16). Despite numerous studies on the association between ocular rigidity (OR) and OAG in the last eighty years (17-23), this remains unclear, and competing hypotheses are highly debated (24). On one side, OR is thought to be higher in glaucomatous eyes, producing higher IOP fluctuations due to rigid ocular walls, and hence more deformation at the ONH. On the other side, OR is thought to be lower in early glaucoma, engendering axonal stretching and damage. According to this theory, increased OR would occur at later stages of the disease.

Challenges that researchers face when studying OR range from a plethora of confounding factors, both ocular and systemic, including ocular volume and shape, scleral thickness, choroidal blood volume, age and ethnicity, which can have an effect on OR (25). The difficulty in diagnosing glaucoma at the earliest phase of the disease is another obstacle. The lack of longitudinal studies to show whether OR contributes primarily to glaucoma or is altered due to the disease hinders our knowledge of this parameter. More importantly, the ability to quantify OR in living human eyes using a reliable and non-invasive method is essential to investigate the role of OR in OAG. Such a method has only recently become available thanks to developments in our laboratory. Based on the Friedenwald equation (26), the method uses video-rate optical coherence tomography (OCT) imaging and automated choroidal segmentation to measure the pulsatile choroidal volume change (ΔV), and Pascal dynamic contour tonometry to measure the corresponding pulsatile pressure change (27). It will be described in more detail in Chapter 3.

The objectives of this thesis work were thus to validate the method developed to measure OR *in vivo*, and to investigate the relevance of OR in ocular diseases, particularly in OAG. More specifically, we sought to 1) To improve the extrapolation of ΔV and evaluate the method's validity and repeatability, 2) To investigate the association between OR and neuro-retinal damage in glaucomatous patients, as well as those with concomitant vasospasticity, 3) To evaluate the association between OR and corneal biomechanical parameters, 4) To assess the association between OR and IOP spikes following therapeutic intravitreal injections, to predict and prevent them in high-risk patients, and 5) To confirm that OR is lower in myopia.

Before addressing this, the following chapter will briefly review ocular hydrodynamics (IOP and aqueous humor dynamics) and hemodynamics (blood flow), as these elements are involved in OR measurement. This will be followed by a review of the most prominent findings pertaining to ocular biomechanics, and will present the current evidence on the link between OR and OAG.

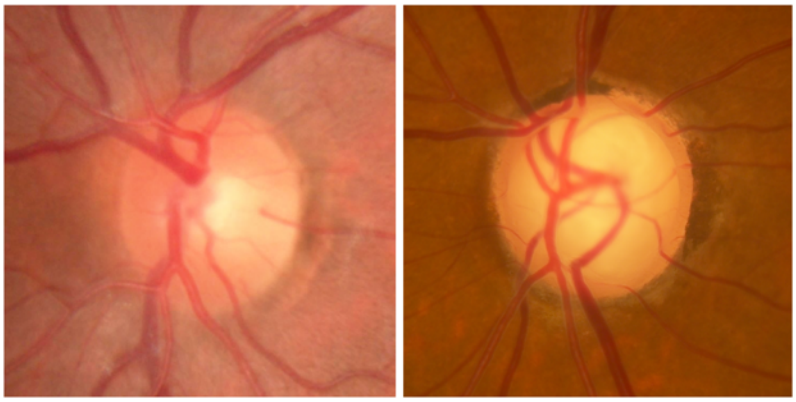

Figure 1. – Glaucomatous optic neuropathy is characterized by the progressive deformation and excavation of tissues at the optic nerve head. Thinning of the neuroretinal rim due to axonal loss, increased cupping and bowing of the lamina cribrosa are clinical hallmarks of this disease. (Courtesy of Dr Lesk and Dr Sayah.)

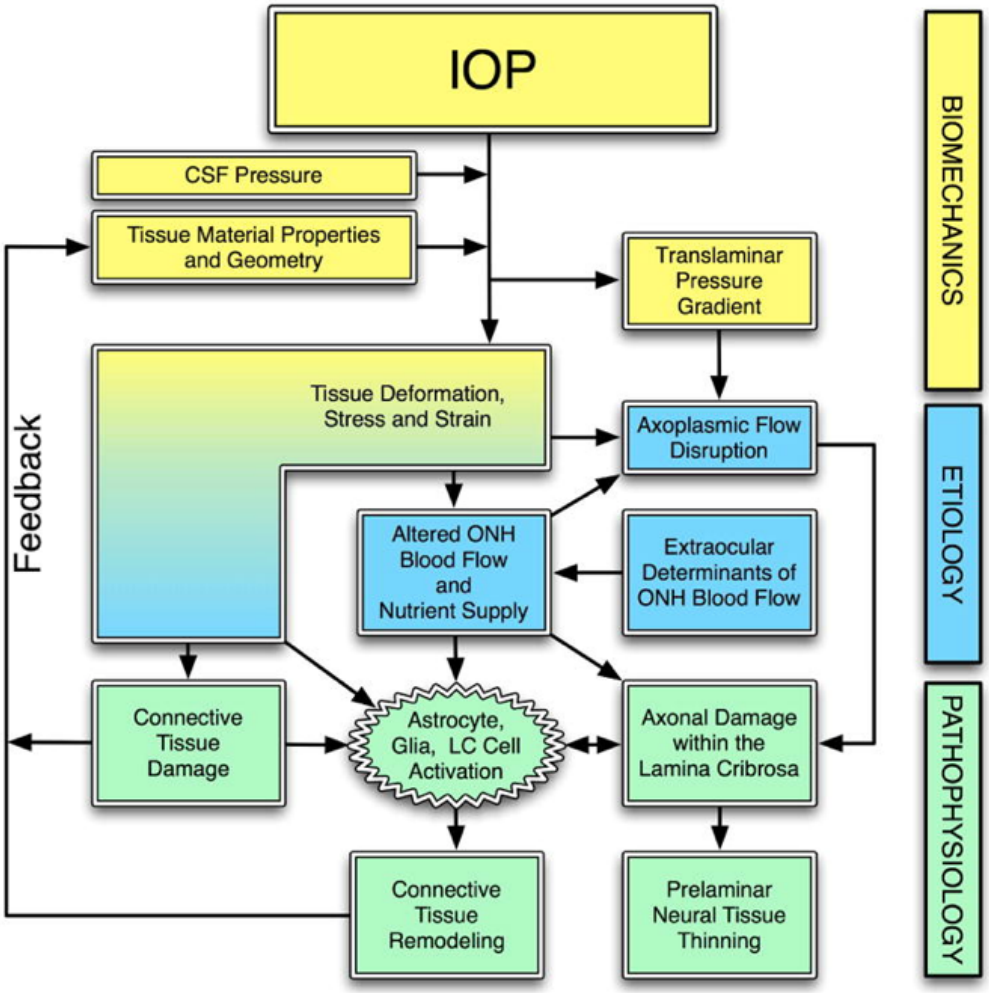

Figure 2. – Representation scheme of the biomechanical paradigm of glaucoma. IOP-induced deformation, stress and strain produce alterations in physiological processes which ultimately lead to axonal loss and glaucomatous damage. (Reprinted from Sigal et al. (15) with permission from Elsevier.)

Chapter 2 – Literature Review

2.1 Aqueous Humor Dynamics and Intraocular Pressure

The eye is a pressurized shell, filled with a colorless fluid of similar composition to plasma – the aqueous humor (AH). AH circulates in the anterior part of the eye, while the vitreous humor, or vitreous body, a gelatinous mass composed primarily of water (98-99.7%) and hyaluronic acid, is found in the retrolental space, with little moving fluid (28). In the eye, AH plays an important role in the nourishment and homeostasis of the cornea and lens, transparent and avascular structures that permit light transmission to the retina.

2.1.1 Aqueous Humor Production and Drainage

AH is continually produced and evacuated. The production of AH occurs in the ciliary processes (Figure 3). From the fenestrated capillaries, through the ciliary process stroma and a double-layered epithelium, it is in the non-pigmented epithelial cells of this double-layer that almost 90% of AH is formed through active secretion (29). AH is secreted into the posterior chamber, traverses the pupil and circulates in the anterior chamber (AC), following a convective flow pattern. This pattern is caused by the temperature difference between the iris (higher temperature) and the cornea (lower temperature) in the AC, producing an upward flow near the iris and a downward flow near the cornea (30).

The evacuation of AH occurs through two routes, the trabecular and uveoscleral pathways. The trabecular or conventional pathway is responsible for 85% of AH outflow from the eye. Its primary constituent is the trabecular meshwork (TM), composed of the uveal meshwork, corneoscleral meshwork and juxtacanalicular tissue, the latter providing the most resistance to AH outflow (31). Driven by the pressure gradient, AH flows out through the TM, across the inner wall of Schlemm's canal, and drains in the collector channels, aqueous veins and episcleral veins (32, 33). When traveling through the uveoscleral pathway, AH flows through the uveal meshwork and anterior face of the ciliary muscle, and drains into the suprachoroidal space and the sclera (29).

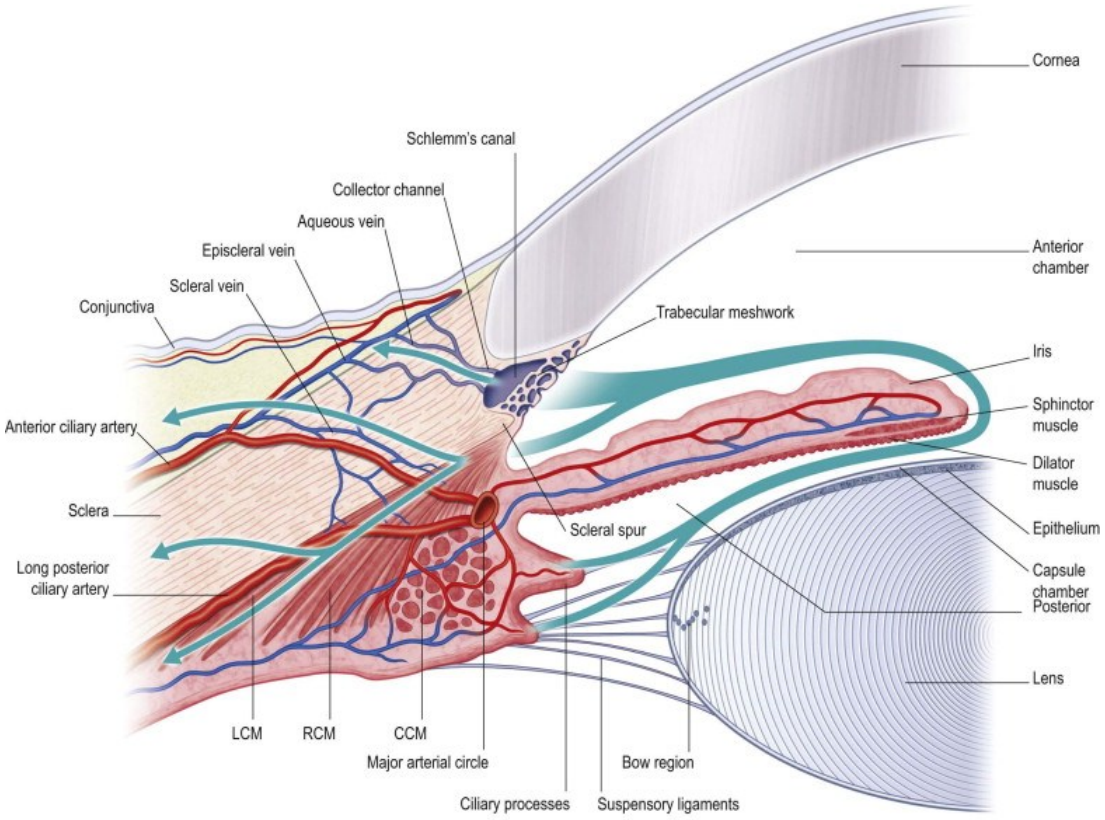

Figure 3. – Schematic representation of the anterior segment of the human eye. Arrows indicate aqueous humor flow pathways. Aqueous humor is formed by the ciliary processes, enters the posterior chamber, flows through the pupil into the anterior chamber, and exits at the chamber angle via the trabecular and uveoscleral routes. (Reprinted from Kaufman, Wiedman (34), with permission from Springer.)

2.1.2 Intraocular Pressure

At steady-state IOP, which is approximately 15 mmHg, the rate of AH production and evacuation are equal (35). In a healthy adult eye, this corresponds to an AH turnover rate of 2.75±0.63µl/min during daytime (36), or about 1-1.5% of the AC volume per minute (37). This state of equilibrium is essential in maintaining physiological processes as well as the shape of the eye.

Many factors are known to affect IOP. These include the circadian rhythm, heartbeat, respiration, exercise, posture, fluid intake, alcohol and cannabis use, as well as topical and systemic medications (38). Age and disease can also affect IOP. This is particularly true for glaucoma, in

which IOP holds an important role both as a risk factor and in its management. Increased resistance of aqueous outflow through the TM is a known risk factor for glaucoma and can cause ocular hypertension (5, 39, 40). From a biomechanical perspective, the stiffness of the TM is thought to increase in glaucoma (41, 42), although the mechanism through which this occurs is not well understood. However, *in vivo* measurement of TM stiffness can be challenging and their interpretation can be problematic as many agents, including topical glaucoma medications, can alter TM function and potentially TM stiffness (43). Currently, the only evidence-based treatment for OAG is to lower IOP, regardless of baseline IOP (44-48). IOP reduction can be carried out using pharmaceuticals, laser trabeculoplasty, surgical procedures, or a combination of these methods. In general, these methods reduce IOP by reducing AH production and/or increasing its evacuation. Some surgical procedures, such as trabeculectomy and drainage devices, create a new exit route to drain the AH and bring the IOP to lower levels.

2.1.3 Tonometry

Tonometry is a crucial part of an eye examination, especially for accurate measurement and management of IOP in glaucoma. Numerous methods have been developed to measure IOP *in vivo*. The main tonometry techniques used in this thesis work, and those historically involved in biomechanical measurements such as the rigidity of the eye, will be briefly described in this section.

One of the first and most commonly used modern device to measure IOP in the world was the Schiötz tonometer (49). As an indentation tonometer, it is based on the principle that a force or weight would produce less indentation in a harder object, or eye. Thus, the amount of indentation would enable IOP estimation, providing that less indentation would be indicative of elevated IOP. To measure IOP, the Schiötz's curved footplate is set on the anesthetized cornea. Different weights, between 5 to 15 g, can be added to the plunger and used to indent the cornea. A table is then used to convert the scale reading to the IOP value in mmHg. One major caveat of the Schiötz is that it is highly dependent on ocular rigidity, leading to underestimation of IOP in eyes with lower rigidity and vice versa (50). Despite the development of updated conversion tables by Friedenwald to correct for OR (51, 52), this method was replaced by Goldmann applanation

tonometry (GAT) in the last quarter of the 20th century, rendering GAT the most used tonometer worldwide.

Applanation tonometry is based on the Imbert-Fick principle, which states that the pressure (P) inside a thin-walled sphere filled with liquid equals the force (F) necessary to flatten its surface divided by the flattened area (A), such that P=F/A (53). In GAT, the anesthetized cornea is flattened by a prism of 3.06 mm diameter (7.35 mm^2). Using fluorescein dye to highlight the tear film, the IOP is determined by varying the applanation force to properly align the superior and inferior mires produced by the prism. Since the Imbert-Fick principles assumes a thin-walled sphere, it does not account for thickness and rigidity. This tends to lead to underestimation of the measured IOP using GAT in thin corneas, and vice versa (54-58). However, no accurate adjustment of GAT-IOP readings for CCT currently exists for individual eyes, as "true" IOP also depends on other biomechanical factors of the cornea which current nomograms do not account for (59, 60). Other applanation tonometers include non-contact tonometry (NCT), pneumotonometry and the Tono-Pen. NCT uses an air pulse of increasing intensity to applanate the cornea. The Ocular Response Analyzer (ORA), a newer type of NCT, measures the biomechanical response of the eye to the rapid air jet-induced deformation at the cornea (61). It yields the Goldmann-correlated IOP (IOPg) and the corneal-compensated IOP (IOPcc), which is less dependent on biomechanical properties, as well as the corneal hysteresis (CH) and corneal resistance factor (CRF). CH and CRF provide information on the viscoelasticity of the cornea and will be described in more detail in the upcoming section on the mechanics of the cornea. Another device based on NCT is the Corneal Visualization Scheimpflug Technology tonometer (Corvis ST). Using a high-speed Scheimpflug camera to visualize and measure corneal deformation in response to an air impulse, the biomechanical corrected IOP (bIOP) is measured, along with various other parameters that describe the viscoelastic properties of the cornea (62). Pneumotonometry uses a 5mm diameter piston with silicone tip and air pressure to flatten the cornea. When the tip and the cornea are both flattened, this corresponds to the IOP (49, 63). The Tono-Pen is a portable tonometer, with an applanating surface and a small plunger protruding slightly from its center. A strain gauge creates an electrical signal that provides an IOP reading when both the plunger and the surrounding surface applanate the anesthetized cornea (63). Each IOP measurement obtained

with this tonometer is an average of multiple IOP readings, and is recorded along with a reliability index ranging from ≤5% to >20%, with the lowest number indicating the highest reliability.

Finally, dynamic contour tonometry (DCT) is a more recent technique that enables the measurement of IOP using the principle of contour matching or Pascal principle. By matching the contour of the cornea, the pressure inside and outside a sphere should be equal. A piezoresistive sensor at the center of the concave tip measures the IOP dynamically when in contact with the cornea (64). When force is exerted on the sensor as it comes in contact with the cornea, the silicon, of which it is composed, becomes more resistant to the small current passing through it. The alteration in resistance is detected and amplified by a wheatstone bridge and is converted to a change in pressure, according to a linear relationship. The three output variables from the Pascal DCT are a quality signal (Q=1 to 5; lower Q is better), the diastolic IOP and the ocular pulse amplitude (OPA), which corresponds to the difference in IOP between the systole and diastole. The IOP measurement from the Pascal DCT, as well as the IOPcc obtained using the ORA, were shown to be independent of central corneal thickness (CCT) and corneal biomechanical properties (65, 66).

2.2 Ocular Hemodynamics

In the human body, the eye is the only place where a direct view to the fundus and blood vessels is possible; it is thus a privileged site for the study of blood flow and its regulatory mechanisms. It is also the organ with the highest metabolism and as such requires a high but regulated blood supply (67, 68). While the measurement of blood flow can contribute to a better understanding of the vasogenic theory of glaucoma (69), it can also bring some insight unto the mechanical theory of this optic neuropathy. In this thesis work, this is relevant for two reasons: 1) the method we developed to estimate the ocular rigidity coefficient involves the measurement of pulsatile choroidal blood flow (as will be described in Chapter 3), and 2) pathological conditions and medications can alter ocular blood flow (70). A review of blood flow and its regulatory mechanisms is thus relevant as it can have an impact on the measurement of OR. The following subsections will focus on the effects of glaucoma, vasospastic disorders and medications on ocular blood flow.

2.2.1 Anatomy of the Ocular Vascular System

Two main vascular systems, retinal and uveal, irrigate the eye, as seen in Figure 4. All blood supply to the eye originates from the ophthalmic artery, which proceeds from the internal carotid artery. The ophthalmic artery is divided into multiple branches, including the central retinal artery (CRA), the anterior ciliary arteries and the short and long posterior ciliary arteries (71). The blood flows out of the eye primarily via the central retinal vein and vortex veins which then drain into the cavernous sinus (71).

The CRA supplies nourishment to the inner retinal layers, from the retinal nerve fiber layer (RNFL) to the outer plexiform layer through two non-fenestrated capillary networks located in the inner nuclear and inner plexiform layers of the retina. The presence of tight junctions between the endothelial cells of these arterioles contributes to the inner part of the blood-retinal barrier. The outer part of this barrier is found at the retinal pigment epithelium cells layer (71).

The retinal arterioles do not supply the foveal avascular zone (FAZ); the absence of superficial blood vessels in this region allows for optimal visual acuity. Rather, the blood input to the FAZ and the outer third of the retina comes from the choroid which proceeds from the short posterior ciliary arteries (SPCA) (72). The choroid represents 80-90% of the total ocular blood volume and flow (73). This characteristic of the choroid is important in the methodology we developed to estimate ocular rigidity. The choroid is essential in maintaining nourishment to the retina, one of the highest oxygen-consuming tissue in the human body (67). It is composed of five layers: Bruch's membrane (BM), the choriocapillaris, Haller's and Sattler's vascular layers, and the suprachoroidea (74). It is also thought to be involved in disease processes such as glaucoma, thermoregulation, secretion of growth factors, and emmetropization (eye growth) (75).

In addition to supplying the choroid, the SPCA form a circular ring called the circle of Zinn and Haller which supplies blood to the prelaminar and laminar portion of the optic nerve head (ONH). The SPCA may also give rise to cilioretinal arteries in about 27% of optic disks, especially in large disks (76). The anterior and long posterior ciliary arteries anastomose to form the major and minor arterial arcades in the anterior part of the eye, supplying nutrients and oxygen to the ciliary body and the iris, and playing a role in AH production (71).

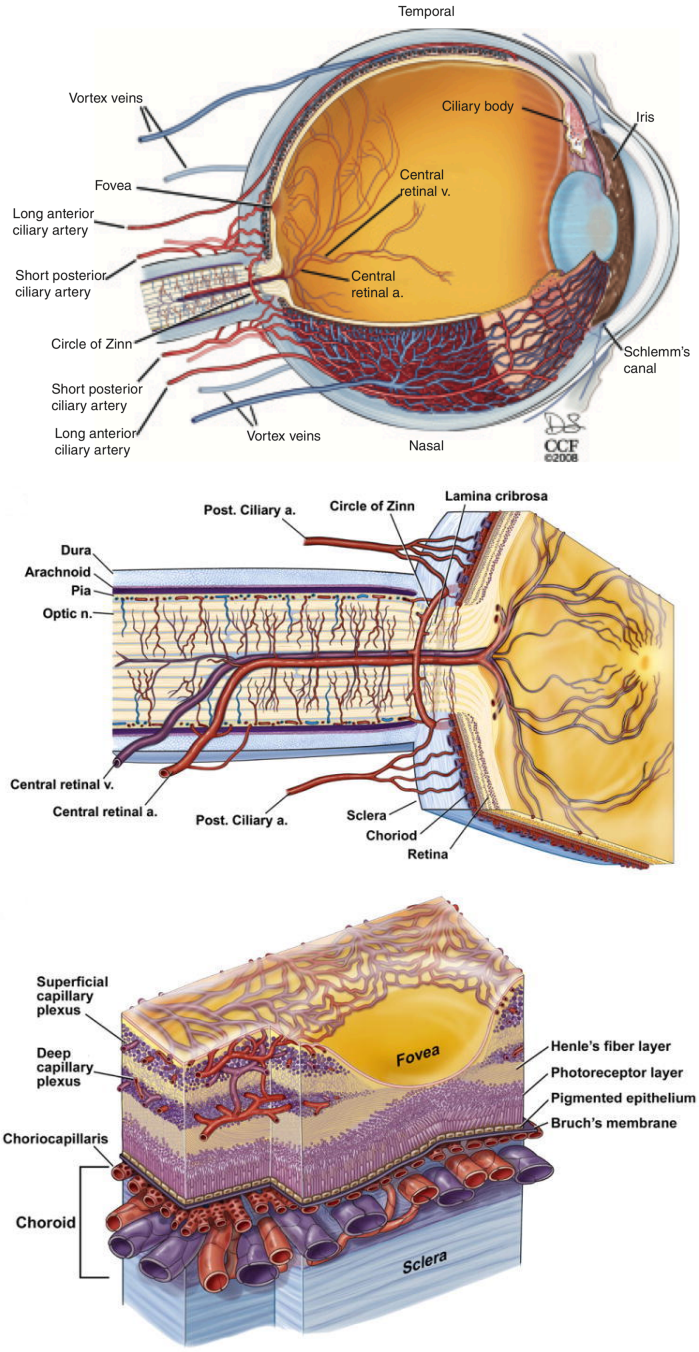

Figure 4. – Anatomy of the ocular vascular system. A) Cutaway drawing of the human eye showing the major blood vessels supplying the retina, choroid and anterior segment. B) Cutaway drawing along the superior–inferior axis of the human eye through the optic nerve, showing the vascular supply in this location. C) Drawing showing the vasculature of the retina and choroid. (Drawings by Dave Schumick. Reprinted from Anand-Apte and Hollyfield (77), with permission from Elsevier.)

2.2.2 Blood Flow and Regulation

Proper homeostasis requires a continuous flow of blood through the capillaries of the body. This flow is governed by the pressure gradient, or perfusion pressure (PP; in mmHg), between the vessel ends, and the resistance (R), or friction, of the circulating blood on the vessel walls. Blood flow (BF) is a measurement of volume in function of time, is described by the following equation (78, 79):

$$BF = \frac{PP}{R}$$

In the eye, the mean PP corresponds to the difference between the mean blood pressure (BP) in the ophthalmic artery and the venous pressure as the blood exits the eye. Since IOP is considered to be almost equal to the venous pressure, the PP at the eye level is defined as follows:

$$PP = \frac{2}{3}\left[DBP + \frac{1}{3}\,(SBP - DBP)\right] - IOP$$

where DBP and SBP are the diastolic and systolic blood pressures respectively (79). This shows that ocular blood flow can be strongly influenced by IOP (80).

Knowing that the resistance to flow in a cylindrical pipe, such as blood vessels, depends on its radius (r), its length (L), the blood's viscosity (η) and the inherent resistance to flow, these elements can be included in the Hagen-Poiseuille law, as follows (78, 79):

$$BF = \frac{PP\ \pi\ r^4}{8\ L\ \eta}$$

An alternative equation, Murray's law (81) may be more adequate for microvascular beds (79):

$$BF = k\ (\frac{r^3}{\sqrt{\eta}})$$

where *k* is a constant that depends on the vessel's length and the blood's viscosity.

Another important element of homeostasis is the ability of the vascular system to regulate. Regulation is usually achieved with the influence of the autonomic nervous system and circulating hormones, as well as local autoregulation (82, 83). Autoregulation is the ability of local tissue to

maintain a constant blood flow despite perturbations such as variations in metabolic demand or in PP (84). In the first condition, the aim is to regulate oxygen and carbon dioxide concentration as well as adenosine, nitric oxide and endothelin-1 (ET-1) levels (82, 83). The second mechanism of autoregulation pertains to mechanical, or myogenic, influences (85, 86), such as changes in PP (or systemic BP or IOP), which can alter vessel diameter to modify the vascular resistance accordingly as shown by the Hagen-Poiseuille and Murray equations (79, 82).

In the eye, the retinal and choroidal systems possess various intrinsic differences (82, 87). Unlike the retinal vasculature, where the lack of autonomic innervation (88) and the blood-retinal barrier (87, 89) limits the effect, the choroid's blood vessels are fenestrated and innervated, and can thus be affected by the body's chemical messengers as well as the autonomic nervous system (82, 87). Another difference is their ability to autoregulate. The retinal vasculature possesses contractile elements, including several layers of smooth muscle cells and a high density of pericytes (82, 90, 91). Retinal blood flow can thus be maintained constant through autoregulation up to an IOP of about 30 mmHg (73, 92). At elevated IOP, retinal blood flow decreases. This may be relevant to glaucoma, considering that retinal circulation provides the inner retina and inner parts of the ONH (73). This ability to autoregulate is widely recognized for the retina, optic nerve, retrobulbar vessels (83, 87, 93-95), and the anterior uveal circulation (73). However it remains nebulous for the choroid, as it was thought not to be autoregulated (73) until recent evidence pointing to the contrary (96, 97).

Many experimental methods have been developed and have enabled the study of autoregulative responses. These methods often involve the alteration of OPP by inducing a significant change in systemic BP, a change in IOP, positional change, or through exercise, and measuring blood flow following perturbation (83). Experiments using flickering light stimuli were also designed to evaluate autoregulative responses of the ocular vasculature by increasing the neuronal activity of the eye, which increases the metabolic demand, and should ultimately lead to increased blood flow (98, 99).

Various studies investigating choroidal blood flow have shown that it remains somewhat constant with PP changes. Riva et al. developed a method based on laser doppler flowmetry to measure

the relative choroidal blood flow subfoveally (100). They found evidence of autoregulation in the choroid in response to acute PP changes due to isometric exercise (101). In their study, when PP increased by up to 67%, an elevation in vascular resistance in the choroid was suggested as the main mechanism for this autoregulation. Other studies showed similar findings by altering IOP or BP through exercise or different means, both in human and rabbit eyes (96, 102-105).

2.2.3 Blood Flow and Glaucoma

Blood flow dysregulation is an independent risk factor to various pathological conditions (70). In glaucoma, impaired autoregulation is thought to be present at all levels of the vascular system (83). While OAG is a multifactorial disease leading to RGC death and visual field loss, it is believed that autoregulative ability as well as OPP play an important role in the development of this condition (106-109).

Some examples of dysregulation include impaired response to posture-induced changes in OPP in the retinal vasculature in OAG patients compared to controls (110), and less retinal vessel reactivity (diameter change) to short-term IOP elevation in OAG than OHT eyes (111). Hafez et al. found markedly improved blood flow in the neuro-retinal rim following therapeutic IOP reduction in OAG eyes, as opposed to eyes with OHT (112). This may indicate that OAG patients have impaired autoregulation in the neuro-retinal rim, whereas OHT patients do not. Studies have also shown impaired autoregulation in the choroidal (113-116) as well as in the retrobulbar vasculature (117-119) in OAG. For example, improvement of choroidal blood flow was demonstrated following trabeculectomy, an IOP-lowering surgery, suggesting impaired choroidal autoregulation in glaucoma (115). A higher susceptibility to IOP-induced glaucomatous damage was also shown to occur in patients with vascular dysregulation, with visual field progression at lower levels of IOP (114). Numerous studies also show an association between reduced blood flow and glaucomatous damage or visual field loss (120-129), and disease progression (130).

While the exact cause of vascular dysregulation in glaucoma is unknown, it could result from an inconsistent supply of oxygen to ocular tissue, or in other words, from alternating periods of hypoxia and reperfusion (131). This phenomenon causes oxidative damage to cells, and mitochondria, which are numerous in the optic nerve head (132) and also present in the

trabecular meshwork (133). Mechanical and ischemic stress is also thought to activate astrocytes, which can lead to reduced trophic functions, tissue remodeling and subsequent ONH excavation (134). The major causes of unstable blood flow and oxidative stress are elevated IOP which exceed the autoregulative capacities, or vasospastic disorders.

2.2.4 Blood Flow and Vasospastic Disorders

Vasospastic disorders are characterized by vascular dysregulation in the extremities, leading to vasospasm, an abnormal constriction of arteries (135). Common examples of vasospastic disorders include Raynaud's disease and migraines. However vasospastic disorders can include a range of signs and symptoms, and may not all result in Raynaud-like manifestations. They can be secondary to a systemic disease or can present in otherwise healthy patients.

Primary vascular dysregulation (PVD) is characterized by the body's abnormal response to stimuli such as temperature and emotional stress, leading to cold hands and/or feet. These symptoms are usually present after puberty but may improve with menopause, suggesting hormonal involvement in PVD. The use of certain medications such as calcium channel blockers which have vasodilatory properties, as well as gingko biloba supplements can have beneficial effects in vasospastic subjects (136, 137).

PVD is thought to be more common in thin women with type-A personalities (138). Several characteristics of PVD have been identified including a reduced feeling of thirst, low blood pressure, and increased ET-1 plasma levels (139). In terms of ocular manifestations, PVD can be associated with splinter hemorrhages, focal rim loss, dense central scotomas, as well as a dysregulation of blood flow to perfusion pressure changes (138, 140, 141). Vasospasticity is thus associated with glaucoma, particularly normal-tension glaucoma (NTG) (142-144).

While testing for ET-1 may be one way to test for vasospasticity, other objective tests exist. The most common include finger laser doppler flowmetry and nailfold capillaroscopy to evaluate the peripheral vascular response to temperature change (138).

There is some evidence that biomechanical stimuli may bring forth abnormal vascular response in vasospastic patients, which renders this condition particularly interesting in the context of this

thesis work. In a previous study, our group showed a greater improvement in rim blood flow following IOP reduction in vasospastic patients compared to non-vasospastic patients, indicating defective autoregulation in patients with vasospasm (145). Another study by Schulzer et al. (144) also demonstrated differences between vasospastic and non-vasospastic patients. More specifically, they showed that within a glaucomatous population, two distinct populations could be identified and each exhibited different characteristics. Interestingly, the group with vasospasticity had a high positive correlation between the mean defect (MD) index of visual field and the maximum IOP (Tmax), while the group with vascular disease, akin to atherosclerosis, showed no correlation between these variables.

2.2.5 Blood Flow and Medication

As discussed previously, reduced blood flow in glaucoma may have adverse effects on the progression of the disease (130, 146). While treatment aimed at lowering IOP is thought to improve OPP and blood flow, the effect of some medication, particularly some systemic hypertensive drugs, can lower the diastolic blood pressure, which in turn lowers the OPP. This can have a significant impact on blood flow regulation, and have a negative effect on glaucoma progression (147-149).

2.2.5.1 Blood Flow and Ocular Hypotensive Medication

Various IOP-lowering agents are commonly used to treat glaucoma. We will focus on the most common and current ones.

Prostaglandin analogues use generally shows an improved ocular blood flow. Most studies on latanoprost showed improved pulsatile ocular blood flow (150-156) as well as beneficial effects on the ONH circulation (157-159), including increased OPP at the optic disc (160). Unoprostone improved ONH circulation (161-165), although no improvement was found in vasospastic subjects (166). Unoprostone also exhibited an antagonistic effect of ET-1 by improving impaired choroidal blood flow (167, 168). Bimatoprost was shown to cause vasoconstriction of the ciliary arteries *in-vitro* at high concentrations (169), tafluprost exhibited a vasodilatory effect *in-vitro* (170) and travoprost did neither (171). Numerous studies with bimatoprost showed no effect on retrobulbar hemodynamics in glaucomatous eyes (172-176), whereas one study found a positive

effect in healthy eyes (177). However, travoprost mostly showed a positive effect on the retrobulbar vasculature (173, 177), as well as a sustained ONH circulation improvement (162). Topical clonidine, an alpha-2 receptor agonist, demonstrated a reduction in OPP in OAG patients (178), and brimonidine showed an increased ocular blood flow in glaucoma patients (179, 180). However, brimonidine has also been associated with decreased nocturnal OPP due to its lowering effect on BP overnight (181). Non-selective β-blockers, particularly timolol, have been associated with unchanged (182-186) or decreased (187-190) ocular blood flow as measured using various techniques. Betaxolol, a β1-selective adrenoceptor antagonist with a probable calcium-channel blocker action, has demonstrated a beneficial effect on blood flow at multiple levels in the eye, including the choroid and ONH circulation (191-194). Topical carbonic anhydrase inhibitors (CAI), dorzolamide and brinzolamide, have both shown enhancing effects on ocular blood flow and its regulation (148, 186, 195, 196). Pilocarpine, a parasympathomimetic vasodilator, displays no effect on ocular blood flow in most studies (197-200). A new class of IOP-lowering drug, rho kinase inhibitors, have been shown to have vasodilatory effects on the conjunctiva (201) and increase ocular blood flow (202).

2.2.5.2 Blood Flow and Systemic Medication

Few studies have been carried out to investigate the role of systemic medications on ocular blood flow. Even fewer have looked at the ocular effects of systemic drugs in glaucoma subjects (137). This section will present the effects of the most common and relevant medications on the eye, as found in the literature.

Systemic CAIs, namely acetazolamide and dorzolamide, have generally been shown to exert a vasodilatory effect on both the brain and the eye, showing increased retinal arterioles' diameter and increased retinal, choroidal and ONH blood flow in the latter (203-206). The dilation of retinal capillaries in an animal model has been linked to decreased extracellular pH (207).

Calcium channel blockers, or antagonists, are among the most prescribed medications to lower blood pressure in hypertensive patients (208). Their mechanism of action involves the inhibition of calcium ions' entry into cells which leads to smooth muscle relaxation and vasodilation. Centrally acting calcium channel blockers appear to increase blood flow in the eye, whereas

peripherally acting calcium channel blockers do not (137). This was shown in multiple reports demonstrating increased blood flow in the ONH and juxtapapillary retina, as well as in other ocular structures including the choroid (209-228). As mentioned previously, calcium channel blockers can also have positive effects on blood flow in vasospastic subjects compared with non-vasospastic subjects (229).

The renin-angiotensin system plays a key role in vasoconstriction, leading to high systemic BP (230). Two classes of medications act on this system to lower BP, namely the angiotensin-converting enzyme (ACE) inhibitors and the angiotensin II receptor blockers (ARB). In the eye, an increase in the velocity of blood flow in the CRA as well as in the posterior ciliary arteries in subjects suffering from essential hypertension treated with an ACE inhibitor was reported (231). The effect of losartan, an ARB, in normal subjects shows some effects on the retrobulbar and choroidal blood flow that can lead to an increased fundus pulse amplitude (232, 233).

Nitric oxide (NO) can lower IOP and increase blood flow through its vasodilatory role on smooth muscle cells, as well a potential autoregulatory effect on the retinal vasculature (234-236). Simvastatin, a drug used to treat dyslipidemia, leads to increased blood velocity and blood flow in the retinal vasculature (237). These effects may be due to increased plasma levels of NO triggered by the drug.

Cannabinoids have IOP-lowering effects as well as vasodilating properties which may be able to increase blood flow in the eye in theory (238, 239). However, they can also cause systemic BP reduction and tachycardia at the same dose required to effectively lower IOP, which may hinder the therapeutic effect of the drug on glaucoma by thus lowering the ocular blood flow (238, 240).

Ginkgo biloba extract is thought to have numerous beneficial properties for the treatment of glaucoma. There is evidence for reduced blood viscosity and vasospasms (137), increased ocular blood flow (241, 242) and neuroprotective properties with ginkgo biloba leading to improved RGC survival (243, 244). Improved visual function was also demonstrated in some patients with NTG (245, 246).

Finally, estrogens and hormonal replacement therapy are thought to have neuroprotective properties (247) and were shown to improve ocular blood flow in both the retrobulbar and retinal circulation (137).

2.2.6 Blood Flow and Systemic Factors

Numerous other factors, including dietary and lifestyle choices as well as overall health can influence ocular blood flow. Some common factors, especially those which can be relevant to glaucoma, will be briefly reviewed in this section.

Caffeine increases blood pressure, decreases heart rate and causes vasoconstriction (248, 249). It was shown to decrease blood flow in the eye in healthy eyes (250-252) and increase IOP slightly, by about 1 mmHg, in glaucoma patients (253-255). The Blue Mountains Eye Study found that glaucoma patients who reported regular caffeine consumption had a higher average IOP (256), which may be explained by an increased AH production due to caffeine (257, 258). However, coffee consumption was not associated with POAG (259, 260).

Alcohol is a vasodilator and was shown to increase blood flow at the ONH level (261), but not in the retrobulbar circulation (262). Its acute consumption was also shown to lower IOP (261-263), and was not found to be a risk factor for POAG (264).

Interestingly, while cigarette smoking is thought to induce vasospasm and increase blood viscosity (265), some studies have instead shown increased cerebral and ocular blood flow in response to nicotine (266-269). This may be due to increased cerebral oxygen consumption in smokers (270). Cigarette smoking however was not found to be an important risk factor for POAG in a large prospective study (271).

Obesity has been associated with elevated IOP and reduced retrobulbar blood flow (272, 273), as well as reduced ocular pulse amplitude (274). Epidemiological studies have shown conflicting results regarding the risk of POAG in obese subjects, with some showing increased risk (275), while others decreased risk (276-278) or no associated risk (279, 280).

Obstructive sleep apnea syndrome (OSAS) is a disorder in which breathing can be interrupted multiple times during sleep. It is characterized by a relaxing of the muscles in the throat, which in

turn cause the upper airway to collapse (281). While the typical OSAS patient is thought to be a middle-aged, obese man who snores loudly, this is not always the case and should be considered when screening for this sleep disorder (282-284). OSAS was found to be associated with POAG, particularly NTG, (285-295). It is thought that a dysregulation of blood flow caused by repetitive hypoxic events as well as insufficient ONH perfusion and increased vascular resistance is probably at play in both of these conditions (285). Systemically, impaired coronary endothelial vasoreactivity (296) and decreased cerebral blood flow (297-302) was found in patients with sleep apnea. However, in the eye, blood flow was found to be unaltered in OSAS subjects compared with controls in most studies (303-306), except in one study where impaired autoregulation in the retrobulbar vasculature of OSAS subjects was reported (307).

Both low and high BP have been found to be associated with glaucoma. Numerous studies have reported an association between low DBP and low OPP and a higher prevalence and/or incidence of OAG (308-311). The Baltimore Eye Survey reported a six-fold increase in the prevalence of OAG in patients with the lowest OPP, suggesting altered ocular blood flow and autoregulation (311). The combination of nocturnal hypotension in patients with low systemic BP, or those with treated hypertension (HTN), and elevated IOP is a risk factor for glaucoma, leading to reduced OPP and ONH ischemia (106, 311-315). An association between HTN and OAG, as well as a correlation between SBP and IOP were also consistently found in several clinical studies, suggesting that chronic HTN may impair blood flow to the ONH (309, 316-321). However, this association was later attributed to the correlation between age and HTN (4). In the context of biomechanics which will be discussed in the following section, altering BP was suggested to have an effect on the pressure-volume relationship in rabbit eyes, by altering blood volume and choroidal blood flow (322). These findings were not corroborated in human studies in the range of clinically encountered BP (23, 323).

Diabetes mellitus is known to damage the endothelium and pericytes of blood vessels, leading to dysfunctional regulation of ocular blood flow in the early stages of the disease, followed by ischemia and vascular proliferation in the later stages of diabetic retinopathy (324). Findings regarding choroidal blood flow in diabetes using subfoveal laser Doppler flowmetry generally indicate a reduction (325, 326) and dysregulation (327) of choroidal blood flow in eyes with

diabetic retinopathy. Although diabetes was initially thought to be a risk factor for glaucoma (328-332), conflicting data suggests that diabetes may not be associated with glaucoma (278, 333-338).

2.3 Ocular Biomechanics

Biomechanics is a rapidly developing field, joining physics and biology, and bringing new insights into physiological and pathophysiological mechanisms. In a normal eye, various forces are constantly being exerted on its walls by surrounding or internal structures, including the extraocular muscles and ciliary muscle, during accommodation for example, as well as by fluids such as the AH and the vascular system during the cardiac cycle (80). Throughout these processes, the shape of the eye and position of its optical components is maintained to ensure optimal vision. In other cases, the mechanical properties of the eye can dictate its behaviour in response to different factors, including IOP, and lead to adverse morphological and functional changes. This is thought to be particularly true in diseases such as OAG, age-related macular degeneration (AMD) and myopia. Hence, understanding the structural and material properties of the eye could help elucidate the mechanisms underlying these potentially-blinding diseases, and in turn have a significant impact on clinical practice.

The following sections will present the main findings pertaining to the biomechanical properties of the eye in OAG, from the most anterior to the most posterior structures. They are adapted from a textbook chapter on Glaucoma and Ocular Rigidity that I co-authored (339). The outer coat of the eye is formed by the cornea and the sclera, two tough connective tissues that make up the corneoscleral shell. Posteriorly, the corneoscleral shell is pierced by the scleral canal through which the retinal ganglion cells' (RGC) axons exit the eye on their way to the brain. The lamina cribrosa (LC), a specialized region of the sclera, spans the scleral canal. It is clear that remodeling of these tissues occurs in glaucoma (14, 340, 341), thus altering the mechanical environment of the optic nerve head (ONH). The properties of these structures will be reviewed with an emphasis on their relevance in glaucoma.

2.3.1 Mechanics of the Cornea

The cornea is the anterior extension of the sclera, and its viscoelastic properties and thickness contribute to the overall rigidity of the eye. The main biomechanical properties of the cornea which can be currently measured and studied in glaucoma are the central corneal thickness (CCT), corneal hysteresis (CH), corneal resistance factor (CRF), and many others, including the ORA waveform parameters and the Corvis ST parameters, that have been studied less extensively.

2.3.1.1 Central Corneal Thickness

CCT is most frequently measured using ultrasound pachymetry, optical pachymetry, Scheimpflug imaging or anterior segment optical coherence tomography (OCT) (342). Initially, CCT was used in the clinical management of glaucoma to correct IOP readings (343). This correction was later shown to be inadequate due to the absence of algorithm to accurately predict the true IOP corrected for CCT (344). The Ocular Hypertension Treatment Study (OHTS) was the first to demonstrate the importance of CCT as a predictor for the development of OAG (5). In this study, a CCT of 555 μm or less was associated with a three-fold increased risk of developing OAG. Further investigation has confirmed CCT to be an independent predictor for the development of POAG (5, 345) as well as a risk factor for the development of visual field (VF) loss in glaucoma patients (346).

Several experiments were carried out to better understand the link between CCT and posterior structures of the eye in glaucoma. While this association remains unclear, due to the absence of correlation between CCT and laminar and scleral thicknesses (347, 348), a thinner cornea was suggested to be associated with a more compliant lamina cribrosa due to larger displacement of the LC with IOP reduction in eyes with lower CCT (349). Furthermore, an inverse relationship was found between CCT and optic disc size or area, perhaps indicating larger and more deformable optic discs with lower CCT (350). In a study involving non-invasive measurement of OR, a positive albeit weak correlation was also found between OR and CCT, indicating that subjects with a thinner cornea may have a more compliant sclera (23). In a similar clinical study, no relationship between OR and CCT was found, arguably due to low statistical power (351).

In subjects with no corneal pathology, CCT remains relatively stable. CCT was reportedly lower in subjects from African descent (AD) and Hispanics compared to Caucasians (352-355), although

this difference was later shown to be dependent upon corneal hysteresis (356). While CCT also decreases with age, and can be altered with some topical treatments (357-359), it is not known to change over time in glaucoma patients as their disease advances (360).

2.3.1.2 Corneal Viscoelastic Properties

The corneal hysteresis (CH) and corneal resistance factor (CRF) can be measured *in vivo* using the Ocular Response Analyzer (ORA; Reichert Ophthalmic Instruments, Inc., Buffalo, NY, USA), a non-contact tonometer that measures the biomechanical response of the eye to a rapid air jet-induced deformation at the cornea (61). The Corneal Visualization Scheimpflug Technology tonometer (Corvis ST: CST; Oculus, Wetzlar, Germany), a more recent device, visualizes and measures corneal deformation also in response to an air impulse using a high-speed Scheimpflug camera (62). It measures numerous parameters, many of which have been shown to be correlated, albeit weakly, with CH and CRF (361). However, these two devices yield different parameters which are not interchangeable.

CH and CRF are considered to be analogous to the viscous and elastic properties of the cornea respectively. As such, CH represents the cornea's ability to absorb and dissipate energy, and is defined as the difference between the inward applanation pressure (P1) and the outward applanation pressure (P2) as seen in Figure 5. CRF provides information about the elastic properties of corneal tissue or their resistance to stress, and is defined as P1-kP2 where k is a constant derived empirically from central corneal thickness (CCT) (362). Both CH and CRF have been shown to be relevant to glaucoma. Typically, average CH and CRF values in non-diseased eyes are around 10.5 mmHg (363, 364). CH was found to be significantly lower in POAG (365-368) compared to controls, while both CH and CRF were found to be higher in OHT eyes than in glaucomatous eyes (369, 370). Numerous studies also associated a lower CH with an increased risk of glaucoma progression (371-374). Furthermore, in a study investigating CH in asymmetric glaucoma progression, worse eyes had significantly lower CH than the less damaged eyes (8.2 ± 1.9 vs 8.9 ± 1.9 mm Hg; $p < 0.001$), while CCT and IOP did not significantly differ between eyes. CH was thus the most discriminative index for predicting the eye with worse VF in asymmetric OAG (375). Moreover, when comparing corneal biomechanical factors, reported findings showed lower CH values to be predictive of glaucoma progression, more so than CCT (371, 372).

How these corneal properties are linked to optic nerve susceptibility and glaucomatous damage remains unclear. Some speculate that the viscoelasticity of the corneal extracellular matrix (ECM) could be related to the properties of the ECM in the LC and peripapillary sclera. This would mean that an eye with a more deformable cornea (low CH) may also be more vulnerable to IOP-induced ONH damage. Some studies on the relationship between CH and ONH morphology have found lower CH to be associated with larger cup-to-disc ratio (376, 377), deeper cup in untreated POAG (376) and small rim area (377). However, another study did not find such correlations in a large, non-glaucomatous cohort (378). When subjected to an acute but transient IOP elevation, glaucomatous eyes have shown a correlation between CH and optic nerve surface displacement, whereas controls did not (366). When IOP was reduced in POAG subjects, greater change in ONH cup area occurred in POAG eyes with lower CH when controlling for baseline IOP and IOP change, but this was not significant when all factors were included in the multivariate model (379). Similarly, no significant association was found between CH and RNFL thickness in glaucomatous subjects when multivariate analyses were carried out (380, 381).

CH is a dynamic property. While it has been shown to decrease only slightly with age (382), it has been shown to have a mild inverse relationship with IOP (383, 384). Consequently, CH can be altered following IOP-lowering therapies such as with topical prostaglandin analogues (PGA) (358). Other surgical IOP-lowering strategies also showed increased CH post-operatively (384, 385), while maintaining a lower CH in the treated eye compared to the contralateral healthy eye in some cases (384). Furthermore, low-baseline CH, but not CCT, can be predictive of a greater magnitude of IOP reduction following treatments such as PGA (29% vs 7.6% IOP reduction with mean CH 7.0 mmHg vs 11.9 mmHg respectively, p=0.006) (386) and selective laser trabeculoplasty (SLT) (387). Ethnic differences point to lower CH in subjects of African Descent (AD) (356), in both healthy and glaucomatous eyes (388). Whether this could be linked to the higher predilection of AD subjects of developing glaucoma remains unknown.

In summary, CH may be more relevant to glaucoma than CCT by its stronger association with disease severity, risk of progression, and effectiveness of glaucoma treatments (389). How these findings can be related to ONH biomechanics remains to be elucidated.

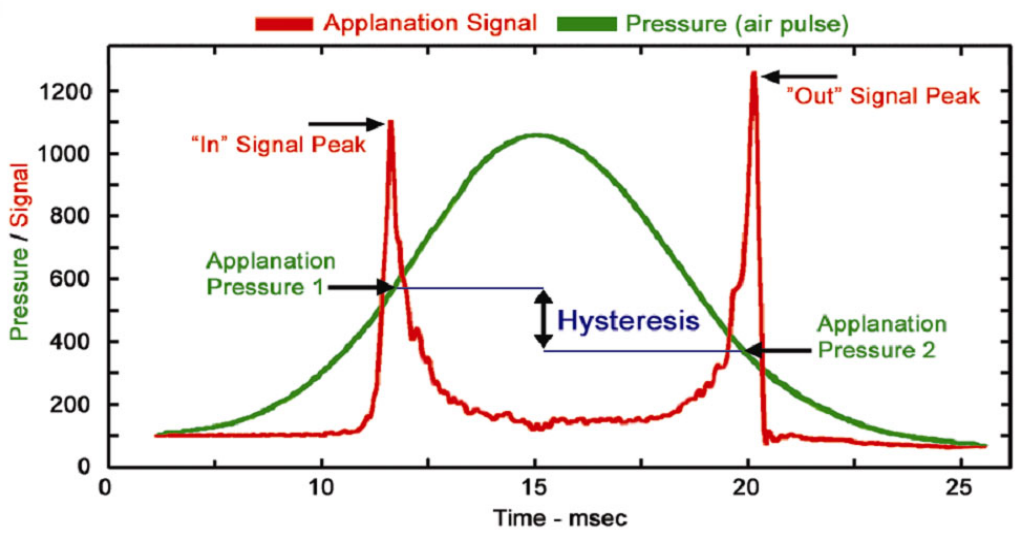

Figure 5. – Ocular Response Analyzer signal showing the cornea's response to deformation by a rapid 30 ms air jet pulse. Infrared light (red signal) is emitted and detected by a photodetector after reflecting on the corneal surface. Following the air jet pulse, the cornea is applanated (green signal) and flattened; this corresponds to the inward applanation pressure (P1). It continues to move inward, becomes concave, then rebounds to reach a second flattened state at an outward applanation pressure (P2), and return to its original shape. Corneal hysteresis is defined as P1-P2. CRF corresponds to P1-kP2 where k is a constant derived empirically from central corneal thickness.

2.3.2 Mechanics of the Globe, or Ocular Rigidity

2.3.2.1 Ocular Rigidity

Seeking to improve the accuracy of tonometry readings and investigate differences between normal and diseased eyes, a prominent ophthalmologist and scientist, Jonas S. Friedenwald, investigated the relationship between the change in intraocular pressure (IOP) and ocular volume (V). This led, in 1937, to his proposal of the "ocular rigidity function":

$$\ln \frac{IOP}{IOP_0} = K\ (V - V_0),$$

where K is the ocular rigidity coefficient (26). Friedenwald's equation was obtained empirically using experimental data on the distensibility of the eyeball recorded previously in enucleated

eyes. The application of this equation is limited to IOP values above 5 mmHg, as at lower IOPs, it suggests that an infinite volume of fluid must be removed from the eye to result in a null IOP (26). Since the sclera, the fibrous envelope of the eye, is responsible for the majority of the ocular globe's rigidity, it is not surprising that the Friedenwald equation can be derived from the mechanical properties (stress-strain relationship) of its primary constituent, collagen (80, 390).

In biomechanics, stress (σ) is the force per unit cross-sectional area (in N/m^2 or Pa) that is exerted on a body. Strain (ε) is the deformation in the direction of the applied force divided by the initial length of the material ($\varepsilon = \Delta l/l_0$). The stress/strain behaviour of the corneoscleral envelope is described as (391-393):

$$\sigma = A[e^{\alpha\varepsilon} - 1],$$

where A and α are material constants. At low strains, $A\alpha$ corresponds to the Young's modulus of the material (80). Young's modulus, or the elastic modulus, is a material property describing its resistance to being deformed when a force is applied to it. The sclera has a high elastic modulus, 5-13 MPa on average according to experiments led on inflated human eyes (394-396), and a very high rupture strength (80). When we evoke ocular rigidity, it refers to a property of both the material and shape of the object. The rigidity of the corneoscleral shell, or ocular rigidity (OR), is thus a measure of the resistance that the eye exerts to distending forces and corresponds to the pressure-volume relationship in the eye as represented in Friedenwald's equation (26). In this equation, a greater K value corresponds to a more rigid eye. A good analogy for this is to think of a rigid eye (high K, or OR) as a soccer ball and of a compliant eye (low K, or OR) as a birthday balloon. Alternative and more accurate formulae were developed, however the Friedenwald function remains the most commonly used to calculate the OR coefficient (25).

OR is considered an important biomechanical property of the eye and is thought to play a key role in the pathogenesis of open-angle glaucoma (OAG) (11, 13, 14, 16, 340, 397), myopia (14) and age-related macular degeneration (AMD) (398, 399). OR has been shown to be altered in these diseases (17, 23, 399, 400). More recently, numerical modeling has provided insight into the profound effect of biomechanical properties of the corneoscleral shell on the level of stress exerted on the ONH (13, 14, 16, 401). These models have shown that forces at the ONH are

considerably higher than the IOP (402). Furthermore, finite element modeling suggested that scleral stiffness could be the most important biomechanical factor in determining strain at the ONH (16). However, its role in their pathogenesis remains to be fully understood and requires further investigation.

The ability to quantify the structural and material properties of the corneoscleral shell could help elucidate the pathophysiological mechanisms of these diseases, and thus improve their diagnosis and treatment. Until now, reported outcomes on the association between OR and glaucoma remain mitigated. Inflation studies in cadaver eyes, and *in vivo* studies using indirect measurements showed higher OR in eyes with established glaucoma (17, 19-21). More recent studies reported low OR in OAG (18, 23), and highest OR in ocular hypertensives (OHT) with no glaucomatous damage (23). Finally, using intraoperative cannulation, one experiment showed no difference between diseased and healthy eyes (22). How can these results be reconciled? The idea that perhaps OR is altered during the course of the disease is an interesting one, although this has not been assessed yet. As early as 1960, Drance postulated that while OR seems to be increased in long-standing glaucoma, decreased OR in untreated glaucoma patients was possible (17). Discrepancies may also be due to confounding factors which can influence OR values. We will hereby address some of these factors.

2.3.2.2 Ocular Rigidity Measurement Methods

Different approaches, both invasive and non-invasive, have been used in the last decades to estimate OR. Each has advantages and limitations. This meant that interpretation of results with non-invasive techniques had to be done carefully, and invasive methods were not suitable for large scale testing.

Historically, OR measurements were performed in cadaver eyes (12, 403-405) or *in vivo* by means of Schiotz tonometry, either paired readings or differential tonometry. This technique consisted of comparing Schiötz and Goldmann tonometry results, but was later considered inaccurate primarily due to the dependence of both indentation and applanation tonometry on the biomechanical properties of the eye (406-409). The most significant source of this variability in OR coefficients originates from the use of weights in Schiötz tonometry, which compress the

ocular wall and displace a significant amount of intraocular fluid (406, 409), but also through the erroneous assumption that the OR of all eyes is standard in the applicability of the conversion table which provides the IOP reading in mmHg (39, 51, 406). Other non-invasive methods were developed to measure OR based on Friedenwald's equation. The first method estimated the ocular volume change (ΔV) by measuring the movement between the cornea and inner retina in response to the cardiac pulse, also known as the fundus pulse amplitude (FPA) (19). Another group measured the change in axial length (AL) following pharmacological IOP reduction to estimate OR (20). Both methods consisted of measuring the anterior to posterior expansion of the corneoscleral shell, which is itself dependent on OR (410). Instead of measuring the response of ocular coats to an increase in volume, choroidal laser Doppler flowmetry was used to estimate the amount of blood injected in the eye with each cardiac pulse as an indicator of ΔV to estimate OR. However this gave only relative values because choroidal blood flow was measured in arbitrary units (23).

Due to the difficulties of quantifying ΔV with other methods, anterior chamber manometry remained the main technique to directly calculate OR in vivo (351, 411-413). This technique is used at the outset of surgery and involves injecting small increments of fluid into the anterior chamber while measuring the resultant change in IOP. It could be considered the "gold standard" for clinical OR measurements, however its invasive nature limited its applicability in clinical use. Instead of injecting known volumes of fluid in the eye and measuring resulting IOP changes to estimate OR, our group has recently developed a non-invasive, clinical method to directly measure OR in living human eyes (27). This method will be described in detail in Chapter 3.

2.3.2.3 Ocular Rigidity and Post-Mortem Changes

Experiments using enucleated eyes often yield higher values of OR when compared to *in vivo* measurements. This is thought to result from the influence of the vasculature and extraocular muscles in living eyes, and of edema in postmortem eyes (351, 413-415). While comparison of glaucomatous and non-glaucomatous eyes remains possible, limited knowledge as to the prior state of the eyes and the history of the disease is known when using human cadaver eyes. Furthermore, dynamic behavior cannot be easily assessed using cadaver eyes.

2.3.2.4 Ocular Rigidity and Glaucoma Severity

In most studies, glaucomatous patients are chosen following diagnostic criteria including signs of axonal and VF damage (19, 20). Since VF defects are detected only after a substantial proportion, up to 57% of RGCs are lost (416-418), these subjects have established glaucoma. Therefore, OR is not often measured near the initiation of glaucoma, and changes may have occurred that modify the initial OR. As well, these cross-sectional experiments do not permit the assessment of how OR changes during the course of glaucoma. Perhaps longitudinal studies will help establish whether OR could be low in early stages and increases with advanced disease, as proposed by Drance (17).

2.3.2.5 Ocular Rigidity and IOP-lowering therapy

In several studies investigating OR in glaucoma, recruited patients are on IOP-lowering therapy. Due to the dependence of OR on IOP, results thus need to be interpreted with caution (25). Furthermore, commonly used IOP-lowering medications may have an effect on OR possibly through alterations of the sclera's composition (18, 419, 420). Some medications, including losartan, an angiotensin II receptor blocker prescribed to lower systemic blood pressure, has been shown to alter scleral remodeling in experimental glaucoma in mice, and exhibit a neuroprotective effect on RGCs (421). Ocular surgical procedures, especially those intending to lower IOP, may also alter OR.

2.3.2.6 Ocular Rigidity and Ocular Volume

The relationship between OR and the diameter or volume of the eye is well known. OR is thought to be lower in longer eyes (23, 422). Previous findings report thinner peripapillary sclera and lamina cribrosa (423), as well as scleral remodeling in elongated eyes (424). Axial myopia is also a known risk factor for glaucoma, with a two- to three-fold increased risk of glaucoma compared to non-myopes (425, 426). Theoretically, this would be due to greater IOP-induced strain in larger eyes (427), and needs to be controlled for in clinical studies investigating OR. This would suggest that the association between axial myopia and glaucoma could be due, at least in part, to the increased compliance of the sclera, leading to increased ONH deformation and susceptibility to axonal damage.

2.3.2.7 Ocular Rigidity and Age

There is evidence for the association between aging and increased OR (351, 419, 428). Induced crosslinking from the accumulation of advanced glycation end products in tissues with aging could be at fault (429, 430). These age-related changes in the composition and thickness of the sclera and optic nerve head would increase lamina cribrosa (LC) and peripapillary sclera (PPS) stiffness (431, 432). Since aging is also a risk factor for glaucoma, a high OR would then be thought to be associated with glaucoma. However, this may not be the case as demonstrated by more recent clinical and computational studies (16, 23) and needs to be further investigated.

2.3.2.8 Ocular Rigidity and Ethnic differences

Through inflation studies and ONH reconstructions from cadaver eyes, ethnic differences were observed between eyes from African descent (AD) and those from European descent (ED). PPS stiffness was reported to be higher in aging AD eyes compared to ED eyes (433). Similarly, AD eyes showed an increase in scleral thickness and LC depth with age, whereas ED eyes did not (432).

2.3.2.9 Ocular Rigidity and Other Factors

While OR may be altered through the course of ocular diseases, choroidal and ocular blood flow can alter OR (323, 428, 434). These have been reviewed in some detail in the previous sections. Pseudoexfoliation syndrome is associated with increased stiffness of the iris (435, 436), and perhaps of the scleral shell. Furthermore, the impact of collagen diseases on OR is not to be neglected, as subjects with osteogenesis imperfecta were found to have lower OR (437) and other collagen or connective tissue disorders have been associated with corneal conditions such as keratoconus, which is characterized by increased compliance of the cornea (438).

The mechanism by which the sclera is altered in glaucoma has not been established, and in vivo studies indicating OR alterations in glaucoma remain sparse. Changes in the content and composition of collagen fibers in glaucomatous eyes and in suspected glaucomatous eyes were found (439). However, while increased OR in established glaucoma may be related to stiffness or thickness of the sclera, no relationship was found between OR and scleral thickness (440). This reinforces that to better understand the fundamental biomechanical paradigm and the forces

that lead to ONH damage, it is perhaps necessary to evaluate OR in conjunction with other factors such as the biomechanical properties of the PPS and the LC, which make major contributions to the stresses and strains in the ONH.

2.3.3 Mechanics of the Lamina Cribrosa

An extension of the sclera, the lamina cribrosa (LC) is a porous disc at the base of the optic nerve head through which the axons composing the optic nerve leave the eye. It features a complex three-dimensional structure composed of a network of flexible beams of connective tissue. As it spans the scleral canal, this fenestrated and vascularized tissue provides mechanical as well as metabolic support to the retinal ganglion cells' axons as they leave the eye (341).

Biomechanically, the LC is a structure of great interest and is thought to be the principal site of axonal damage in glaucoma (6, 9, 441). The LC is significantly more compliant and thinner compared to the surrounding sclera. It corresponds to about one-tenth of the sclera's stiffness and one-third of the peripapillary scleral (PPS) thickness (341). It is thus considered a 'weak spot' in the corneoscleral shell (402). Its vulnerability is further exacerbated by its surroundings. On one side the intraocular space and on the other the retrobulbar space represent high (IOP) and low (cerebrospinal fluid pressure, or CSFP) pressure environments respectively, creating a translaminar pressure gradient (TLPG) across this barrier (442). The TLPG, estimated as the difference between IOP and CSFP divided by the laminar thickness (443, 444), would generally produce an outward bowing of the LC. IOP-induced circumferential stress can also act on the ONH via the corneoscleral shell and PPS to expand the scleral canal. Both these elements can give rise to considerable stress and strain, even at normal levels of IOP (402, 445). In turn, this can induce morphological changes within these structures (134, 446-449), but also disrupt axoplasmic flow within the RGC axons at the LC level (7, 441, 450-453) and impinge on the delicate ONH vasculature leading to reduced blood flow (454). LC deformation is thus mediated by IOP, CSFP, as well as the geometrical and material properties of the sclera and LC of the individual eye (341). Eye-specific characteristics thus mediate the susceptibility to glaucoma in individuals at any given IOP.

Chronic IOP elevation and transient IOP elevations were found to produce tissue remodeling in the ONH through various pathways, including through the activation of astrocytes and LC cells (134, 455-457). Stretching induces remodeling of the extracellular matrix in the LC (447-449). This remodeling can alter the stiffness of the LC and in turn, play a role in the development of OAG. Laminar stiffness is shown to increase with age (405, 429, 458), more so in patients of African origin (432, 459, 460). A plethora of studies have investigated LC mobility in *ex vivo* (12, 403-405, 461) and histological studies (12, 462-465) as well as in monkey eyes (462, 466, 467) and living human eyes (468-472), and more recently through engineering modeling (16, 401, 473). Some have suggested an initial hypercompliance in early glaucoma (462, 467) and most have documented increased rigidity later in the course of the disease (12, 403-405, 461, 462, 466, 468, 474). Morphologically, glaucomatous changes to the laminar structure have been shown to manifest as posteriorizing of the LC insertion into the sclera, increased cupping and focal laminar defects (341). Focal defects such as laminar holes and disinsertions were found to be linked with disk hemorrhages (475-478) and RNFL defects (479, 480). Enlargement of the laminar pores were also found, particularly in the superior and inferior quadrants where early glaucomatous RNFL defects and VF loss are most common (463). Laminar posteriorizing was greater in glaucomatous eyes compared to controls (481), and greater LC depth was found in high-tension glaucoma compared to NTG (482). Posteriorizing of the LC insertion and peripheral LC were shown in OAG eyes compared with age-matched controls, the latter being more displaced in the vertical meridian (483). This was consistent with the findings in asymmetric glaucoma where prelaminar tissue was thinner and the LC was more posterior in the eye with VF loss compared to the contralateral eye with no VF defect (484).

In experiments involving significant IOP reduction or elevation, LC displacement was shown to bend in either direction (ie. inward or outward) (485, 486). This can be dependent on its initial position and the stiffness of the surrounding tissue. When OAG subjects were divided in three groups according to disease severity, and anterior LC depth (ALD) was imaged using optical coherence tomography (OCT) prior to and after significant IOP reduction, the results showed posterior displacement of the LC in the group with lesser VF damage, anterior displacement in the group with moderate damage and close to no displacement in subjects with greater glaucoma

damage (485). Perhaps these results suggest that the LC is stiffer in advanced glaucoma, and that the group with less VF damage has a more compliant sclera. In other words, while a compliant PPS would expand with high IOP, producing a taut pulling of the lamina and an expansion of the scleral canal, IOP reduction would reverse this expansion. The LC would hence move outward, back to its original position as the IOP is reduced, as illustrated in Figure 6. However, this remains to be verified. As more imaging tools are developed to study the biomechanical behavior of the LC, a small and relatively inaccessible structure of the eye, it will become possible to assess glaucomatous changes over time.

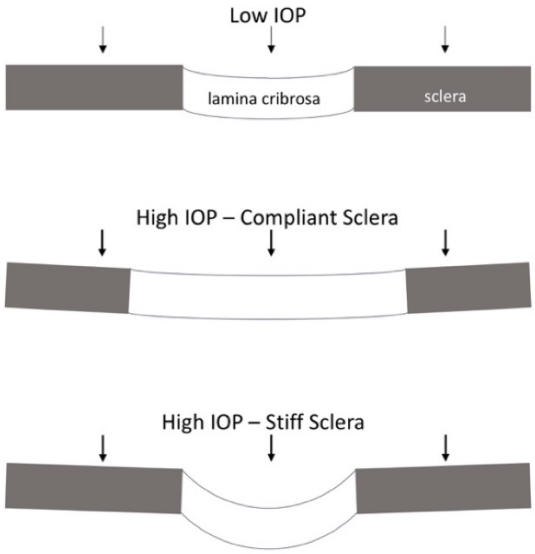

Figure 6. – Behavior of the lamina cribrosa when subjected to low or high IOP. When the sclera is compliant, increased IOP pulls the LC taut due to the expansion of the sclera and scleral canal. When the sclera is stiff, minimal scleral deformation occurs. Instead, the LC deforms posteriorly under the effect of IOP.

Chapter 3 – Method Developed to Measure Ocular Rigidity

Our group has developed the first non-invasive and direct method to measure ocular rigidity (OR) in living human eyes (27). Based on Friedenwald's equation, this approach involves video-rate optical coherence tomography (OCT) imaging coupled with automated choroidal segmentation to measure the pulsatile ocular volume change, as well as Pascal dynamic contour tonometry (DCT) to measure the pulsatile intraocular pressure (IOP) change. The novelty of this method consists mainly in its ability to measure the pulsatile ocular volume change from OCT videos. Every step of the method is described in detail in this chapter.

3.1 Pulsatile Ocular Volume Change

OCT is a medical imaging technique that uses low coherence interferometry to produce high-resolution cross-sectional images (487). Since the eye is transparent, it is a privileged site for OCT imaging. The basic principles behind this technology are similar to the Michelson interferometer, as seen in Figure 7.

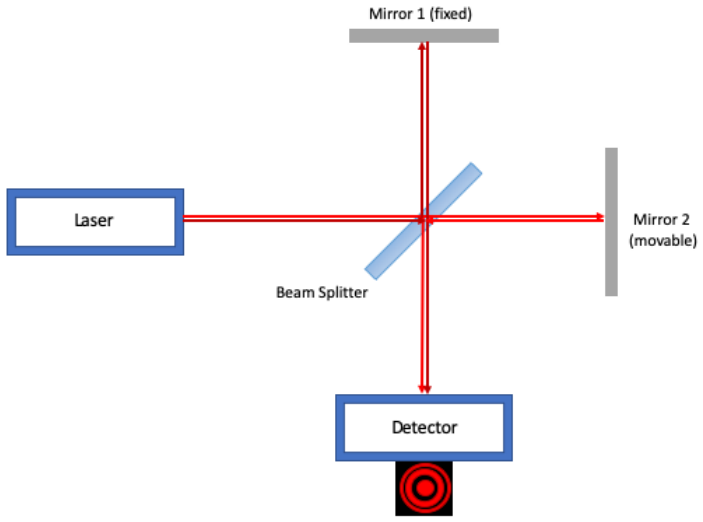

Figure 7. – Michelson interferometer. A laser light is shone and passes through a beam splitter. One beam travels to the sample (Mirror 1) and another to the reference arm (Mirror 2). Both light beams then travel to a photodetector. If they are detected simultaneously (ie. if the distance traveled by both beams is the same), an interference pattern forms.

By shining a polychromatic laser light into the eye, an image of its structures can be reconstructed based on their reflectivity and the detection of the reflected light's interference patterns.

Using dynamic video-rate OCT imaging, the first step of our method requires the measurement of the pulsatile ocular volume change, or volumetric changes of the eye due to choroidal filling. In other words, it detects the amount of blood pumped into the eye with each heartbeat. In each frame of the video, automated segmentation is carried out to measure choroidal thickness (CT). In the time-series, the change in CT associated with the cardiac cycle, or ΔCT, is measured. Considering that the choroid represents close to 90% of the total ocular blood flow, a simple mathematical model is used to extrapolate the pulsatile ocular volume change (ΔV) from ΔCT.

To capture the pulsatility of the choroid, OCT imaging is carried out at 8 Hz, corresponding to an averaging of 5 b-scans per frame, with an axial and lateral resolution of 3.9 µm and 11 µm respectively. Using the Spectralis Spectral-Domain OCT (Heidelberg Engineering GmbH, Heidelberg, Germany) and a custom software enabling video-rate imaging, a single 30° wide b-scan is acquired centered at the fovea. To optimize the visualization of the choroid-sclera interface (CSI), the azimuthal angle of the b-scan is chosen accordingly, and enhanced depth imaging (EDI) mode is used. Once acquisition starts, four hundred images are acquired per video in less than a minute. The heart rate is measured simultaneously using a finger oximeter.

In order to process all images, measure ΔCT, and ultimately compute OR, a fully automated algorithm was developed using Matlab (The MathWorks, Natick, MA). Preprocessing begins by trimming unwanted a-scans from the time-series, for example to remove a-scans near the optic disk where no choroid is present (Fig. 8A). Low quality images (Spectralis Quality metric <20) are excluded from the time-series. All remaining images are registered, or aligned to the first one, without further transformation. Segmentation of the retina-vitreous interface (RVI) and the anterior and posterior interfaces of the retinal pigmented epithelium (RPE) is carried out (Fig. 8B). The RVI is found using Canny Edge Detector. The RPE corresponds to the dark-to-bright transition below the retina, while Bruch's membrane (BM) corresponds to the steepest light-to-dark transition below the RPE. The b-scans are then flattened with respect to the RPE to facilitate CSI segmentation (Fig. 8C).

Precise detection of the CSI is based on graph search using an edge-probability weighting scheme. This numerical approach has been shown to be more robust in detecting the CSI compared with existing algorithms (27, 488). This strategy detects potential nodes and minimizes the path across the nodes based on weights assigned to each connection. Nodes are pixels that could potentially be a part of the CSI interface. They are located at regions of high local contrast. Nodes are found using the smoothed first and second gradient (derivative) of image intensity along each A-scan. Connections link the nodes to each other, based on horizontal and vertical distance thresholds. A depth of 585 µm, or 150 pixels, from the BM is also established to limit the location of the CSI (Fig. 9). In other words, graph search is similar to Google Maps, where nodes are the street corners and connections are the streets, and a combination of these determines the shortest and best path that will make up the choroidal boundary. In this way, the algorithm measures the BM-CSI distance, or CT, in each frame as well as ΔCT through the time-series (Fig. 10A).

To ensure that CT fluctuations in the time-series are due to the pulsatile blood flow, frequency components from the spectral analysis must coincide with the first and second harmonics of the heart rate frequency which is measured simultaneously using an oximeter. A frequency spectrum analysis is carried out. Similar to a Fourier transform, a Lomb-Scargle periodogram is used intead since the imaging is sampled unevenly due to the OCT's eye-tracker (Fig. 10B).

Once we measure the fluctuations in submacular CT associated with the heart rate, we use a simple spherical model of the eye to extrapolate ΔV from ΔCT. The choroid is modeled as the volume between two equal spheres shifted by ΔCT. The radius (R) of each sphere is set as half of the ocular axial length (AL), the distance between the anterior surface of the cornea and the RPE, measured using optical biometry (IOL Master 500, Carl Zeiss Meditec AG, Dublin, USA). In this model, the pulsatile ocular volume change is thus estimated as:

$$\Delta V = \pi R^2 \Delta CT .$$

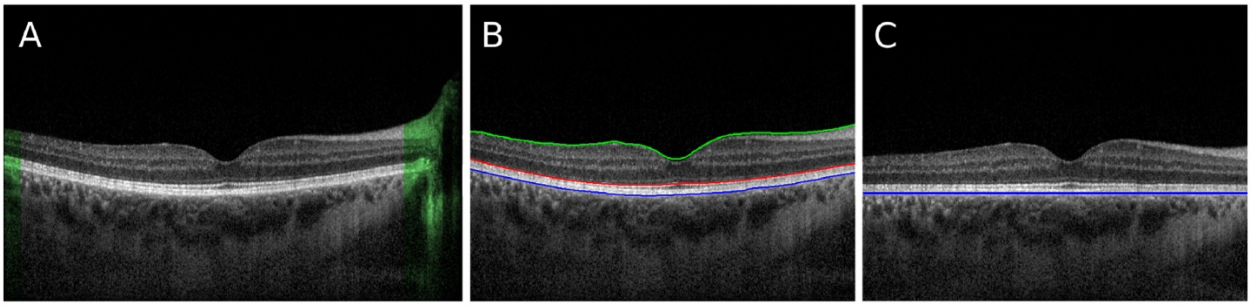

Figure 8. – Automated segmentation of retinal layers of interest from OCT images. The image in A is a typical frame from the video series. A) A-scans where the choroid is absent (highlighted in green) are discarded from all frames. B) Segmentation of the outmost layers of the retina: RVI is indicated in green, anterior RPE in red, and posterior RPE in blue. C) The A-scans are shifted so that the blue layer appears flattened. (Reprinted from Beaton et al. (27) with permission from The Optical Society.)

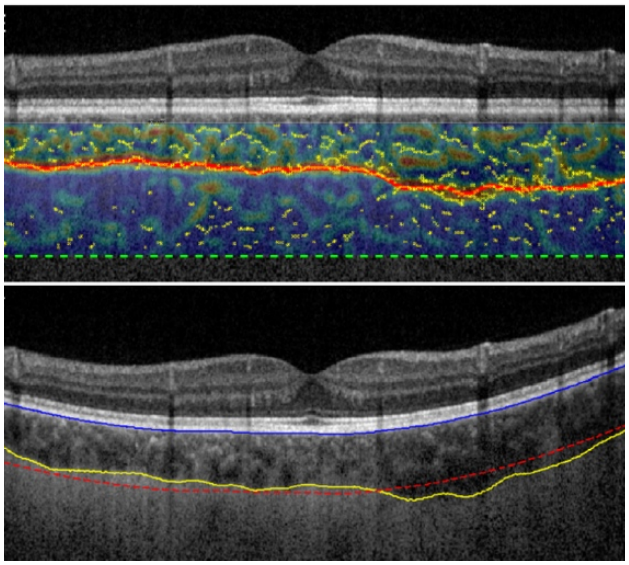

Figure 9. – Top) Heatmap showing pixels which are very likely to lie on a boundary, including node locations (yellow) and the CSI (red line). The b-scan is flattened and the green dashed line shows the limit of 585 µm below the Bruch's beyond which nodes are discarded. Bottom) The original b-scan overlaid with the RPE (blue), CSI (yellow) and the mean CT (red dotted line). (Reprinted from Beaton et al. (27) with permission from The Optical Society.)

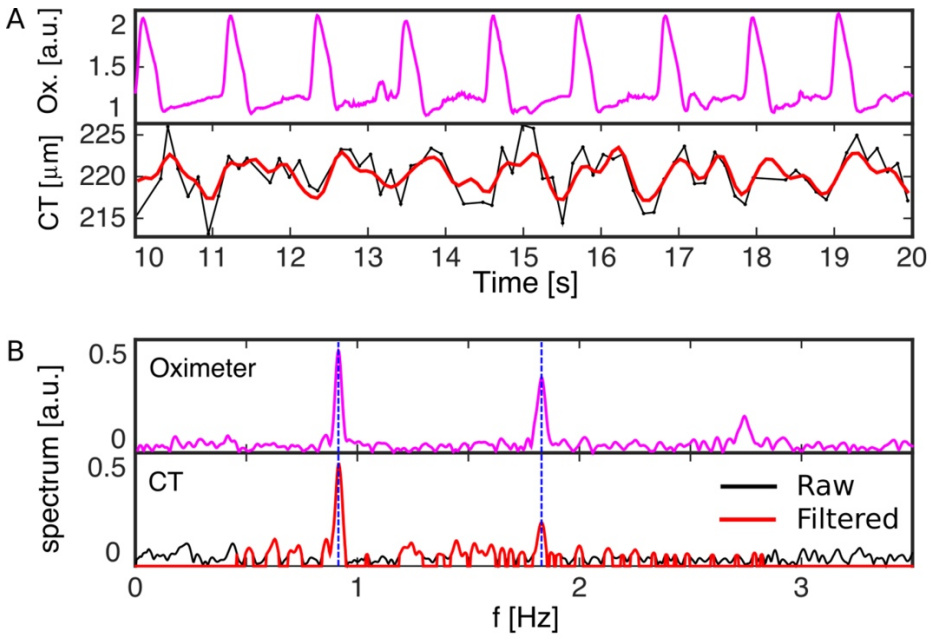

Figure 10. – A) Frequency spectrum analysis of CT fluctuations in time, showing the oximeter signal, raw fluctuations of CT versus time (black) and band-pass filtered CT signal (red). B) Frequency spectrum of the oximeter signal (top), and CT signal (bottom), where the offset component has been omitted. The filtered frequency band for the CT spectrum is shown in red. The dashed blue lines indicate the two first harmonics of the measured heart rate which are observed in both signals. (Reprinted from Beaton et al. (27) with permission from The Optical Society.)

3.2 Pulsatile Intraocular Pressure Change

The pulsatile IOP change can be obtained using the Pascal DCT (Ziemer Ophthalmic Systems AG, Port, Switzerland), a tonometer which is independent of the properties of the cornea (65, 489-491). The Pascal DCT provides two outputs: the diastolic IOP (492) and the ocular pulse amplitude (OPA). The OPA corresponds to the difference between the systolic and diastolic IOP. Only measurements with a quality index above 3 were considered. An alternative way to present the expression IOP/IOP_0 from the Friedenwald equation would be Systolic IOP/Diastolic IOP, where Systolic IOP = Diastolic IOP + OPA. Correspondingly, ΔV, or $V\text{-}V_0$, as measured using our algorithm is defined as the ocular volume change with the cardiac cycle. These volumetric and pressure

changes thus permit the calculation of the OR coefficient using Friedenwald's equation (26). We obtain a single value for the overall OR of the corneoscleral shell.

The possibility of using other methods such as pneumatonometry to measure the ocular pulse amplitude is not excluded. However, we speculate that the Pascal DCT may be more adequate to measure OPA and estimate OR due to less sensitivity to corneal biomechanical properties (65, 493).

Chapter 4 – Method Improvement, Validation and Repeatability Assessment

We have improved the method to measure OR using a more anatomically accurate mathematical model of choroidal thickness, and have also assessed the validity and repeatability of the method. This work titled “Non-invasive in vivo measurement of ocular rigidity: Clinical validation, repeatability and method improvement” has been published in 2019 in Experimental Eye Research (494).

This chapter presents the text as it was published. The authors are Diane N. Sayah, Javier Mazzaferri, Pierre Ghesquière, Renaud Duval, Flavio Rezende, Santiago Costantino and Mark R. Lesk.

Published Article

Experimental Eye Research 190 (2020) 107831

Contents lists available at ScienceDirect

Experimental Eye Research

journal homepage: www.elsevier.com/locate/yexer

Non-invasive *in vivo* measurement of ocular rigidity: Clinical validation, repeatability and method improvement

Diane N. Sayah[a,b], Javier Mazzaferri[a], Pierre Ghesquière[a], Renaud Duval[b,c], Flavio Rezende[b,c], Santiago Costantino[a,b,c,**], Mark R. Lesk[a,b,c,*]

[a] Centre de Recherche de l'Hôpital Maisonneuve-Rosemont, Montréal, Québec, H1T 2M4, Canada
[b] Département d'ophtalmologie, Faculté de Médecine, Université de Montréal, Montréal, Québec, H3T 1J4, Canada
[c] Centre Universitaire d'ophtalmologie de l'Université de Montréal de l'Hôpital Maisonneuve-Rosemont, CIUSSS-E, Montréal, Québec, H1T 2M4, Canada

ARTICLE INFO

Keywords:
Glaucoma
Open-angle glaucoma
Ocular rigidity
Ocular biomechanics
Clinical method
Choroid
Optical coherence tomography

ABSTRACT

Ocular rigidity (OR) is thought to play a role in the pathogenesis of glaucoma, but the lack of reliable non-invasive measurements has been a major technical challenge. We recently developed a clinical method using optical coherence tomography time-lapse imaging and automated choroidal segmentation to measure the pulsatile choroidal volume change (ΔV) and calculate OR using Friedenwald's equation. Here we assess the validity and repeatability of this non-invasive technique. We also propose an improved mathematical model of choroidal thickness to extrapolate ΔV from the pulsatile submacular choroidal thickness change more accurately. The new mathematical model uses anatomical data accounting for the choroid thickness near the equator. The validity of the technique was tested by comparing OR coefficients obtained using our non-invasive method (OR_{OCT}) and those obtained with an invasive procedure involving intravitreal injections of Bevacizumab (OR_{IVI}) in 12 eyes. Intrasession and intersession repeatability was assessed for 72 and 8 eyes respectively with two consecutive measurements of OR. Using the new mathematical model, we obtained OR values which are closer to those obtained using the invasive procedure and previously reported techniques. A regression line was calculated to predict the OR_{IVI} based on OR_{OCT}, such that $OR_{IVI} = 0.655 \times OR_{OCT}$. A strong correlation between OR_{OCT} and OR_{IVI} was found, with a Spearman coefficient of 0.853 ($p < 0.001$). The intraclass correlation coefficient for intrasession and intersession repeatability was 0.925, 95% CI [0.881, 0.953] and 0.950, 95% CI [0.763, 0.990] respectively. This confirms the validity and good repeatability of OR measurements using our non-invasive clinical method.

1. Introduction

The stiffness of the corneoscleral shell is an important biomechanical property of the eye and plays a key role in elucidating the pathophysiology of various ocular diseases, particularly open-angle glaucoma (Burgoyne et al., 2005; Downs et al., 2008; Fechtner and Weinreb, 1994; Sigal and Ethier, 2009; Sigal et al., 2005, 2009), age-related macular degeneration (Friedman, 1997; Friedman et al., 1989) and myopia (Burgoyne et al., 2005). Ocular rigidity (OR) has been shown to be altered in these diseases (Drance, 1960; Friedman et al., 1989; Pallikaris et al., 2006; Wang et al., 2013), and finite element modelling suggests that the stiffness of the sclera is the most influential factor on the optic nerve head's response to variations in intraocular pressure (IOP) in glaucoma (Sigal et al., 2005, 2009). However, its role in their pathogenesis remains to be fully understood and requires further investigation.

To achieve this, the ability to quantify OR in living human eyes using a reliable and non-invasive method is essential. Such a method has only recently become available (Beaton et al., 2015).

Historically, a comparison of Schiötz and Goldmann tonometry results in living eyes was considered a non-invasive but indirect method to measure OR. This technique was later considered inaccurate primarily due to the dependence of both indentation and applanation tonometry on the biomechanical properties of the eye (Gloster and

* Corresponding author. Hôpital Maisonneuve-Rosemont, Centre de soins ambulatoires, Rez-de-chaussée, F-117, 5415 Boul. de l'Assomption, Montréal, Québec, H1T 2M4, Canada.
** Corresponding author. Hôpital Maisonneuve-Rosemont, Centre de soins ambulatoires, Rez-de-chaussée, F-117, 5415 Boul. de l'Assomption, Montréal, Québec, H1T 2M4. Canada.

https://doi.org/10.1016/j.exer.2019.107831
Received 7 June 2019; Received in revised form 5 September 2019; Accepted 4 October 2019
Available online 10 October 2019
0014-4835/

Abbreviations

ACD	Anterior chamber depth
AL	Ocular axial length
AL_{adj}	Adjusted axial length
CI	Confidence interval
CSI	Choroid-sclera interface
CT	Choroidal thickness
D	Diopters
DCT	Dynamic Contour Tonometry
EDI	Enhanced depth imaging
ICC	Intraclass correlation coefficient
IOP	Intraocular pressure
I-T	Inferior-temporal
IVI	Intravitreal injection
LSO	Line-scanning ophthalmoscope
OCT	Optical coherence tomography
OPA	Ocular pulse amplitude
OR	Ocular rigidity
OR1	First measurement of ocular rigidity
OR2	Second measurement of ocular rigidity
OR_{IVI}	Ocular rigidity coefficients obtained using an invasive procedure involving intravitreal injections
OR_{OCT}	Ocular rigidity coefficients obtained using our non-invasive, OCT-based method
$OR_{OCT\text{-}new}$	OR_{OCT} values evaluated with the newly proposed mathematical model
$OR_{OCT\text{-}old}$	OR_{OCT} values evaluated with the old mathematical model
SD-OCT	Spectral domain optical coherence tomography
SE	Spherical equivalent
S-T	Superior-temporal
VEGF	Vascular endothelial growth factor
ΔCT	Pulsatile choroidal thickness change
ΔV	Pulsatile choroidal volume change

Perkins, 1957; Jackson, 1965; Moses and Grodzki, 1969; Perkins and Gloster, 1957). The most significant source of this variability in OR coefficients originates from the use of weights in Schiötz tonometry, which compress the ocular wall and displace a significant amount of intraocular fluid (Jackson, 1965; Moses and Grodzki, 1969), but also through the erroneous assumption that the OR of all eyes is standard in the applicability of the conversion table which provides the IOP reading in mmHg (Friedenwald, 1957; Grant, 1951; Jackson, 1965).

A recently developed non-invasive technique to measure OR, based on choroidal laser Doppler flowmetry gave only relative values because choroidal blood flow was measured in arbitrary units (Wang et al., 2013).

Anterior chamber manometry is the main technique used to directly calculate OR *in vivo* (Eisenlohr et al., 1962; Pallikaris et al., 2005; Ytteborg, 1960a, 1960b). It is done by injecting known volumes of fluid into the eye, measuring the resultant IOP changes, and estimating OR using the Friedenwald pressure-volume relationship (Friedenwald, 1937):

$$\ln \frac{IOP}{IOP_0} = K(V - V_0) \quad (1)$$

However this technique involves the intraoperative cannulation of the anterior chamber (Pallikaris et al., 2005). Its invasive nature limits the technique's applicability to consenting participants who require an intraocular surgical procedure, preventing the investigation of OR in a wider selection of subjects as well as follow-up measurements.

Our group has developed the first non-invasive and direct clinical method to measure OR in living human eyes (Beaton et al., 2015). The approach is based on video-rate Spectral Domain optical coherence tomography (OCT) and Pascal Dynamic Contour Tonometry (DCT). The novelty of the method consists mainly in its ability to measure the pulsatile ocular volume change directly from OCT videos. In other words, the amount of blood pumped into the eye with each heartbeat is detected through the automated segmentation of the choroid. The segmentation algorithm is based on graph theory using an edge-probability weighting scheme that enables the precise detection of the choroid's boundaries. The algorithm measures choroidal thickness (CT) in each frame, and also the pulsatile choroidal thickness change (ΔCT) throughout the time-series. This numerical approach is described in detail in our previous paper (Beaton et al., 2015) and was shown to be more robust in detecting the choroid-sclera interface (CSI) than other existing algorithms (Beaton et al., 2015; Mazzaferri et al., 2017). To ensure that CT fluctuations in the time-series are due to the pulsatile blood flow, frequency components from the spectral analysis must coincide with the first and second harmonics of the heart rate frequency which is measured simultaneously using an oximeter.

Considering that the choroid represents approximately 90% of the blood flow in the eye (Alm and Bill, 1973), we estimate the pulsatile ocular volume change (ΔV) from the measured ΔCT. More specifically, we measure the fluctuations in submacular CT associated with the heart rate and use the axial length and a mathematical two-spheres model of the eye to extrapolate the choroidal volume from choroidal thickness. The ocular pulse amplitude (OPA), corresponding to the change in IOP between the systole and diastole, is measured with a tonometer which is independent of the properties of the cornea (Andreanos et al., 2016; Mangouritsas et al., 2011; Ozcura et al., 2017). These volumetric and pressure changes thus permit the calculation of the OR coefficient using Friedenwald's equation (Friedenwald, 1937). We obtain a single value for the overall OR of the corneoscleral shell.

The purpose of this study is to assess the validity and repeatability of this non-invasive method. To do so, we also proposed a new and more anatomically accurate mathematical model of choroidal thickness to derive the pulsatile ocular volume change (ΔV) from the measured pulsatile choroidal thickness change (ΔCT). Comparison of OR coefficients with those obtained using an invasive procedure involving intravitreal injections was performed. Repeated measurements using the non-invasive method were compared.

2. Material and methods

This study followed the tenets of the Declaration of Helsinki and was approved by the Maisonneuve-Rosemont Hospital institutional review board. Informed consent was obtained from all participants prior to testing.

2.1. Validity assessment

2.1.1. Proposal of a new mathematical model of choroidal thickness

A two-sphere mathematical model was previously proposed by our group to derive the pulsatile ocular volume change (ΔV) from the submacular pulsatile change in choroidal thickness (ΔCT) corresponding to choroidal filling (Beaton et al., 2015). Since our OCT measurements are made over an 8 mm length under the macula, an extrapolation must be used to account for the entire choroid. In this model, ΔV was estimated as:

$$\Delta V = \pi R^2 \Delta CT \quad (2)$$

A first order approximation of a spherical eye model was used, in which the choroid was modeled as the volume between two spheres shifted by ΔCT. The radius (R) of each sphere was set as half of the axial length as measured using optical biometry. OR coefficients were ultimately computed using Friedenwald's ocular rigidity function

(Equation (1)), where $V - V_0$ is equal to ΔV, as obtained from video-rate choroidal imaging with enhanced depth imaging (EDI) mode (Spectralis SD-OCT, Heidelberg Engineering GmbH, Heidelberg, Germany) using automated segmentation, and where $\frac{IOP}{IOP_0}$ is equal to $\frac{Systolic\ IOP}{Diastolic\ IOP}$ or $\frac{IOP + OPA}{IOP}$ as measured using the Pascal DCT (Ziemer Ophthalmic Systems AG, Port, Switzerland). Of note, the IOP reading obtained using this tonometer corresponds to the diastolic IOP, whereas the OPA is the difference between the systolic and diastolic IOP (Ziemer Group Company, 2012).

While it is known that the choroid extends anteriorly until the ora serrata, this simple model did not account for the choroid in the periphery of the eye and underestimated choroidal filling by exhibiting a negligible (null) choroidal thickness change at the equator and beyond (see Fig. 1A).

The new mathematical model we hereby propose accounts for the equatorial choroid and its thickness change according to anatomical data provided both by the literature and our experiments as will be described below.

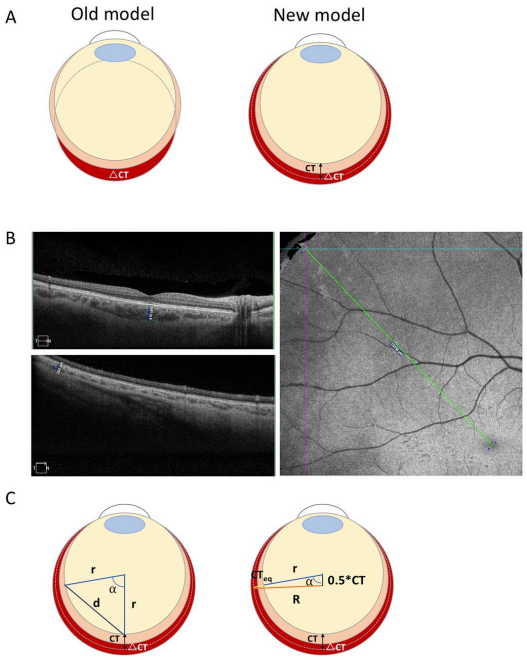

Fig. 1. A) Left: Original mathematical model used to extrapolate the pulsatile ocular volume change (ΔV). This model describes ΔV as two spheres with diameter equal to the axial length (AL), shifted by the pulsatile choroidal thickness change (ΔCT). Right: New mathematical model of choroidal thickness featuring a smaller sphere with diameter equal to AL_{adj} (corresponding to the measured AL, excluding the anterior chamber depth), fixed to a larger sphere with diameter of (AL_{adj} + CT) at the center of the pupil. The diameter of the larger sphere increases by ½ ΔCT at systole and decreases by the same amount at diastole, equivalent to a net expansion of ΔCT at each heartbeat. Note that figures are not to scale. B) B-scans acquired with the PLEX Elite 9000 OCT showing the measurement of the subfoveal CT (top-left) and of the equatorial CT (bottom-left) using the built-in caliper. To the right, an example of a superior-temporal fundus image is shown with the measured distance between the fovea and the location nearest the equator using the built-in caliper. C) Left: Mathematical model displaying the radius *r* of the small sphere, the distance *d* between the fovea and the closest location to the equator, and the angle *α* opposite to *d*. Right: Geometrical arrangement showing the same angle *α*, the radius *R* of the larger sphere, as well as $CT_{equator}$, the CT measurement to be solved to calculate the theoretical ratio ($CT_{equator}/CT_{subfovea}$).

The model now includes two spheres of different diameters overlapping each other at the center of the pupil (see Fig. 1A). The inner sphere spans anteriorly from the limbus to the submacular retinal pigmented epithelium. Since the anterior chamber depth (ACD) is not considered within the diameter of these spheres, an adjusted axial length (AL_{adj}) was considered. As the old model did not require ACD measurements, this parameter is not available for subjects in this study. For this reason, an average ACD-to-AL ratio was calculated from the literature in a similar population to be 13% (Foster et al., 2010; Jivrajka et al., 2008). Thus, in our model, AL_{adj} will be defined as 87% of the biometry measured AL. The radius *r* of the inner sphere is equal to half of the adjusted axial length. The outer sphere is larger, spanning from the limbus to the submacular choroid-sclera boundary. The thickness of the sclera is not accounted for in this model as it is not relevant in the extrapolation of the ΔV from ΔCT, and the subsequent computation of OR using Friedenwald's equation. The average radius *R* of the outer sphere accounts for half of the adjusted AL plus the average measured CT at the macula. We define ΔCT as the peak-to-peak amplitude of CT change between the diastole (minimum thickness) and systole (maximum thickness) as measured by our segmentation algorithm in the time-series (Beaton et al., 2015). This sphere's average diameter thus increases by ΔCT/2 at systole due to choroidal filling, and decreases by ΔCT/2 at diastole. The net movement of the larger sphere's diameter at each heartbeat is thus equal to ΔCT.

In this model, the pulsatile ocular volume change is represented by the following equation:

$$\Delta V = \left(\frac{4}{3}\pi\right)\left(R_{systole}^3 - R_{diastole}^3\right) \quad (3)$$

where $R_{systole} = \frac{(AL_{adj} + CT + \Delta CT/2)}{2}$ and $R_{diastole} = \frac{(AL_{adj} + CT - \Delta CT/2)}{2}$.

This equation was further simplified to first order, assuming ΔCT is relatively very small:

$$\Delta V \cong \frac{\pi}{2}(AL_{adj} + CT)^2 \Delta CT \quad (4)$$

Of note, equal OR coefficients were obtained using Equations (3) and (4). This last equation was used to derive the pulsatile ocular volume change from the pulsatile choroidal thickness change in our new mathematical model. OR coefficients were calculated using Friedenwald's equation.

2.1.2. Ratio of the choroidal thickness measurements near the equator and subfoveally

Choroidal imaging was performed using the PLEX Elite 9000 Swept Source OCT (Carl Zeiss Meditec, Dublin, CA). The montage feature was used to acquire scans at the macula, in the superior-temporal (S-T) and inferior-temporal (I-T) quadrants in six eyes of six participants (4M, 2F; 31 ± 9 years of age). Refractive error differed between participants: one was a hyperope (spherical equivalent (SE) +3.00 diopters(D)), two were myopes (SE -6.00 and -10.00 D) and three were emmetropes (SE plano). All participants were healthy and had negative ocular and systemic history.

Choroidal thickness measurements were carried out manually at three locations: subfoveally, as well as in the S-T and I-T quadrants, at ~13.2 mm from the fovea, as shown in Fig. 1B. This distance was chosen for practical reasons, as it is the furthest distance from the fovea, and nearest to the equator where both the line-scanning ophthalmoscope (LSO) fundus image and the choroid layer were visible in all participants.

The ratio between the thickness of the choroid near the equator and at the macula was calculated. This ratio was compared to the theoretical ratio computed from our new mathematical model of choroidal thickness.

To compute this ratio from the mathematical model, we assumed an

Table 1
Patients' characteristics at baseline.

Gender (Female/Male)		145/115
Age (years)[a]		68 ± 12
Ethnicity	African Descent	21
	Caucasian	231
	Other (Hispanic, Asian, …)	8
Ocular Conditions	Healthy	121
	Glaucoma	120
	Retinal disease (Exudative macular degeneration, venous occlusion, diabetic retinopathy, …)	19
Pascal DCT Intraocular Pressure (mmHg)[a]		18.3 ± 5.2
Ocular Pulse Amplitude (OPA) (mmHg)[a]		3.0 ± 1.3
Ocular Axial Length (mm)[a]		24.21 ± 1.35
Choroidal Thickness (CT) (μm)[a]		185 ± 58
Pulsatile CT Change (ΔCT) (μm)[a]		10.5 ± 5.4
Old Model – Pulsatile Ocular Volume Change (ΔV) (μL)[a]		4.8 ± 2.3
New Model – Pulsatile Ocular Volume Change (ΔV) (μL)[a]		7.3 ± 3.6
Old Model - Ocular Rigidity Coefficient (1/μL)[a]		0.0382 ± 0.0193
New Model – Ocular Rigidity Coefficient (1/μL)[a]		0.0248 ± 0.0125
Systemic Blood Pressure	Systolic (mmHg)[a]	135 ± 19
	Diastolic (mmHg)[a]	78 ± 9

[a] Data is presented as: mean ± standard deviation.

eye with dimensions (AL, CT and ΔCT) corresponding to the average measurements obtained from a database of 260 eyes, both healthy and diseased (115M, 145F; 68 ± 12 years of age) with OR measurements using our technique. Baseline characteristics of the subjects included in the database are presented in Table 1. These dimensions include an AL of 24.21 mm (AL_{adj} of 21.06 mm); a CT of 185 μm; and ΔCT of 10.5 μm. We solved for the choroidal thickness near the equator (at ~13.2 mm from the fovea) using geometry, and calculated the ratio using the average macular CT as measured using our custom automated segmentation algorithm (Fig. 1C).

To calculate CT at the equator (CT_{eq}), the following equation was derived, where α is defined in Fig. 1C:

$$CT_{eq} = \frac{1}{2}CT\cos\alpha + \sqrt{R^2 - \left(\frac{1}{2}CT\sin\alpha\right)^2} - r \quad (5)$$

Similar calculations were carried out to find the theoretical ΔCT near the equator as well according to:

$$\Delta CT_{eq} = \frac{1}{2}\Delta CT\left(\frac{R - \frac{1}{2}CT\,sin^2(\alpha)}{\sqrt{R^2 - \left(\frac{1}{2}CT\,sin\,\alpha\right)^2}} + cos\,\alpha\right) \quad (6)$$

The equator-to-macula ΔCT ratio was computed to allow adequate comparison between the old and new mathematical models.

2.1.3. Evaluation of ΔV and OR values using the new mathematical model

Comparison of ΔV and OR was carried out between the old values obtained using the two-spheres model described previously in Beaton et al. (2015) and the new values obtained using this more anatomically accurate mathematical model of choroidal thickness. The ratio between the old and new values was derived from Equations (2) and (4) to evaluate the effect of our more detailed model on these parameters.

2.1.4. Comparison of the non-invasive and invasive measurements of ocular rigidity

The optical technique we developed to measure OR non-invasively was compared to an invasive procedure in order to assess its validity. An in-office alternative approach to the anterior chamber manometry technique was adopted in our protocol to measure OR invasively. Twelve subjects who require intravitreal injections (IVIs) of Bevacizumab, an anti-vascular endothelial growth factor (VEGF) agent, as treatment for a pre-existing retinal condition were enrolled in our study.

Participants were required to have clear media, steady fixation, and the ability to fixate a target light with the study or contralateral eye. Patients with surgically treated glaucoma (trabeculectomy or tube shunt) were excluded because of the rapid outflow of aqueous.

The OR coefficient was measured in the affected eye using our OCT-based technique as previously described, followed by the invasive procedure, on the same day, rendering each subject its own control. The latter, which is also based on Friedenwald's ocular rigidity function, consists of the IVI of a known volume of fluid, 50 μL, in the affected eye and the measurement of the resulting IOP spike.

Immediately prior to asepsis and eyelid speculum placement but with the patient in the semi-supine position, the IOP was measured once in the test eye using the Tono-Pen XL (Reichert Technologies), a portable tonometer. Within 10–15 s of the injection (30-gauge needle) by the retina specialist following standard clinical procedures, with the patient still semi-supine, the speculum was removed and the IOP re-measured once again by the same examiner. The final averaged IOP measurement using the Tono-Pen XL was completed within 30 s following the IVI. Each IOP measurement obtained with this tonometer was an average of four valid IOP readings, and had a statistical reliability index of ≤5%.

The correlation between OR coefficients obtained for the same eye using both the OCT-based method and the invasive procedure was calculated with SPSS. This was done with the OR values obtained using the new mathematical model.

2.2. Repeatability assessment

To assess the intrasession repeatability of our novel method, seventy-two participants (35M, 37F; 66 ± 13 years of age) were recruited, and one eye was examined per participant.

Two consecutive measurements of OR were obtained and compared.

For fourteen participants, OR repeatability was assessed by carrying out all measurements twice on the examined eye within the same session, including video-rate OCT imaging as well as IOP measurements using the Pascal DCT and ocular axial length (AL) measurements using the IOL Master 500 (Carl Zeiss Meditec AG, Dublin, USA). For fifty-eight other participants, only video-rate OCT imaging using the Spectralis SD-OCT was carried out twice on the examined eye within the same session, and OR was computed. Each data set was then analyzed and OR measurements were calculated using the newly proposed mathematical model.

Intersession (between-visits) repeatability of our method was also assessed in eight participants (2M, 6F; 42 ± 16 years of age at initial visit). At two visits one week apart, IOP measurements, biometry and video-rate OCT imaging were carried out. Two OR measurements were thus obtained using the new mathematical model.

Repeatability was assessed by means of paired *t*-test, Bland-Altman plot and the intraclass correlation coefficient (ICC) based on an absolute agreement, 2-way mixed-effects model using SPSS (SPSS Inc, Chicago, IL).

3. Results

3.1. Validity assessment

3.1.1. New mathematical model of choroidal thickness

The new mathematical model is composed of one small and one larger sphere overlapping at the center of the pupil and accounts for the choroid, as illustrated in Fig. 1A. Considering the previously mentioned database of 260 subjects, this model yields values of ΔV which are 1.55 larger than the ones obtained with the previous model, and values of

OR which are 0.65 times smaller than the old ones. The average of newly calculated values of ΔV and OR is 7.3 ± 3.6 μL and 0.0248 ± 0.013 μL^{-1} respectively. Hence, the old model underestimated ΔV and overestimated OR values compared to the newly proposed one.

3.1.2. Ratio of the choroidal thickness measurements near the equator and subfoveally

The choroidal thickness was measured subfoveally, as well as in the S-T and I-T quadrants. Table 2 features the average CT measurements under the fovea and near the equator, along with the ratio of the CT near the equator over the macular CT in six participants. The equator-to-macula CT ratio from this experimental data is 49% for emmetropic eyes, and 50% for all eyes regardless of refractive error.

Theoretical and experimental data were also compared by solving for CT near the equator in the mathematical model, as shown in Fig. 1C. The equator-to-macula CT ratio was 60%, in the theoretical eye model. The theoretical equator-to-macula ΔCT ratio in the new model was also 60%, whereas it was 0% in the previous model. The higher value seems more realistic, but has not been tested experimentally for comparison, since the quality required for video-rate OCT imaging and precise ΔCT measurement is not adequate near the equatorial choroid despite extreme gaze positioning and stable fixation (as opposed to less challenging static images).

3.1.3. Comparison of the non-invasive and invasive measurements of ocular rigidity

Twelve subjects (7M, 5F; 66 ± 10 years of age) were included in the validity study. Medical indications for IVIs included branch retinal vein occlusions (n = 4), diabetic macular edema (n = 3), exudative age-related macular degeneration (n = 2), chronic central serous chorioretinopathy (n = 2) and idiopathic juxtapapillary choroidal neovascular membrane (n = 1). Initial mean IOP was 17 ± 5 mmHg and the mean IOP change following IVI was 20 ± 11 mmHg as measured using the Tono-Pen XL. Systolic and diastolic blood pressures were 148 ± 26 and 79 ± 10 mmHg respectively. The mean IOP and OPA measured using Pascal DCT tonometry were 20.3 ± 3.3 mmHg and 3.3 ± 0.7 mmHg respectively, whereas the mean axial length was 23.31 ± 0.80 mm and measured ΔCT was 12.8 ± 5.0 μm.

OR coefficients obtained for a same eye using our non-invasive imaging technique (OR_{OCT}) and the invasive procedure involving IVIs (OR_{IVI}) were compared. The Spearman correlation coefficient between OR_{IVI} and OR_{OCT} is 0.853 ($p < 0.001$). For a same eye, a strong correlation was thus obtained between the techniques, although the invasive procedure yielded smaller values of OR compared to the OR coefficients obtained non-invasively. A simple regression line was calculated to predict the OR_{IVI} based on OR_{OCT}. A significant regression equation was found using the new mathematical model, with an R^2 of 0.74. The equation of the line is $OR_{IVI} = 0.655 \times OR_{OCT}$, as shown in Fig. 2.

Average OR_{OCT} values were evaluated for the newly proposed mathematical model ($OR_{OCT\text{-}new}$), as well as for the previously used model ($OR_{OCT\text{-}old}$). As such, the average values of $OR_{OCT\text{-}new}$ and $OR_{OCT\text{-}old}$ are 0.022 ± 0.011/μL and 0.034 ± 0.018/μL respectively, whereas the average value of OR_{IVI} is 0.015 ± 0.007/μL, indicating that the fine-tuning of the mathematical model of choroidal thickness led to reduced OR value differences between the non-invasive optical technique and the invasive procedure.

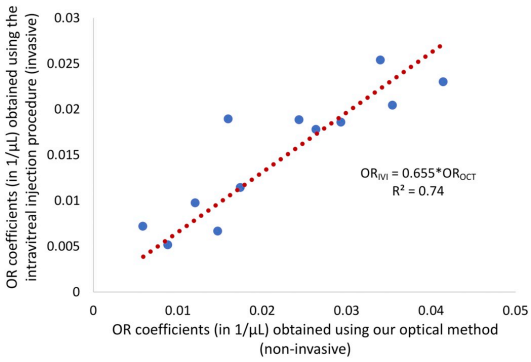

Fig. 2. Linear regression plot showing a strong positive correlation ($\rho = 0.853$, $p < 0.001$) between OR coefficients (in μL^{-1}) obtained non-invasively (OR_{OCT}) and invasively (OR_{IVI}) in 12 eyes from 12 subjects with pre-existing retinal conditions requiring an intravitreal injection (IVI) of Bevacizumab. A significant regression equation (dotted line) was found with an R^2 of 0.74. The equation of the regression line is $OR_{IVI} = 0.655 \times OR_{OCT}$. The OR_{OCT} coefficients were computed using the improved mathematical model proposed in this paper.

3.2. Repeatability assessment

Intrasession repeatability was assessed for seventy-two participants (35M, 37F; 66 ± 13 years of age), including 38 with healthy eyes, 33 with glaucomatous eyes and one with exudative AMD. Mean Pascal-IOP was 18.5 ± 3.7 mmHg, OPA was 3.0 ± 1.0 mmHg, AL was 24.47 ± 1.50 mm and systolic and diastolic blood pressures were 138 ± 23 and 79 ± 10 mmHg respectively.

Out of these 72 subjects, a first group (n = 14) underwent repeated OCT imaging, Pascal DCT and biometry twice in order to obtain two repeated OR values. In the second group (n = 58), only OCT video acquisitions were carried out twice to obtain repeated OR values. In both groups, no statistically significant difference was found among repeated OR measurements ($p > 0.05$).

For both groups, the Bland-Altman plot shows good agreement between the first (OR1) and the second (OR2) non-invasive OR measurements obtained in each examined eye (Fig. 3A and C) (Bland and Altman, 1986; Giavarina, 2015).

For the first group with all repeated measurements, the Pearson correlation coefficient between OR1 and OR2 was 0.887, demonstrating a strong direct correlation between both measurements, as can also be seen in the linear correlation plot of OR1 and OR2 in Fig. 3B. The single measures ICC for the repeated measurements of the OR coefficient was 0.891 with a 95 percent confidence interval (CI) of [0.694, 0.964], showing good test-retest reliability. The average measures ICC was 0.942 with a 95% CI of [0.820, 0.982], indicating excellent reliability.

Table 2
Experimental data featuring choroidal thickness (CT) measurements in μm at various locations (subfoveally, superior-temporal (S-T) quadrant and inferior-temporal (I-T) quadrant) as well as the average distance away from the fovea, in μm, where CT measurements were performed in 6 healthy eyes with various refractive errors. The ratio between CT near the equator and subfoveally is indicated in %.

	Average Subfoveal CT	Average S-T CT	Average I-T CT	Average distance to the fovea	Average ratio (%): equator/fovea
Emmetropes only (n = 3)	415.7	212.3	194.3	13172.8	48.9
All subjects (n = 6)	369.0	189.7	175.8	13201.3	49.5

All thickness and distance measurements are in micrometers.

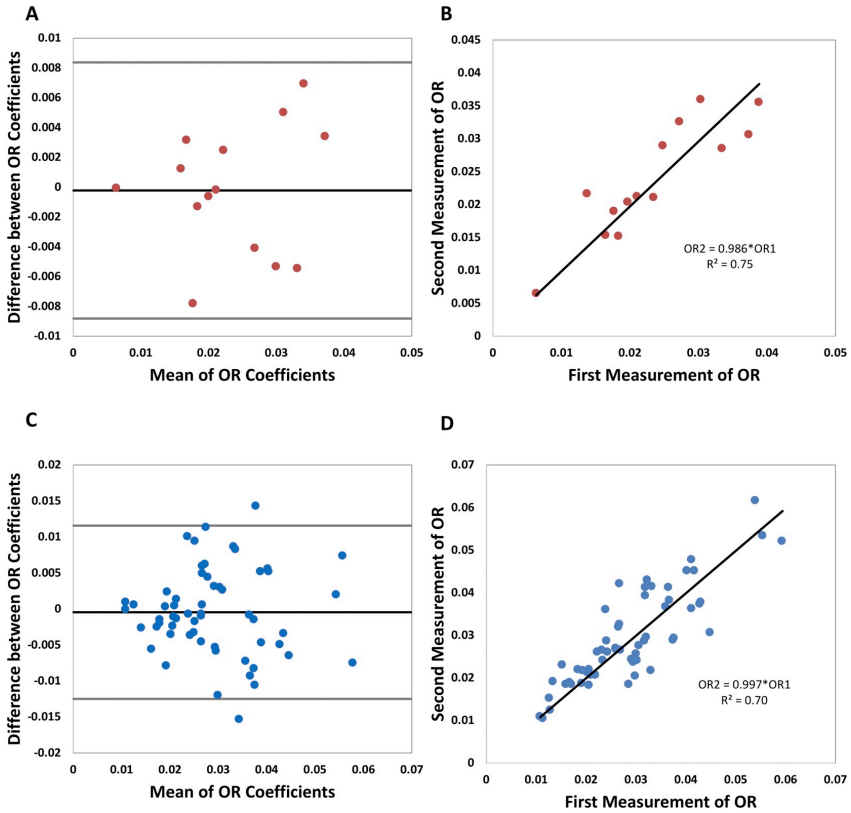

Fig. 3. Intrasession Repeatability. A) Bland-Altman plot showing agreement between two intrasession repeated measurements of ocular rigidity coefficients (in μL^{-1}) as measured using our novel method in 14 eyes from 14 subjects. Pascal DCT, biometry and OCT imaging were carried out twice. The horizontal axis represents the average of the two OR measurements ((OR1 + OR2)/2). The vertical axis represents the difference between the first and second OR coefficients measured (OR1 - OR2). The central horizontal black line corresponds to the mean of the difference. The upper and lower horizontal gray lines correspond to the upper and lower bounds of the 95% confidence interval of the difference between OR1 and OR2. B) Linear correlation plot showing a good correlation ($r = 0.887$, $p < 0.001$) between the first and second measurements of the ocular rigidity coefficient in these same 14 eyes using our non-invasive OR measurement method. C) Bland-Altman plot showing agreement between two repeated OR measurements in 58 eyes from 58 other subjects, where only OCT video acquisition was carried out twice. D) Linear correlation plot showing a good correlation ($r = 0.850$, $p < 0.001$) between OR1 and OR2 in these 58 eyes.

For the second group, the Pearson correlation coefficient between OR1 and OR2 was 0.850, also indicating a strong direct correlation between intra-session repeated OR measurements (Fig. 3D). The single measures ICC for the repeated measurements of the OR coefficient was 0.851 with a 95% CI of [0.761, 0.909]. Similarly, the average measures ICC was 0.920 with a 95% CI of [0.865, 0.952] for the second group, indicating excellent reliability.

When combining all 72 subjects, the Pearson correlation was 0.860 ($p < 0.001$), and the single and average measures ICC were 0.861, 95% CI [0.787, 0.911] and 0.925, 95% CI [0.881, 0.953] respectively. The repeatability parameters were thus comparable whether all measurements, including OCT, DCT and AL were repeated or whether only OCT measurements were repeated.

The OR coefficient of eight healthy eyes from 8 subjects (2M, 6F; 42 ± 16 years of age) was measured at two separate visits one week apart. Initial mean Pascal-IOP was 15.3 ± 1.2 mmHg, OPA was 2.5 ± 0.7 mmHg and AL was 24.25 ± 1.52 mm. At the second visit, mean Pascal-IOP was 15.5 ± 1.1 mmHg, OPA was 2.7 ± 1.0 mmHg and AL was 24.25 ± 1.52 mm. No statistically significant difference was found in any parameter among the two visits ($p > 0.05$).

The Bland-Altman plot showed good agreement between both OR measurements (Fig. 4A). The mean differences were small, as was the range of 95% confidence intervals. The Pearson correlation coefficient between OR1 and OR2 is 0.924 ($p = 0.001$), demonstrating a strong direct correlation between both measurements, as seen also in Fig. 4B. The single measures ICC for the repeated measurements of the OR coefficient was 0.905 with a 95 percent confidence interval (CI) of [0.617, 0.980], showing good test-retest reliability. The average measures ICC was 0.950 with a 95% CI of [0.763, 0.990], indicating excellent reliability.

4. Discussion

We have developed a non-invasive and direct clinical method to measure OR in living human eyes (Beaton et al., 2015). This technique is based on the measurements of the pulsatile ocular volume change from video-rate OCT imaging and automated choroidal segmentation, and the pulsatile IOP change using Pascal tonometry, to compute the OR coefficient using Friedenwald's equation.

In assessing the validity of our technique, we considered our

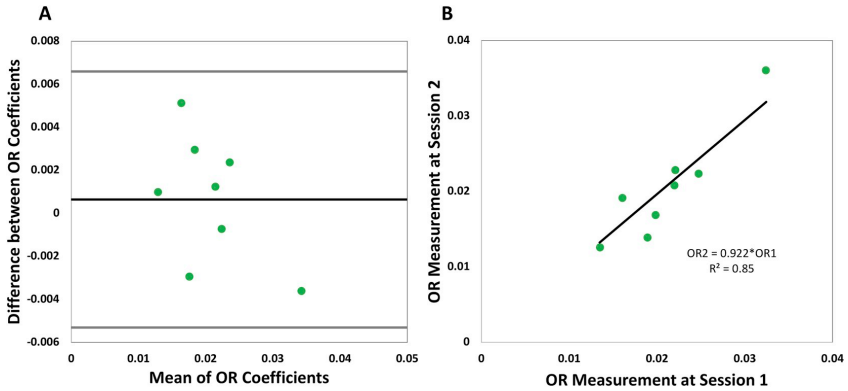

Fig. 4. Intersession Repeatability. A) Bland-Altman plot showing agreement between two intersession repeated measurements of ocular rigidity (in μL^{-1}) as measured using our non-invasive optical method. Measurement of OR was carried out in 8 eyes from 8 subjects at two visits, one week apart. The horizontal axis represents the average of the two OR measurements ((OR1 + OR2)/2). The vertical axis represents the difference between OR coefficients measured at the first and second visit (OR1 - OR2). The central horizontal black line corresponds to the mean of the difference. The upper and lower horizontal gray lines correspond to the upper and lower bounds of the 95% confidence interval of the difference between OR1 and OR2. B) Linear correlation plot showing a good correlation ($r = 0.924$, $p = 0.001$) between OR1 and OR2 in these 8 eyes.

previous model for extrapolating the pulsatile ocular volume change from the CT change under the macula to be oversimplified since it does not appropriately consider the peripheral shape of the choroid. The mathematical model we propose here accounts for anatomical characteristics of the choroid. Despite the significant improvements to the model, it considers the globe to be spherical and as such, should not be applied for eyes that present with a staphyloma or other shape irregularities. Furthermore, in future iterations, measurement of both AL and ACD will be performed in individual eyes instead of using a fixed ratio such as was done in this study.

To compare the new mathematical model with experimental data, we estimated the experimental ratio of equator/subfoveal CT to ~50% (Table 2). The calculated theoretical ratio was 60%, displaying a slight overestimation of the CT near the equator compared with our experimental data, but corresponding well with the range found in the literature (~48%–67%) (Kubota et al., 1993; Shen et al., 2016; Spraul et al., 2002). These values remain global estimations within a simple model and were not calculated for every individual eye according to axial length differences.

Compared to the previous mathematical model, the new OR values are 0.65 times lower and are thus closer to values obtained using invasive techniques, as shown in this paper and as previously reported in manometric studies. More precisely, mean OR values obtained with our improved method compared with manometric studies led in subjects within the same age group are 0.025/μL and about 0.022/μL respectively (Dastiridou et al., 2009, 2013a, 2013b; Panagiotoglou et al., 2015), rendering them similar although not identical.

Moreover, this model remains simple enough to be used in clinical settings as it requires easily measurable properties of the eye. To further facilitate this method's implementation in clinic, we do not exclude the possibility of using other methods such as pneumatonometry to measure the ocular pulse amplitude. However, we speculate that the Pascal DCT may be more adequate to measure OPA and estimate OR due to less sensitivity to corneal biomechanical properties (Boehm et al., 2008; De Moraes et al., 2008).

Of course, both the emergence of wide-field OCT and the ability to carry out video-rate imaging with a wider scan could provide useful information about the shape and thickness of the peripheral choroid and further improve the extrapolation of ΔV from the submacular CT change. While the model we propose provides significant improvements compared to the old model, the capacity to image and compute the actual ora to ora pulsatile CT change would be ideal. This is currently being explored by our group.

Additional evaluation of this technique's validity was carried out, including comparing it to an invasive procedure. While anterior chamber manometry has been used to measure OR by another group, intravitreal injections of Bevacizumab were a more practical comparator because there was no extra procedure or prolongation of a procedure involved. Furthermore, since each participant underwent both techniques to compare the obtained OR coefficients, the effect of ocular diseases and other parameters known to influence OR were controlled for in this study.

As our non-invasive technique yielded consistently higher values than OR values obtained invasively (although the new mathematical model significantly reduced this gap), the invasive procedure used in our study has potential limitations which one must acknowledge. These include lens status, the possibility of reflux following IVIs and inaccurate IOP spike measurement due to time constraints. The first could provide facilitated passage of the injected drug from the vitreal cavity to the anterior chamber, potentially influencing IOP measurement post-IVI. While 3 out of 12 eyes in this study were pseudophakic and 9 were phakic, larger scale studies have not shown significant differences in IOP spikes following IVI in phakic and pseudophakic eyes (Fuest et al., 2014; Lemos-Reis et al., 2014). The second would result in an overestimation of the injected volume of fluid, and consequently an underestimation of OR_{IVI}. The third considers the 20–30 s delay between the IVI and the completion of the post-IVI IOP measurement as a possibility to underestimate the IOP spike and, consequently, the OR coefficient. In other words, if simultaneous IOP measurement to the IVI was possible, the measured IOP spike would be larger, thus resulting in a higher OR_{IVI} value. We speculate that this value would be closer to OR_{OCT} obtained in the same eye using our optical method, and also closer to OR values obtained in manometric studies. Our results showed however that OR_{OCT} and OR_{IVI} are strongly correlated (Fig. 2), further confirming the validity of our non-invasive method for measuring OR *in vivo*. The validity of our technique is also substantiated by the good correlation previously observed between OR and axial length, as well as the correlation showing increased OR with age (Beaton et al., 2015; Sayah et al., 2016).

As invasive procedures are not suited for large scale studies, these results imply that our non-invasive optical method for measuring OR *in vivo* could be applied in clinical research to reliably estimate OR and

investigate its role in diseases of the eye.

To further validate our technique, we assessed its intrasession and between-visits repeatability in 72 and 8 subjects respectively. The Bland-Altman plot and the correlation coefficients showed good agreement and correlation respectively (Bland and Altman, 1999; Giavarina, 2015; Koo and Li, 2016). According to the guidelines provided by Koo and Li (2016), the ICC also demonstrated good to excellent test-retest reliability. This shows that *in vivo* OR measurements obtained within the same session and between two sessions using our non-invasive method are indeed repeatable. Clinically, the large range of OR values present in the general population (0.0044–0.0607/μL in our database of 260 subjects) should signify an ability to accurately discriminate rigid from compliant eyes.

A limitation of the intrasession repeatability study is the absence of repeated IOP and AL measurements in 58 eyes evaluated. This means that true intersession repeatability has been assessed on 14 eyes. However, despite the smaller number of eyes having repeated measurements of all parameters, good repeatability was obtained for both groups. Similarly, the evaluation of intersession repeatability has been carried out in a small number of eyes, however good repeatability was also found, confirming negligible change in OR between sessions in healthy eyes.

Recent technological advances in OCT could further improve the repeatability of our technique by improving the quality of the acquired images and thus the ability to detect the CSI. Swept-source OCT was introduced and is thought to provide better visualization of the choroid than SD-OCT, due to higher image acquisition speed and the use of a tunable laser with longer wavelengths which allows for enhanced penetration into ocular tissue (Copete et al., 2014; Lavinsky and Lavinsky, 2016). Studies have shown that increased light scattering in deeper tissues can hinder proper visualization of the CSI, particularly in a thicker choroid (Copete et al., 2014; Tan et al., 2015). This is minimized with swept-source OCT where CT could be measured in 100% of cases, and with greater accuracy, according to a comparative study by Copete et al. (2014).

Finally, implications for the development and validation of our non-invasive method are significant, as its application in research and clinics will help elucidate the role of OR in the pathogenesis of ocular diseases. We speculate that ultimately this method could become a new diagnostic tool for assessing and predicting the progression of glaucomatous optic neuropathy and other diseases.

Funding

This work was supported by the Canadian Institutes of Health Research (S.C. and M.R.L.), the Natural Sciences and Engineering Research Council of Canada (S.C.), the Fonds de Recherche en Ophtalmologie de l'Université de Montréal (M.R.L. and S.C.), the Fonds de Recherche du Québec - Santé (S.C. and D.N.S.) and the Glaucoma Research Society of Canada (M.R.L.).

References

Alm, A., Bill, A., 1973. Ocular and optic nerve blood flow at normal and increased intraocular pressures in monkeys (Macaca irus): a study with radioactively labelled microspheres including flow determinations in brain and some other tissues. Exp. Eye Res. 15, 15–29.

Andreanos, K., Koutsandrea, C., Papaconstantinou, D., Diagourtas, A., Kotoulas, A., Dimitrakas, P., Moschos, M.M., 2016. Comparison of Goldmann applanation tonometry and Pascal dynamic contour tonometry in relation to central corneal thickness and corneal curvature. Clin. Ophthalmol. 10, 2477–2484.

Beaton, L., Mazzaferri, J., Lalonde, F., Hidalgo-Aguirre, M., Descovich, D., Lesk, M.R., Costantino, S., 2015. Non-invasive measurement of choroidal volume change and ocular rigidity through automated segmentation of high-speed OCT imaging. Biomed. Opt. Express 6, 1694–1706.

Bland, J.M., Altman, D.G., 1986. Statistical methods for assessing agreement between two methods of clinical measurement. Lancet 1, 307–310.

Bland, J.M., Altman, D.G., 1999. Measuring agreement in method comparison studies. Stat. Methods Med. Res. 8, 135–160.

Boehm, A.G., Weber, A., Pillunat, L.E., Koch, R., Spoerl, E., 2008. Dynamic contour tonometry in comparison to intracameral IOP measurements. Invest. Opthalmol. Vis. Sci. 49, 2472–2477.

Burgoyne, C.F., Downs, J.C., Bellezza, A.J., Suh, J.K., Hart, R.T., 2005. The optic nerve head as a biomechanical structure: a new paradigm for understanding the role of IOP-related stress and strain in the pathophysiology of glaucomatous optic nerve head damage. Prog. Retin. Eye Res. 24, 39–73.

Copete, S., Flores-Moreno, I., Montero, J.A., Duker, J.S., Ruiz-Moreno, J.M., 2014. Direct comparison of spectral-domain and swept-source OCT in the measurement of choroidal thickness in normal eyes. Br. J. Ophthalmol. 98, 334–338.

Dastiridou, A.I., Ginis, H., Tsilimbaris, M., Karyotakis, N., Detorakis, E., Siganos, C., Cholevas, P., Tsironi, E.E., Pallikaris, I.G., 2013a. Ocular rigidity, ocular pulse amplitude, and pulsatile ocular blood flow: the effect of axial length. Invest. Opthalmol. Vis. Sci. 54, 2087–2092.

Dastiridou, A.I., Ginis, H.S., De Brouwere, D., Tsilimbaris, M.K., Pallikaris, I.G., 2009. Ocular rigidity, ocular pulse amplitude, and pulsatile ocular blood flow: the effect of intraocular pressure. Invest. Opthalmol. Vis. Sci. 50, 5718–5722.

Dastiridou, A.I., Tsironi, E.E., Tsilimbaris, M.K., Ginis, H., Karyotakis, N., Cholevas, P., Androudi, S., Pallikaris, I.G., 2013b. Ocular rigidity, outflow facility, ocular pulse amplitude, and pulsatile ocular blood flow in open-angle glaucoma: a manometric study. Invest. Opthalmol. Vis. Sci. 54, 4571–4577.

De Moraes, C., Prata, T., Liebmann, J., Ritch, R., 2008. Modalities of tonometry and their accuracy with respect to corneal thickness and irregularities. J. Opt. 1, 43–49.

Downs, J.C., Roberts, M.D., Burgoyne, C.F., 2008. Mechanical environment of the optic nerve head in glaucoma. Optom. Vis. Sci. 85, 425–435.

Drance, S.M., 1960. The coefficient of scleral rigidity in normal and glaucomatous eyes. Arch. Ophthalmol. 63, 668–674.

Eisenlohr, J.E., Langham, M.E., Maumenee, A.E., 1962. Manometric studies of the pressure-volume relationship in living and enucleated eyes of individual human subjects. Br. J. Ophthalmol. 46, 536–548.

Fechtner, R.D., Weinreb, R.N., 1994. Mechanisms of optic nerve damage in primary open angle glaucoma. Surv. Ophthalmol. 39, 23–42.

Foster, P.J., Broadway, D.C., Hayat, S., Luben, R., Dalzell, N., Bingham, S., Wareham, N.J., Khaw, K.T., 2010. Refractive error, axial length and anterior chamber depth of the eye in British adults: the EPIC-Norfolk Eye Study. Br. J. Ophthalmol. 94, 827–830.

Friedenwald, J.S., 1937. Contribution to the theory and practice of tonometry. Am. J. Ophthalmol. 20, 985–1024.

Friedenwald, J.S., 1957. Tonometer calibration; an attempt to remove discrepancies found in the 1954 calibration scale for Schiotz tonometers. Trans. Am. Acad. Ophthalmol. Otolaryngol. 61, 108–122.

Friedman, E., 1997. A hemodynamic model of the pathogenesis of age-related macular degeneration. Am. J. Ophthalmol. 124, 677–682.

Friedman, E., Ivry, M., Ebert, E., Glynn, R., Gragoudas, E., Seddon, J., 1989. Increased scleral rigidity and age-related macular degeneration. Ophthalmology 96, 104–108.

Fuest, M., Kotliar, K., Walter, P., Plange, N., 2014. Monitoring intraocular pressure changes after intravitreal Ranibizumab injection using rebound tonometry. Ophthalmic Physiol. Opt. 34, 438–444.

Giavarina, D., 2015. Understanding Bland Altman analysis. Biochem. Med. 25, 141–151.

Gloster, J., Perkins, E.S., 1957. Ocular rigidity and tonometry. Proc. R. Soc. Med. 50, 667–674.

Grant, W.M., 1951. Clinical measurements of aqueous outflow. Arch. Ophthalmol. 46, 113–131.

Jackson, C.R., 1965. Schiotz tonometers. An assessment of their usefulness. Br. J. Ophthalmol. 49, 478–484.

Jivrajka, R., Shammas, M.C., Boenzi, T., Swearingen, M., Shammas, H.J., 2008. Variability of axial length, anterior chamber depth, and lens thickness in the cataractous eye. J. Cataract Refract. Surg. 34, 289–294.

Koo, T.K., Li, M.Y., 2016. A guideline of selecting and reporting intraclass correlation coefficients for reliability research. J. Chiropr. Med. 15, 155–163.

Kubota, T., Jonas, J.B., Naumann, G.O., 1993. Decreased choroidal thickness in eyes with secondary angle closure glaucoma. An aetiological factor for deep retinal changes in glaucoma? Br. J. Ophthalmol. 77, 430–432.

Lavinsky, F., Lavinsky, D., 2016. Novel perspectives on swept-source optical coherence tomography. Int. J. Retin. Vitr. 2, 25.

Lemos-Reis, R., Moreira-Goncalves, N., Melo, A.B., Carneiro, A.M., Falcao-Reis, F.M., 2014. Immediate effect of intravitreal injection of bevacizumab on intraocular pressure. Clin. Ophthalmol. 8, 1383–1388.

Mangouritsas, G., Mourtzoukos, S., Mantzounis, A., Alexopoulos, L., 2011. Comparison of Goldmann and Pascal tonometry in relation to corneal hysteresis and central corneal thickness in nonglaucomatous eyes. Clin. Ophthalmol. 5, 1071–1077.

Mazzaferri, J., Beaton, L., Hounye, G., Sayah, D.N., Costantino, S., 2017. Open-source algorithm for automatic choroid segmentation of OCT volume reconstructions. Sci. Rep. 7, 42112.

Moses, R.A., Grodzki, W.J., 1969. Ocular rigidity in tonography. Doc. Ophthalmol. 26, 118–129.

Ozcura, F., Yildirim, N., Tambova, E., Sahin, A., 2017. Evaluation of Goldmann applanation tonometry, rebound tonometry and dynamic contour tonometry in keratoconus. J. Opt. 10, 117–122.

Pallikaris, I.G., Kymionis, G.D., Ginis, H.S., Kounis, G.A., Christodoulakis, E., Tsilimbaris, M.K., 2006. Ocular rigidity in patients with age-related macular degeneration. Am. J. Ophthalmol. 141, 611–615.

Pallikaris, I.G., Kymionis, G.D., Ginis, H.S., Kounis, G.A., Tsilimbaris, M.K., 2005. Ocular rigidity in living human eyes. Invest. Opthalmol. Vis. Sci. 46, 409–414.

Panagiotoglou, T., Tsilimbaris, M., Ginis, H., Karyotakis, N., Georgiou, V., Koutentakis, P., Pallikaris, I., 2015. Ocular rigidity and outflow facility in nonproliferative diabetic retinopathy. J. Diabetes Res. 2015, 141598.

Perkins, E.S., Gloster, J., 1957. Further studies on the distensibility of the eye. Br. J. Ophthalmol. 41, 475–486.
Sayah, D.N., Mazzaferri, J., Beaton, L., Lalonde, F., Hidalgo, M., Costantino, S., Lesk, M.R., 2016. Ocular rigidity: a novel non-invasive clinical method. Invest. Ophthalmol. Vis. Sci. 57 (12) ARVO E-Abstract 3551.
Shen, L., You, Q.S., Xu, X., Gao, F., Zhang, Z., Li, B., Jonas, J.B., 2016. Scleral and choroidal thickness in secondary high axial myopia. Retina 36, 1579–1585.
Sigal, I.A., Ethier, C.R., 2009. Biomechanics of the optic nerve head. Exp. Eye Res. 88, 799–807.
Sigal, I.A., Flanagan, J.G., Ethier, C.R., 2005. Factors influencing optic nerve head biomechanics. Invest. Opthalmol. Vis. Sci. 46, 4189–4199.
Sigal, I.A., Flanagan, J.G., Tertinegg, I., Ethier, C.R., 2009. Modeling individual-specific human optic nerve head biomechanics. Part II: influence of material properties. Biomechanics Model. Mechanobiol. 8, 99–109.
Spraul, C.W., Lang, G.E., Lang, G.K., Grossniklaus, H.E., 2002. Morphometric changes of the choriocapillaris and the choroidal vasculature in eyes with advanced glaucomatous changes. Vis. Resour. 42, 923–932.
Tan, C.S., Ngo, W.K., Cheong, K.X., 2015. Comparison of choroidal thicknesses using swept source and spectral domain optical coherence tomography in diseased and normal eyes. Br. J. Ophthalmol. 99, 354–358.
Wang, J., Freeman, E.E., Descovich, D., Harasymowycz, P.J., Kamdeu Fansi, A., Li, G., Lesk, M.R., 2013. Estimation of ocular rigidity in glaucoma using ocular pulse amplitude and pulsatile choroidal blood flow. Invest. Opthalmol. Vis. Sci. 54, 1706–1711.
Ytteborg, J., 1960a. The effect of intraocular pressure on rigidity coefficient in the human eye. Acta Ophthalmol. 38, 548–561.
Ytteborg, J., 1960b. Further investigations of factors influencing size of rigidity coefficient. Acta Ophthalmol. 38, 643–657.
Ziemer Group Company, 2012. Pascal Dynamic Contour Tonometry: User Manual. (Port, Switzerland).

Supplementary Findings

While the following data was not published along with the article presented in this chapter, it is interesting to include it here as food for thought.

Analysis of the data from the 260 subjects included in the previous study showed a relatively strong correlation between OR and ΔV as seen in Figure 11. The Spearman correlation coefficient was -0.764 ($p<0.001$).

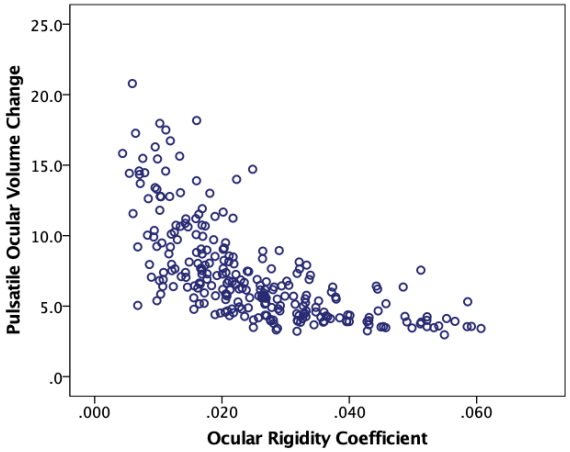

Figure 11. – Scatterplot showing the relationship between ocular rigidity and the pulsatile ocular volume change in 260 subjects.

The most obvious explanation for this strong inverse correlation could be the use of Friedenwald's equation to calculate OR from ΔV. However, one may also question whether OR could perhaps influence choroidal filling by exerting some resistance on the bolus of blood. This would mean that a more rigid eye would exert more resistance and therefore limit the amount of blood entering the choroid. This hypothesis could be consistent with pathological processes documented elsewhere in the body, where reduced blood flow was found with increased arterial stiffness (495, 496). However, this remains to be verified. Furthermore, the potential effects of central hemodynamics changes on ΔV will need to be investigated.

Chapter 5 – Lower Ocular Rigidity is Associated with Glaucomatous Neuro-Retinal Damage

In an effort to better understand the link between OR and glaucoma, we investigated the association between OR and quantitative parameters of neuro-retinal damage. This work titled "Ocular Rigidity as a Risk Factor for Neuro-Retinal Damage in Glaucoma" has been submitted to a peer-reviewed journal.

The authors of this work are Diane N. Sayah, Javier Mazzaferri, Denise Descovich, Santiago Costantino and Mark R. Lesk.

Abstract

Purpose: Ocular rigidity (OR) is an important biomechanical property, thought to be relevant to the pathophysiology of open-angle glaucoma (OAG). This study aims to evaluate the relationship between OR and neuro-retinal damage caused by glaucoma.

Methods: One hundred eighteen eyes from 118 subjects (25 with healthy eyes, 26 with suspect discs and 67 with OAG) were included in this study. OR was measured using a non-invasive clinical method developed by our group. We also measured central corneal thickness (CCT), corneal hysteresis (CH) and corneal resistance factor (CRF). Pearson and partial correlations were performed to evaluate the relationship between OR and glaucomatous damage represented by ganglion cell complex (GCC) and retinal nerve fiber layer (RNFL) thicknesses.

Results: Significant positive correlations were found between OR and minimum GCC thickness (r=0.304, p=0.002), average GCC thickness (r=0.285, p=0.004 respectively), rim area (r=0.287, p=0.002), and RNFL thickness in the inferior quadrant (r=0.255, p=0.007). After adjusting for age, sex and ethnicity, significant correlations were found between OR and minimum and average GCC thickness (r=0.322, p=0.001 and r=0.298, p=0.003 respectively), rim area (r=0.257, p=0.007), average RNFL thickness (r=0.278, p=0.003) and RNFL thickness in the inferior (r=0.287, p=0.002) and superior (r=0.239, p=0.012) quadrants.

Conclusion: In this study, we found a positive correlation between structural OCT-based parameters and OR, perhaps indicating more neuro-retinal damage in less rigid eyes. These findings could provide insight into the pathophysiology of OAG.

Introduction

Glaucoma is the leading cause of irreversible blindness in the world, resulting in damage to the retinal ganglion cells (RGC) that form the optic nerve, and in visual field loss. Elevated intraocular pressure (IOP) was traditionally associated with the pathogenesis of open-angle glaucoma (OAG), the main form of glaucoma. Evidence has since shown that factors other than IOP must underlie the susceptibility of the optic nerve head (ONH) to glaucomatous injury. This is corroborated by the occurrence of OAG with IOP in the normal range, and the absence of OAG in most patients with elevated IOP (5). Recent biomechanical modelling has suggested that scleral stiffness, the main contributor to ocular rigidity (OR), is the greatest factor to influence strain (deformation) at the optic nerve head in glaucoma, perhaps more so than IOP. A more compliant sclera would lead to increased ONH strain levels (16, 397) and more neuronal damage.

Over the last eighty years, the role of OR in the pathophysiology of glaucoma has been studied (17, 26). Despite this, the association between OR and glaucoma is not well established, and competing hypotheses are highly debated. On one side, OR is thought to be higher in glaucomatous eyes, producing higher IOP fluctuations due to rigid ocular walls, and hence more deformation at the ONH and lamina cribrosa levels. Inflation studies in cadaver eyes, and *in vivo* studies using indirect measurements showed higher OR in eyes with established glaucoma (17, 19-21). On the other side, OR is thought to be lower in early glaucoma, leading to axonal stretching and damage. According to this theory, increased OR would occur at later stages of the disease. Studies have reported low OR in OAG (17, 18, 23), and highest OR in ocular hypertensives with no glaucomatous damage (23). However, another study using intraoperative cannulation showed no difference in OR between diseased and healthy eyes (22). A plethora of challenges and confounding factors have made this question difficult to resolve (25), including the ability to quantify OR in living human eyes using a reliable, direct and non-invasive method. Such a method has only recently become available (27, 494). It estimates the OR coefficient using Friedenwald's

equation (26), where the pulsatile ocular volume change is measured from video-rate OCT imaging coupled with automated choroidal segmentation, and the pulsatile IOP change is measured using Pascal dynamic contour tonometry.

To test the hypothesis that low OR is a risk factor for glaucomatous damage, this study will evaluate the relationship between OR and glaucomatous structural damage such as the ganglion cell complex (GCC) and retinal nerve fiber layer (RNFL) thicknesses.

Methods

This study followed the tenets of the Declaration of Helsinki and was approved by the Maisonneuve-Rosemont Hospital institutional review board. Informed consent was obtained from all participants prior to testing.

Adult subjects with healthy eyes, suspect discs or primary open-angle glaucoma were recruited in this study. A complete ocular examination was performed for all participants. Normal subjects had intraocular pressure (IOP) less than 21 mmHg, normal optic nerve appearance on fundus exam, normal visual fields and no other ocular disease. Subjects with suspect discs had increased cup-to-disc ratio or asymmetry of optic nerve appearance, with no detectable functional or structural damage. IOP in this group could be within normal range or elevated, and if there was a history of elevated IOP, could be treated with topical IOP-lowering agents. Subjects with OAG had open (non-occludable) angles on gonioscopy, a glaucomatous optic nerve appearance, as well as repeatable structural and/or functional findings with optical coherence tomography (OCT) imaging and Humphrey visual field (VF; Zeiss Humphrey Systems, Dublin, California, USA) testing (SITA standard threshold 24–2 strategy). According to this definition, pre-perimetric glaucoma patients were also included in the glaucoma group. Participants were required to have clear media, steady fixation, and the ability to fixate a target light with the study or contralateral eye. Patients with a previous history of intraocular surgery (except cataract extraction) including trabeculectomy, tube shunt, and refractive surgery were excluded. Other exclusion criteria included secondary glaucoma, non-glaucomatous optic neuropathy, any retinopathy, and documented systemic collagen disease.

Ocular rigidity (OR) was measured using a non-invasive method involving video-rate OCT imaging and Pascal dynamic contour tonometry (DCT) (27, 494). This method is based on Friedenwald's equation (419, 494), which permits the ocular rigidity coefficient to be estimated as the following pressure-volume relationship:

$$ln\frac{IOP}{IOP_0} = OR \times (V - V_0).$$

The OR coefficient thus obtained is a single value for the overall OR of the corneoscleral shell.

Through dynamic OCT imaging (Spectralis SD-OCT, Heidelberg Engineering GmbH, Heidelberg, Germany) with enhanced depth imaging (EDI) coupled with automated choroidal segmentation, we obtain a direct measurement of the volume of blood pumped into the choroid with each heartbeat – the pulsatile ocular volume change (ΔV, or $V - V_0$). The method is described in detail in our previous papers (27, 494). Briefly, the choroidal segmentation algorithm is based on graph theory using an edge-probability weighting scheme that enables the precise detection of the choroid's boundaries, and has been shown to be more robust in detecting the choroid-sclera interface compared with existing algorithms (27, 488). It measures the choroidal thickness change (ΔCT) associated with the cardiac cycle through the time-series. To ensure that CT fluctuations in the time-series are due to the pulsatile blood flow, high frequency components from the spectral analysis must coincide with the first and second harmonics of the heart rate frequency which was measured simultaneously using an oximeter.

Since the choroid represents approximately 90% of the blood flow in the eye (82), ΔV can be estimated from the measured ΔCT. The ΔV is calculated according to the following equation : $\Delta V = (\pi/2)(AL_{adj} + CT)^2 \, \Delta CT$, where AL_{adj} is the ocular axial length (AL) measured using the IOL Master 500 (Carl Zeiss Meditec AG, Dublin, USA) and adjusted for the anterior chamber depth (ACD) (494). The pulsatile pressure change was measured using the Pascal DCT (Ziemer Ophthalmic Systems AG, Port, Switzerland). This tonometer provides an IOP reading corresponding to the diastolic IOP, as well as the ocular pulse amplitude (OPA) which is the change in IOP between the systole and diastole. This non-invasive methodology has been previously validated and was also shown to have good repeatability (494).

Structural OCT-based parameters such as ganglion cell complex (GCC) and retinal nerve fiber layer (RNFL) thicknesses were acquired using the Cirrus 5000 OCT (Carl Zeiss Meditec AG, Dublin, USA). These parameters characterize and quantify the retinal layers that contain neuronal structures that form the optic nerve. The GCC corresponds to the ganglion cell layer and inner plexiform layer thicknesses combined. These structural parameters can be presented as average, minimum and sectoral thicknesses. The neuro-retinal rim area, average and minimum GCC thicknesses, average RNFL thickness and RNFL thickness in the superior, temporal and inferior quadrants were considered.

Additional measurements were acquired including IOP by Goldmann applanation (GAT-IOP), central corneal thickness (CCT) using optical pachymetry, corneal hysteresis (CH) and corneal resistance factor (CRF) using the Ocular Response Analyzer (ORA; Reichert Technologies, Depew, NY). Maximum historic IOP (Tmax) and glaucoma medications were also recorded for each participant.

Statistical analyses were performed using SPSS statistical software (version 23; SPSS, Inc., Chicago, IL). Descriptive statistical analysis of baseline demographics was carried out and presented as the mean ± standard deviation. Pearson correlations between OR and neuro-retinal damage in all eyes were assessed. Correlation coefficients were compared between OR and known risk factors such as CCT, CH, CRF and Tmax. Partial correlations were also calculated to adjust for potential covariates. For all statistical tests, a p-value inferior to 0.05 was considered significant.

Results

One hundred eighteen subjects (25 with healthy eyes, 26 with suspect discs and 67 with early to advanced OAG) were recruited. One eye per subject was included in the study; 64 (54%) were right eyes. Of the 118 participants, 57 (48%) were male, 100 (85%) were Caucasian, 11 (9%) were from African origins, 4 (3%) were Hispanic and 3 (3%) were from another ethnic origin. A description of their baseline characteristics is presented in Table 1. In the OAG group the average visual field mean defect (MD) was -3.85 ± 5.01 dB. Comparison of OR with other known risk factors for glaucoma, namely CCT, CH, CRF and Tmax, and their correlation with glaucomatous damage is shown in Table 2. Significant positive correlations were found between OR and the minimum

and average GCC thicknesses (r=0.304, p=0.002 and r=0.285, p=0.004 respectively). Direct correlations were also found between OR and rim area (r=0.287, p=0.002), as well as OR and the RNFL thickness in the inferior quadrant (r=0.255, p=0.007). These correlations were generally greater than those found for CH, CRF and CCT, albeit usually lower than those found for Tmax. To illustrate the association between OR and some of these parameters, Figure 12 displays the scatter plots for OR and the rim area, the minimum GCC thickness, the average RNFL thickness, and the RNFL thickness in the inferior quadrant. After adjusting for age, sex and ethnicity, Pearson correlation coefficients between OR and each OCT-based parameter are shown in Table 3. Rim area was also adjusted for disc area. Significant correlations were found between OR and minimum and average GCC thickness (r=0.322, p=0.001 and r=0.298, p=0.003 respectively), rim area (r=0.257, p=0.007), average RNFL thickness (r=0.278, p=0.003) and RNFL thickness in the inferior (r=0.287, p=0.002) and superior (r=0.239, p=0.012) quadrants.

Age (years)	65 ± 11
Axial length (mm)	24.43 ± 1.41
GAT-IOP (mmHg)	17 ± 5
DCT-IOP (mmHg)	18.8 ± 4.0
Ocular Pulse Amplitude (mmHg)	3.1 ± 1.2
Tmax (mmHg)	22 ± 6
Central Corneal Thickness (µm)	536 ± 41
Corneal Hysteresis (mmHg)	9.0 ± 2.0
Corneal Resistance Factor (mmHg)	9.6 ± 1.9
Ocular Rigidity (μL^{-1})	0.0254 ± 0.0127
Rim area (mm^2)	1.01 ± 0.28
Minimum GCC Thickness (µm)	68 ± 11
Average GCC Thickness (µm)	72 ± 8
Average RNFL Thickness (µm)	79 ± 12
Superior Quadrant RNFL Thickness (µm)	96 ± 18
Temporal Quadrant RNFL Thickness (µm)	58 ± 13
Inferior Quadrant RNFL Thickness (µm)	99 ± 20

Data is presented as the mean ± standard deviation. GAT-IOP = IOP measured by Goldmann applanation tonometry; DCT-IOP = IOP measured using Pascal dynamic contour tonometry; OPA = Ocular pulse amplitude; Tmax = Maximum IOP; GCC = Ganglion cell complex; RNFL = Retinal nerve fiber layer.

Table 1. – Baseline characteristics of participants.

	Ocular Rigidity	Central Corneal Thickness (CCT)	Corneal Hysteresis (CH)	Corneal Resistance Factor (CRF)	Intraocular Pressure (Tmax)
Rim area	**0.287 (0.002)**	**0.208 (0.034)**	**0.312 (0.002)**	**0.245 (0.014)**	**-0.257 (0.012)**
Minimum GCC Thickness	**0.304 (0.002)**	0.133 (0.212)	**0.271 (0.012)**	0.168 (0.124)	**-0.505 (<0.001)**
Average GCC Thickness	**0.285 (0.004)**	0.141 (0.185)	0.179 (0.101)	0.069 (0.531)	**-0.392 (<0.001)**
Average RNFL Thickness	**0.220 (0.017)**	**0.200 (0.039)**	0.182 (0.066)	0.154 (0.120)	**-0.389 (<0.001)**
Superior Quadrant RNFL Thickness	0.177 (0.062)	0.071 (0.469)	0.089 (0.385)	0.000 (0.999)	**-0.308 (0.003)**
Temporal Quadrant RNFL Thickness	0.041 (0.668)	**0.243 (0.014)**	0.148 (0.148)	**0.204 (0.046)**	**-0.226 (0.029)**
Inferior Quadrant RNFL Thickness	**0.255 (0.007)**	0.115 (0.250)	**0.204 (0.045)**	0.133 (0.193)	**-0.470 (<0.001)**

Table 2. – Comparison of the association between parameters of structural damage in glaucoma and ocular rigidity, as well as with other known risk factors. Pearson correlation coefficients and significance values are shown (in bold, if $p < 0.05$).

	Correlation with Ocular Rigidity
Rim Area	**0.257 (0.007)**
Minimum GCC Thickness	**0.322 (0.001)**
Average GCC Thickness	**0.298 (0.003)**
Average RNFL Thickness	**0.278 (0.003)**
Superior Quadrant RNFL Thickness	**0.239 (0.012)**
Temporal Quadrant RNFL Thickness	0.045 (0.642)
Inferior Quadrant RNFL Thickness	**0.287 (0.002)**

Table 3. – Partial correlation between ocular rigidity, rim area, GCC and RNFL thicknesses in the superior, temporal and inferior quadrants. Pearson correlation coefficients adjusted for age, sex and ethnicity (and disc area for the correlation with the rim area) and significance values are shown (in bold, if $p < 0.05$).

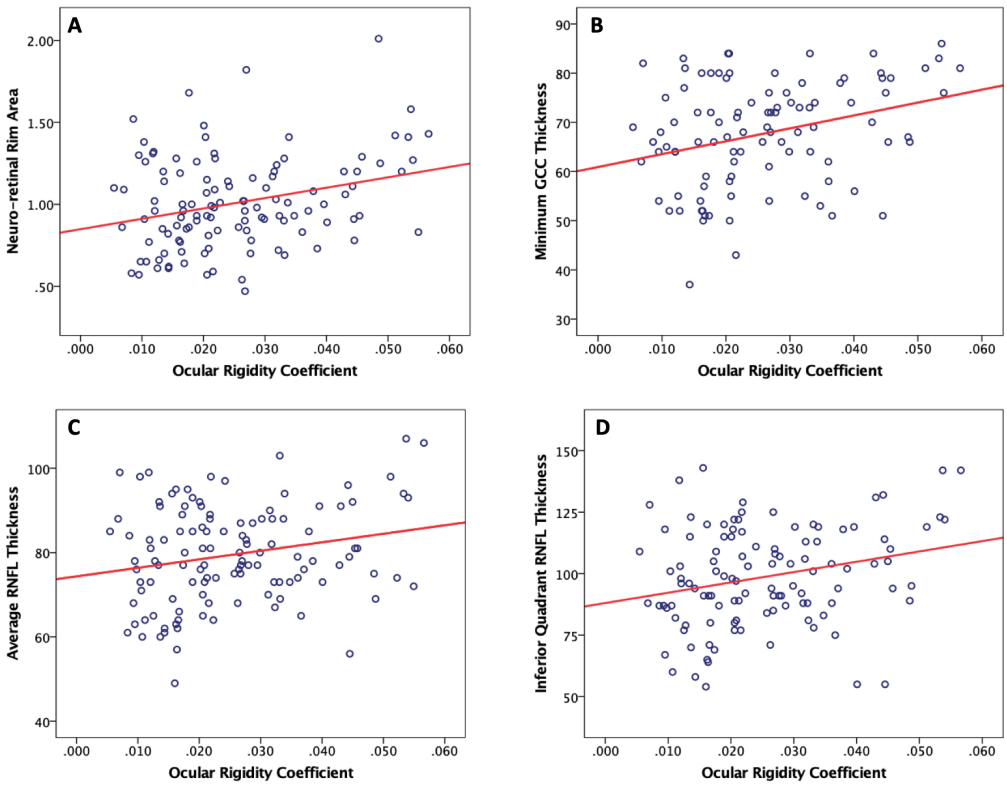

Figure 12. – Scatter plots showing significant correlations between ocular rigidity coefficients and the A) neuro-retinal rim area (r=0.287, p=0.002; Rim Area=0.85+6.33*OR); B) minimum ganglion cell complex (GCC) thickness (r=0.304, p=0.002; GCC=60.92+262*OR); C) average retinal nerve fiber layer (RNFL) thickness (r=0.220, p=0.017; Average RNFL=74.36+202*OR); D) RNFL thickness in the inferior quadrant (r=0.255, p=0.007; Inferior Quadrant RNFL=88.05+420*OR).

Discussion

In this study, we found modest but positive correlations between OR and structural OCT-based parameters. This suggests that neuro-retinal damage due to glaucoma, reflected by a thinner GCC or RNFL, is associated with less rigid eyes.

The strength of the correlations obtained with OR are comparable to or greater than the ones obtained with CCT, CH and CRF, parameters that have been extensively investigated and are

recognized as important risk factors for the development and progression of glaucoma (5, 345, 346, 371-375). Various studies have found associations between these parameters and optic nerve parameters including rim area (349, 350, 366, 372, 497-500). However, limited evidence of a relationship between corneal biomechanical parameters and RNFL has been shown (380, 381, 501). Since elevated IOP leads to glaucomatous damage, an inverse correlation exists between Tmax and the thickness of the structural parameters whereas a direct correlation is found with CCT, CH and CRF, since their values are lower in glaucomatous eyes compared to controls (365-368). Subjective assessment of our correlations suggests better correlations between OR and OCT parameters than between CCT, CH or CRF and the same parameters, although we did not test this statistically. These findings imply that OR is an important risk factor for glaucoma, at least as important as these widely-recognized corneal biomechanical parameters.

In our study population, which includes healthy eyes and others over the glaucoma spectrum, there was a correlation between Rim Area and OR that was similar to that obtained with Tmax. This could be further verified by assessing the strength of correlations between OR and Bruch's membrane opening-minimum rim width (BMO-MRW) in future studies, as this parameter was found to have improved diagnostic capacity for early glaucoma (502). However, correlations with GCC and RNFL parameters were lower (although often significant) for OR than for Tmax. These parameters are usually considered to be affected earlier in glaucoma than rim area. Further studies will be required to confirm and clarify the cause of this observation.

Unlike the recorded Tmax, which is most commonly the initial untreated IOP, OR evolves over the course of the disease, and this evolution may impact the strength of our correlations. If low OR contributes to the initiation of glaucomatous damage but subsequently the sclera becomes more rigid during the course of the disease and with aging (17, 21, 23, 26, 351, 428), correlations would be hard to observe except in the earliest glaucoma patients. In this study we attempted to include only relatively early glaucoma patients as evidenced by the OCT parameters shown in Table 1, but in general we recruited few patients (n=9) with visual field mean defect worse than -6dB. Since approximately half of the ONH axons are damaged before the standard visual field is affected, it is possible that stronger correlations between OCT parameters and OR would have been found if recruitment in the glaucoma group had been limited to patients with even earlier damage.

Comparatively, Tmax may reflect the highest stress imposed on the ONH during the disease history at a given period prior to treatment (14) . It often does not change during the course of the disease but if it does it is because it *increases*, further strengthening correlations as the disease progresses.

To our knowledge, this study shows, for the first time, that across the spectrum of glaucoma the rigidity of the corneo-scleral shell is correlated with OCT-based parameters that quantify neuro-retinal damage. More specifically, a more compliant eye is found to be associated with thinner GCC, RNFL, and neuroretinal rim. We could speculate that this association may be due to increased deformation (strain) of the load-bearing tissues of the ONH and peripapillary retina in eyes with lower OR. This deformation would occur with pulsatile, diurnal, or episodic changes in IOP and would lead to axonal deformation and stretching as well as to connective tissue changes, contributing to glaucomatous optic neuropathy. Early glaucomatous damage is thought to manifest in the macular region, where over 30% of the RGCs are located (503), as well as in the inferior peripapillary region (504, 505). Perhaps our findings, which included stronger correlations in the macular GCC and inferior RNFL, could thus signify that OR may play a greater role in the early stages of glaucoma. Our analysis is complicated by the fact that OR changes with age as the sclera becomes more rigid, but also because it is possible that glaucoma itself eventually causes the sclera to become stiffer thereby erasing the relationship to low OR found early in the disease (17, 21, 23, 26, 351, 428). To show to what degree OR contributes primarily to glaucoma and is altered by the disease process would require longitudinal assessment of OR at all stages of the disease, but especially in very early disease. While further investigation is warranted to confirm the role of OR in glaucoma, and to explore its value in detecting early glaucoma, our findings provide insight into the pathophysiology of OAG.

Chapter 6 – Ocular Rigidity and Neuro-Retinal Damage in Vasospastic Patients: A Pilot Study

As a continuity to the previous study, our aim was to investigate whether OR could play a greater role in certain subgroups of glaucoma patients. We had reasonable evidence to suggest that patients with concurrent vasospasticity could be more susceptible to glaucoma in response to biomechanical stimuli. (Manuscript in preparation)

Abstract

Purpose: Evidence suggests that ocular blood flow dysregulation in vasospastic patients could occur in response to biomechanical stimuli. This may contribute to the optic nerve head's susceptibility in glaucoma. As a continuity of the previous study (Chapter 5), we aimed to evaluate the role of vasospasticity in the association between ocular rigidity (OR), and neuro-retinal damage, expecting OR to play a greater role in the pathophysiology of glaucoma in subjects with vasospasm.

Methods: OR was measured non-invasively using the method developed by our group. Structural OCT-based parameters including retinal nerve fiber layer (RNFL) and macular ganglion cell complex (GCC) thicknesses were acquired using the Cirrus 5000 SD-OCT. Vasospasticity was assessed by a standardized questionnaire based on existing validated questionnaires and adapted to our requirements, and atherosclerosis was evaluated based on Broadway and Drance's (1998) "overall cardiovascular disease score". Correlations between OR and structural parameters were assessed in patients with concurrent vasospasticity, as well as those with atherosclerosis and no vasospasticity.

Results: In the vasospastic group, significant correlations were found between OR and the minimum GCC thickness (r_s=0.681, p=0.030), the average RNFL thickness (r_s=0.745, p=0.013) and the RNFL in the temporal quadrant (r_s=0.772, p=0.009), indicating more damage with lower OR. In contrast, no similar correlation was found in the atherosclerotic group (r_s=0.219, p=0.282; r_s=0.190, p=0.261; and r_s=0.179, p=0.319 respectively).

Conclusion: These results may indicate more structural damage in less rigid eyes of vasospastic patients, and also that OR may play a greater role in glaucoma in vasospastic patients than in atherosclerotic patients, providing insight unto the pathophysiology of OAG.

Introduction

Glaucoma is an ocular disease characterized by structural damage to retinal ganglion cells (RGC) and axons that compose the optic nerve, resulting in visual field loss and leading to blindness too often. This disease is known to be multifactorial. The main mechanisms thought to explain the pathogenesis of this blinding disease include the mechanical and vascular theories. The first postulates that elevated mechanical stress and strain lead to axonal damage and RGC loss (12-14). An individual's predisposition to develop glaucoma may depend on eye-specific geometrical and material properties, such as ocular rigidity (OR). The second proposes reduced perfusion pressure and vascular dysregulation as the main culprits leading to the optic neuropathy (506, 507). This means that the balance between intraocular pressure (IOP) and blood pressure (BP) in the ocular circulation is disturbed, affecting the optic nerve and resulting in pathological changes (508). However, these mechanisms are most probably not mutually exclusive, but rather intertwined. It is hypothesized that ocular biomechanics can mediate blood flow along with other processes in the eye (15).

Vasospasticity, or primary vascular dysregulation (PVD), is characterized by the body's abnormal response to stimuli such as temperature and emotional stress, leading to cold extremities (509). Vasospasticity is a risk factor for glaucoma (143, 510-512), and renders the eye more susceptible to damage in response to IOP or OPP changes due to defective autoregulation (509). An example of this is shown by Hafez et al. (145) who reported that following therapeutic IOP reduction in OAG patients, there were significantly greater increases in neuroretinal rim blood flow in patients with vasospastic disease compared to non-vasospastic patients, indicating defective autoregulation in these patients. Furthermore, evidence suggests that patients with PVD could present ocular blood flow dysregulation in response to biomechanical stimuli, contributing to the optic nerve head's susceptibility in glaucoma (142-144).

It was previously shown that low OR is correlated with neuro-retinal damage in glaucoma (Chapter 5). In the current study, the aim is to evaluate the role of vasospasticity in the association between ocular rigidity (OR), an important biomechanical property of the globe, and neuro-retinal damage. OR is expected to play a greater role in the pathophysiology of glaucoma in subjects with a concurrent vasospastic syndrome.

Methods

This study followed the tenets of the Declaration of Helsinki and was approved by the Maisonneuve-Rosemont Hospital institutional review board. Informed consent was obtained from all participants prior to testing.

OR was measured using a non-invasive optical method described previously (27, 494). Briefly, this method involves the measurement of the pulsatile ocular volume change using dynamic optical coherence tomography (OCT) imaging, and a custom segmentation algorithm, as well as the pulsatile IOP change using the Pascal tonometer (27). This non-invasive methodology has been previously validated and was also shown to have good repeatability (494). The OR coefficient is then computed using Friedenwald's equation (26). Structural OCT-based parameters including macular ganglion cell complex (GCC) and retinal nerve fiber layer (RNFL) thicknesses were acquired using the Cirrus 5000 OCT (Carl Zeiss Meditec AG, Dublin, USA).

Adults with healthy eyes, suspect discs or open-angle glaucoma (OAG) were recruited in this study. Participants were questioned about their systemic health, and medical records were reviewed. Vasospasticity, atherosclerosis and other vascular risk factors were assessed by a questionnaire, based on similar studies (140, 513-516). An "overall cardiovascular disease score" was calculated for each patient, where the five elements considered were: hypertension, ischemic heart disease, cerebral ischemic disease, diabetes and/or hemodynamic crisis (140). A score superior or equal to 1/5 indicated the presence of vascular disease or atherosclerosis. Participants were divided into a vasospastic group and a vascular disease group, according to the collected data. The questionnaire developed and used in this study is shown in Figure 13.

Statistical analyses were performed using SPSS statistical software (version 23; SPSS, Inc., Chicago, IL). Descriptive analysis of baseline demographics was carried out and presented as the mean ± standard deviation. To compare the vasospastic and atherosclerotic groups, a t-test, or equivalent based on distribution and equality of variances assessment, or chi-square test was used where applicable. Correlations between OR and structural parameters were assessed in the two groups of participants for comparison. For all statistical tests, a p-value inferior to 0.05 was considered significant.

Results

Out of the 118 subjects included in our previous study, forty-seven were considered for this study, as 10 were only vasospastic (without atherosclerosis), and 37 were only atherosclerotic (without vasospasm and/or migraine). Subjects who were neither vasospastic nor atherosclerotic were not analyzed in the present study. Of the 47 subjects included in this study, twenty-six (55%) were male, 39 (83%) were Caucasian, 7 (15%) were from African origins and 1 (2%) was Hispanic. One eye per subject was included; 25 (53%) were right eyes, 8 were healthy, 11 had suspect discs and 28 had early to advanced OAG. The baseline characteristics of all included participants are shown in Table 4. The assumption of homogeneity of variance was respected for all variables following Levene's Test for Equality of Variances ($p>0.05$). Due to unequal sample size and non-normal distribution, a Mann-Whitney U test and chi-square test were carried out. The Spearman correlations between OR and parameters of neuro-retinal damage in the vasospastic group and atherosclerotic group are shown in Table 5. In the vasospastic group, significant correlations were found between OR and the minimum GCC thickness ($r_s=0.681$, $p=0.030$), average RNFL thickness ($r_s=0.745$, $p=0.013$) and the RNFL in the temporal quadrant ($r_s=0.772$, $p=0.009$), indicating more damage with lower OR. In contrast, no similar correlation was found in the atherosclerotic group ($r_s=0.219$, $p=0.282$; $r_s=0.190$, $p=0.261$; and $r_s=0.179$, $p=0.319$ respectively). Figures 14 and 15 display the relationship between OR coefficients and neuro-retinal damage parameters in the vasospastic group and the atherosclerotic group respectively.

QUESTIONNAIRE (FOR INVESTIGATOR'S USE) Date: ____ /____ /____

Developed by Sayah DN, et al. 2020

Glaucoma Research Laboratory, University of Montreal, QC, Canada

Patient ID: _____ Name : _____ Date of Birth: _____

1. Do you have cold hands or feet (possibly also in the summer) or have other people ever told you that your hands are cold?
    - Are your hands or feet cold when other people's are not?
2. Do your fingers change color when they are exposed to cold temperature?
    - Do they turn white, blue, or both?
3. Do you suffer from migraines?

    If answer is positive, refer to the International Headache Society Diagnostic criteria to confirm.
4. Do you smoke?
    - Smoker/ ex-smoker / non-smoker
        - Duration of smoking (years)?
        - Average daily number of cigarettes (or other) smoked?
5. Do you have a history of cardiovascular diseases? (score __ / 5)
    - Hypertension?
    - Diabetes? Type I / II / gestational
    - Ischemic heart disease? Angina, infarction, valve problem, arrythmia
    - Cerebral ischemic disease? Stroke, transient ischemic attack
    - Hemodynamic crisis? Blood loss, transfusion, heart stoppage
6. What medication do you take? Ask for list.
    - Ask specifically for blood pressure (calcium channel blockers), cholesterol, diabetes (per os, insulin), heart medication, estrogen replacement therapy
    - Other
7. Do you suffer from sleep apnea? (refer to the STOP-BANG questionnaire)
8. What is your height and weight?
    - Calculate the body-mass index
9. Caffeine / Alcohol consumption:
    - How many cups of caffeinated beverage do you drink every day?
    - How much alcoholic beverages do you drink every day? (more or less than 7 oz)

Figure 13. – Questionnaire developed to establish the presence of vasospasticity, cardiovascular diseases, and other vascular risk factors.

	Vasospastic Group (n=10)	Atherosclerotic Group (n=37)	p-value
Eye (OD / OS)	4 / 6	21 / 16	0.279
Sex (M / F)	3 / 7	23 / 14	0.073
Ethnicity (Caucasian / Other)	8 / 2	31 / 6	0.550
Diagnosis (Healthy / Suspect / OAG)	2 / 1 / 7	6 / 10 / 21	0.591
History of Migraines	3	0	0.009
Age (years)	63±12	66±9	0.929
Axial length (mm)	24.74±1.27	24.33±1.22	0.419
GAT-IOP (mmHg)	16±4	17±4	0.476
DCT-IOP (mmHg)	18.8±4.0	18.7±3.7	1.000
Ocular Pulse Amplitude (mmHg)	2.9±1.3	3.0±1.3	0.692
Ocular Rigidity (μL^{-1})	0.026±0.015	0.023±0.013	0.711
Average GCC Thickness (µm)	71±10	69±9	0.768
Minimum GCC Thickness (µm)	68±12	66±11	0.689
Average RNFL Thickness (µm)	80±15	79±13	0.828
Inferior Quadrant RNFL Thickness (µm)	96±26	101±20	0.600
Temporal Quadrant RNFL Thickness (µm)	57±18	58±12	0.356
Superior Quadrant RNFL Thickness (µm)	97±23	97±19	0.966
6^{th} Clock Hour RNFL Thickness (µm)	103±36	108±29	0.487
7^{th} Clock Hour RNFL Thickness (µm)	106±28	108±28	0.810
8^{th} Clock Hour RNFL Thickness (µm)	62±27	58±14	0.524
9^{th} Clock Hour RNFL Thickness (µm)	46±9	48±10	0.452
10^{th} Clock Hour RNFL Thickness (µm)	64±19	67±17	0.435
11^{th} Clock Hour RNFL Thickness (µm)	108±27	106±28	0.944
12^{th} Clock Hour RNFL Thickness (µm)	97±31	96±25	0.788
Data is presented as the mean ± standard deviation where applicable.			

Table 4. – Baseline characteristics of participants in the vasospastic and atherosclerotic groups.

	Vasospastic Group	Atherosclerotic Group
Average GCC Thickness	0.479 (0.162)	0.128 (0.532)
Minimum GCC Thickness	**0.681** **(0.030)**	0.219 (0.282)
Average RNFL Thickness	**0.745** **(0.013)**	0.190 (0.261)
Inferior Quadrant RNFL Thickness	0.418 (0.229)	0.148 (0.412)
Temporal Quadrant RNFL Thickness	**0.772** **(0.009)**	0.179 (0.319)
Superior Quadrant RNFL Thickness	0.450 0.192	-0.001 (0.994)
6th Clock Hour RNFL Thickness	0.596 (0.069)	0.114 (0.528)
7th Clock Hour RNFL Thickness	**0.661** **(0.038)**	0.001 (0.998)
8th Clock Hour RNFL Thickness	**0.875** **(0.001)**	0.027 (0.883)
9th Clock Hour RNFL Thickness	0.628 (0.052)	0.244 (0.171)
10th Clock Hour RNFL Thickness	**0.648** **(0.043)**	**0.350** **(0.046)**
11th Clock Hour RNFL Thickness	0.552 (0.098)	0.164 (0.362)
12th Clock Hour RNFL Thickness	0.389 (0.266)	-0.230 (0.197)

Table 5. – Comparison of the association between ocular rigidity and structural damage in glaucoma in the vasospastic group and atherosclerotic group. Spearman correlation coefficients and significance values are shown (in bold, if $p < 0.05$).

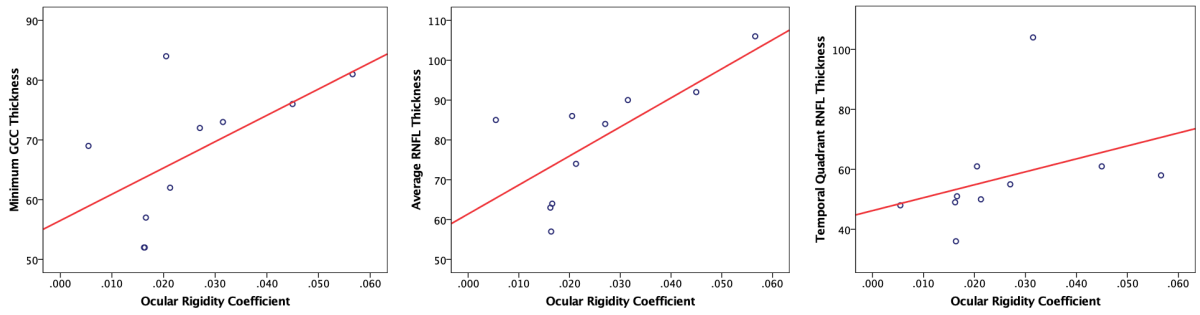

Figure 14. – Relationship between ocular rigidity coefficients and neuro-retinal damage parameters in the vasospastic group. Scatter plots showing significant correlations between ocular rigidity coefficients and the A) minimum ganglion cell complex (GCC) thickness (r=0.681, p=0.030; GCC=56.51+440*OR); B) average retinal nerve fiber layer (RNFL) thickness (r=0.745, p=0.013; Average RNFL=61.42+729*OR); C) RNFL thickness in the temporal quadrant (r=0.772, p=0.009; Temporal Quadrant RNFL=46.23+432*OR).

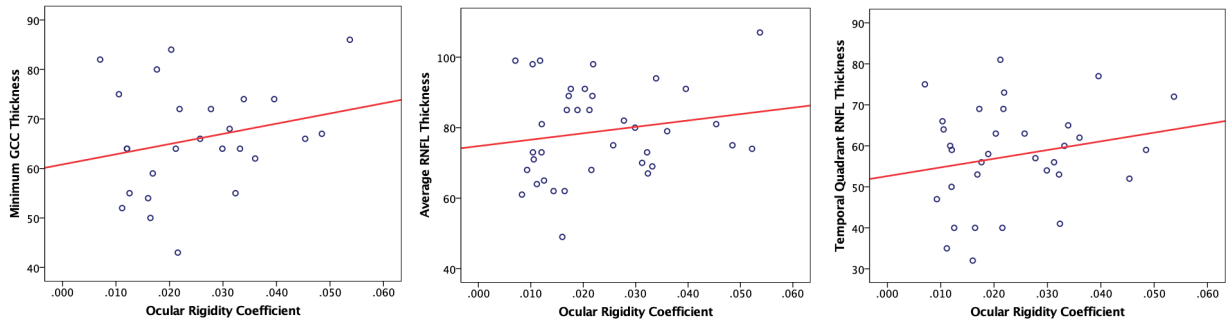

Figure 15. – Relationship between ocular rigidity coefficients and neuro-retinal damage parameters in the atherosclerotic group. Scatter plots showing significant correlations between ocular rigidity coefficients and the A) minimum ganglion cell complex (GCC) thickness (r=0.219, p=0.282; GCC=60.81+206*OR); B) average retinal nerve fiber layer (RNFL) thickness (r=0.190, p=0.261; Average RNFL=74.77+182*OR); C) RNFL thickness in the temporal quadrant (r=0.179, p=0.319; Temporal Quadrant RNFL=52.62+212*OR).

Discussion

In this pilot study, we found a strong correlation between OR and OCT-based parameters of neuro-retinal damage in the vasospastic group, indicating more damage in eyes with lower OR (Table 5). This confirms OR as a risk factor for neuro-retinal damage in glaucoma, perhaps more so in subjects with concurrent vasospasticity. In comparison, the atherosclerotic group showed no correlation between OR and these parameters, except for a weak positive correlation with RNFL in the 10^{th} clock hour. Despite the small number of subjects which limits statistical power, the results clearly suggest two distinct sub-populations with distinct characteristics within the initial heterogeneous population. This corroborates the findings by Schulzer et al. (144) who previously reported two distinct and statistically significantly different subgroups within a population of subjects with low and high-tension glaucoma. In their study, the group with vasospasticity showed a positive correlation between the visual field mean defect and the maximum historic IOP (Tmax), indices of glaucomatous functional damage and biomechanics respectively. In contrast, the group with vascular disease, akin to atherosclerosis, showed no correlation between these variables. The authors argued that this finding may indicate the presence of different pathogenic mechanisms leading to glaucoma. As such, they showed that the first group, although smaller (n=15), may be more sensitive to the biomechanical environment in the eye, whereas the second, larger group (n=45) may present disturbed coagulation and biochemical measurements suggestive of ischemic vascular disease.

The positive correlation found between OR and the OCT-based parameters reflecting glaucomatous neuro-retinal damage is consistent with our previous findings in a non-homogeneous population (Chapter 5).

We recognize some limitations of our study and that these should be addressed in future studies. First, the small size of the groups, particularly the vasospastic group, must be increased to permit additional statistical testing (including adjusting for potential covariates), increase the statistical power and to strengthen our conclusions. It is interesting to note, however, that the proportion of vasospastic to atherosclerotic subjects reported in the previous study (15 and 45) and in our study (10 and 37) is almost equivalent. Perhaps this may be representative of the proportion of

vasospasticity in such a population. Second, the presence of both vasospasticity and atherosclerosis in our study was established by questioning of the patient by the investigator and through review of the medical records. Although it is based on validated and previously published questionnaires (140, 513-516), the questionnaire used in this study has not been validated integrally. Objective, quantitative measurements methods for vasospasticity include finger blood flow and nailfold capillaroscopy, and should be used in future studies. Nevertheless, a number of studies have been published using only a questionnaire to establish the presence of vasospastic syndrome with seemingly good reliability without engaging in additional testing (513, 516, 517). Furthermore, in a cohort of 123 patients, the subjective complaint of cold extremities was significantly correlated with objective peripheral vasospastic testing (140). No hematological or biochemical measurements were carried out specifically for the purpose of this study.

While the presence of migraines is thought to be a possible surrogate for vascular dysregulation (516, 518), all vasospastic subjects in this study did not also report a history of migraines. However, this is consistent with previous reports that not all patients with vasospastic syndrome suffer from migraine (519).

Finally, our study demonstrates for the first time that OR and parameters of neuro-retinal damage are highly correlated in vasospastic subjects, compared to the group with ischemic vascular disease. In other words, this may indicate more structural damage in less rigid eyes, and perhaps also that OR may play a greater role in this subgroup of glaucoma patients. Vasospasticity, a known risk factor in glaucoma, may render the vasculature of the eye to be more susceptible to biomechanical stimuli, including IOP. In clinical practice, this may translate into an increased benefit for therapeutic IOP-lowering in vasospastic patients, especially those with lower OR. These findings provide insight into the pathophysiology of OAG, although further investigation is warranted to confirm the role of OR in glaucoma, and elucidate why and how low OR may play a greater role in certain subgroups of glaucoma patients.

Chapter 7 – Limited Association between Ocular Rigidity and Corneal Biomechanical Parameters

Corneal biomechanical parameters have been widely adopted in clinical practice as surrogate measurements for the eye's overall biomechanical properties represented by OR. In this study, we aimed to investigate the relationship between CH, CRF and CCT with OR. This work is titled "Association between Ocular Rigidity and Corneal Biomechanical Parameters in Healthy and Glaucomatous eyes" and has been authored by Diane N. Sayah, Javier Mazzaferri, Denise Descovich, Santiago Costantino and Mark R. Lesk. (Manuscript in preparation)

Abstract

Introduction: To investigate the relationship between ocular rigidity (OR), and corneal biomechanical parameters, such as the corneal hysteresis (CH) and corneal resistance factor (CRF), as well as the central corneal thickness (CCT), in healthy and glaucomatous eyes.

Methods: One hundred forty-five eyes from 145 patients (66 healthy eyes, 79 glaucomatous eyes) were recruited in this prospective cross-sectional observational study. OR was measured non-invasively by video-rate optical coherence tomography (OCT) imaging coupled with automated choroidal segmentation, and dynamic contour tonometry. The OR coefficient was calculated using Friedenwald's equation. CH and CRF were measured by the Ocular Response Analyzer. CCT was measured using ultrasound pachymetry. Bivariate and partial Pearson correlations were carried out to evaluate the relationship between OR and corneal biomechanical parameters.

Results: CH, CRF and CCT were significantly lower in glaucoma patients compared with controls. OR was lower in the glaucoma group, however this difference did not attain significance (p=0.124). In the normal group, no associations were found between OR and the corneal biomechanical parameters. Only a weak positive correlation between OR and CH was found in the OAG group (r=0.267, p=0.017). In this same group, after adjusting for age, sex, ethnicity, GAT-IOP and CCT, the correlation was no longer significant between OR and CH (r=0.210, p=0.073), while a positive correlation was found between OR and CRF (r=0.255, p=0.028).

Conclusion: The current study demonstrates no association between corneal biomechanical parameters and OR, except for a weak correlation between OR and CRF in glaucomatous eyes. This reinforces the notion that corneal biomechanical parameters are not a surrogate measurement for ocular rigidity and provides insight unto the pathophysiology of glaucoma.

Introduction

Ocular biomechanics are thought to play an important role in many diseases of the eye, including open-angle glaucoma (OAG). The ability to quantify the structural and material properties of the corneoscleral shell could help elucidate the pathophysiological mechanisms of this blinding disease, and potentially improve its diagnosis and treatment.

Corneal biomechanical properties have been extensively studied in the last decade, due to easy-to-use and readily-available measurement methods. Corneal hysteresis (CH) and corneal resistance factor (CRF) are biomechanical parameters which correspond to the viscous and elastic properties of the cornea respectively. The Ocular Response Analyzer (ORA; Reichert Technologies, Depew, NY), a non-contact tonometer, enables their measurement by analyzing the deformation of the cornea in response to a rapid air jet pulse (61). Infrared light is emitted, reflected on the cornea and detected by a photodetector. Following the air jet pulse, the cornea is flattened; this corresponds to the inward applanation pressure (P1). It continues to move inward then rebounds, reaching a second flattened state at an outward applanation pressure (P2), to take back its original shape. CH represents the cornea's ability to absorb and dissipate energy, and is defined as the difference between P1 and P2. CRF provides information about the elastic properties of corneal tissue or their resistance to stress, and is defined as P1-kP2 where k is a constant derived empirically from central corneal thickness (CCT) (362). CCT is another relevant corneal parameter in glaucoma. Generally measured using ultrasound pachymetry, and widely adopted in clinical practice, it was first used to correct IOP readings (343). The importance of CCT as an independent risk factor and predictor for the development of OAG (5, 345) and visual field loss (346) was later demonstrated. Similarly, CH was found to be significantly lower in POAG compared to controls (365-368). Numerous studies also associated a lower CH with an increased risk of glaucoma

progression (371-374), with a higher predictive value of glaucoma progression than CCT (371, 372).

How these corneal properties are linked to the ocular globe's biomechanical properties and to the optic nerve's susceptibility in glaucoma remains unclear. Ocular rigidity (OR) characterizes the resistance that the whole eye exerts to distending forces and is defined as the pressure-volume relationship in the eye (26). As the anterior extension of the sclera, the cornea contributes to the overall rigidity of the eye. However, the stiffness of the sclera is the major contributor to OR. Finite element modeling has shown scleral stiffness to be the most influential biomechanical factor of strain at the optic nerve head (16). Until now, only three studies have attempted to evaluate the association between OR and corneal parameters including CH, CRF and CCT. In one study where OR was measured using laser Doppler flowmetry and Pascal tonometry, a positive but weak correlation was found between OR and CCT (rho = 0.121, p=0.05) (23), indicating that subjects with a thinner cornea may have a more compliant sclera. No correlation was found in another study using an invasive measurement method (r=0.22, p=0.12) (351). OR measured using Schiötz tonometry, an indirect measurement method that was shown to be inaccurate due to its dependence on the eye's biomechanical properties, has shown no correlation with CH (p=0.39), but was negatively correlated with CRF (r=-0.41, p=0.02) in 25 healthy subjects (520).

In this paper, we aim to measure OR and investigate the relationship between OR and corneal biomechanical parameters including CH, CRF and CCT in both healthy and glaucomatous eyes. The measurement of OR will be carried out using a reliable, non-invasive and direct method that was developed by our group and recently validated (27, 494).

Methods

This prospective cross-sectional observational study was approved by the Maisonneuve-Rosemont Hospital Institutional Review Board and conformed to the principles of the Declaration of Helsinki. Informed consent was obtained from all participants prior to testing.

Adult subjects with healthy eyes or with OAG were recruited in this study. A complete ocular examination was performed for all participants. Normal subjects had intraocular pressure (IOP)

less than 21 mmHg, normal optic nerve appearance on fundus exam, normal visual fields and no other ocular disease. Subjects with OAG had open (non-occludable) angles on gonioscopy, a glaucomatous optic nerve appearance, as well as repeatable structural and/or functional findings with optical coherence tomography (OCT) imaging and Humphrey visual field (VF; Zeiss Humphrey Systems, Dublin, California, USA) testing (SITA standard threshold 24–2 strategy). According to this definition, pre-perimetric glaucoma patients were also included in the glaucoma group. Exclusion criteria for this study were prior intraocular surgery (except remote cataract extraction), corneal pathology, and contact lens wear. Subjects were also excluded if they had corneal, lens, or media opacities that resulted in poor retinal OCT quality, had unsteady fixation, or were unable to fixate a target with the contralateral eye.

Ocular rigidity (OR) was measured using a non-invasive method involving video-rate OCT imaging and Pascal dynamic contour tonometry (DCT) (27, 494). This method is based on Friedenwald's equation (419), which permits the ocular rigidity coefficient to be estimated as the following pressure-volume relationship: $ln\, IOP/IOP_0 = OR \times (V - V_0)$. The OR coefficient thus obtained is a single value for the overall OR of the corneoscleral shell.

Through dynamic OCT imaging (Spectralis SD-OCT, Heidelberg Engineering GmbH, Heidelberg, Germany) with enhanced depth imaging (EDI) coupled with automated choroidal segmentation, we obtain a direct measurement of the volume of blood pumped into the eye with each heartbeat – the pulsatile ocular volume change (ΔV, or $V - V_0$). The choroidal segmentation algorithm is described in detail in our previous paper (27). Briefly, it is based on graph theory using an edge-probability weighting scheme that enables the precise detection of the choroid's boundaries, and has been shown to be more robust in detecting the choroid-sclera interface compared with existing algorithms (27, 488). It measures the choroidal thickness change (ΔCT) associated with the cardiac cycle through the time-series. Since the choroid represents approximately 90% of the blood flow in the eye (82), ΔV can be estimated from the measured ΔCT. The ΔV is calculated according to the following equation : $\Delta V = (\pi/2)(AL_{adj} + CT)^2\, \Delta CT$, where AL_{adj} is the ocular axial length (AL) measured using the IOL Master 500 (Carl Zeiss Meditec AG, Dublin, USA) and adjusted for the anterior chamber depth (ACD) (494). The pulsatile pressure change was measured using the Pascal DCT (Ziemer Ophthalmic Systems AG, Port, Switzerland). This

tonometer provides an IOP reading corresponding to the diastolic IOP, as well as the ocular pulse amplitude (OPA) which is the change in IOP between the systole and diastole.

This non-invasive methodology has been previously validated and was also shown to have good repeatability (494).

Corneal biomechanical parameters, namely CH and CRF, were obtained using the Ocular Response Analyzer (ORA) (61). Measurements were repeated at least twice and up to four times if the waveform score was below 6.0, in which case the acquisition with the highest waveform score was considered. Other relevant variables were measured, including CCT using a standard ultrasound pachymeter and IOP by Goldmann applanation tonometry (GAT).

Descriptive statistical analysis of baseline demographics was assessed using SPSS. To compare biomechanical parameters' values between the normal and OAG groups, a t-test was used. To further evaluate the relationship between OR, CH, CRF and CCT, multicollinearity was assessed, followed by bivariate and partial Pearson correlations, adjusting for potential covariates. A p-value <0.05 was considered statistically significant.

Results

A total of 145 eyes from 145 subjects (66 normal and 79 with OAG; 66±13 years of age; 45% males) were included in this study. A description of the demographics of the normal and OAG groups is presented in Table 6. The average values of biomechanical parameters, including CH, CRF, CCT and OR are presented in Table 7. Lower CH, CRF and CCT were found in glaucomatous eyes compared to controls ($p<0.001$, $p=0.009$ and $p=0.001$ respectively). OR was lower in the OAG group, however this difference did not attain statistical significance ($p=0.124$). Table 8 shows the Pearson correlation coefficients and p-values between all relevant variables for the normal and OAG groups respectively. No multicollinearity was found, with a variance inflation factor inferior to 2.5 among all variables.

CH and CRF were positively correlated with each other as well as with CCT. In the normal group, no associations were found between OR and the corneal biomechanical parameters (see Tables 8 and 9). Only a weak positive correlation between OR and CH was found in the OAG group

(r=0.267, p=0.017) (Table 8). In this same group, after adjusting for age, sex, ethnicity, GAT-IOP and CCT, the correlation was no longer significant between OR and CH (r=0.219, p=0.058), while a positive correlation was found between OR and CRF (r=0.294, p=0.010) (Table 9).

	Healthy (n=66)	**OAG (n=79)**
Study eye (OD / OS)	39/27	34/45
Sex (Female / Male)	38/28	42/37
Ethnicity (Caucasian / Other)	61/5	70/9
Age (years) [a]	65±17	67±10
Axial length (mm) [a]	23.84±1.18	24.65±1.43
GAT-IOP (mmHg) [a]	15±3	17±6
DCT-IOP (mmHg) [a]	16.8±2.7	19.6±5.3
MD (dB) [a]	-0.02±0.2	-5.0±6.1
[a] Data is presented as the mean ± standard deviation. GAT-IOP = IOP measured by Goldmann applanation tonometry; DCT-IOP = IOP measured using Pascal dynamic contour tonometry; MD = Visual field mean deviation.		

Table 6. – Baseline characteristics of subjects in the healthy and OAG groups.

	Healthy (n=66)	**OAG (n=79)**	**p-value**
Ocular rigidity coefficient (1/µL) [a]	0.0278±0.0139	0.0244±0.0126	0.124
Corneal hysteresis (mmHg) [a]	10.1±1.8	8.6±1.9	<0.001
Corneal resistance factor (mmHg) [a]	10.1±1.7	9.3±1.8	0.009
Central corneal thickness (µm) [a]	549±36	529±37	0.001
[a] Data is presented as: mean ± standard deviation.			

Table 7. – Average ocular rigidity, corneal hysteresis, corneal resistance factor and central corneal thickness values in the healthy and OAG groups.

	Age	AL	GAT-IOP	DCT-IOP	CCT	CH	CRF	OR
Healthy Group								
CCT	0.150 (0.229)	0.012 (0.922)	0.205 (0.120)	-0.053 (0.673)		**0.422** (<0.001)	**0.600** (<0.001)	-0.007 (0.956)
CH	-0.071 (0.573)	-0.194 (0.120)	-0.192 (0.145)	**-0.353** (0.004)	**0.422** (<0.001)		**0.781** (<0.001)	0.051 (0.687)
CRF	-0.058 (0.644)	-0.038 (0.761)	**0.318** (0.014)	0.161 (0.196)	**0.600** (<0.001)	**0.781** (<0.001)		0.013 (0.920)
OR	-0.024 (0.846)	**-0.494** (<0.001)	-0.116 (0.383)	-0.148 (0.237)	-0.007 (0.956)	0.051 (0.687)	0.013 (0.920)	
Glaucoma Group								
CCT	-0.171 (0.132)	0.162 (0.155)	**0.328** (0.003)	**0.247** (0.028)		**0.471** (<0.001)	**0.575** (<0.001)	0.031 (0.787)
CH	-0.129 (0.258)	0.091 (0.423)	**-0.253** (0.024)	**-0.382** (0.001)	**0.471** (<0.001)		**0.455** (<0.001)	**0.267** (0.017)
CRF	**-0.295** (0.008)	0.100 (0.382)	**0.376** (<0.001)	**0.289** (0.010)	**0.575** (<0.001)	**0.455** (<0.001)		0.129 (0.259)
OR	0.139 (0.222)	**-0.381** (0.001)	**-0.265** (0.018)	**-0.281** (0.012)	0.031 (0.787)	**0.267** (0.017)	0.129 (0.259)	

Table 8. – Pearson correlation coefficients and significance values between OR, CH, CRF, CCT and other relevant variables for the healthy and OAG groups.

	Covariates	**Healthy Group**	**OAG Group**
OR and CCT	Age, sex, ethnicity, GAT-IOP, CRF	-0.004 (0.975)	-0.006 (0.959)
OR and CH	Age, sex, ethnicity, GAT-IOP, CCT	-0.033 (0.813)	0.210 (0.073)
OR and CRF	Age, sex, ethnicity, GAT-IOP, CCT	-0.013 (0.926)	**0.255 (0.028)**

Table 9. – Pearson correlation coefficients adjusted for confounding variables (and significance values) between OR, CH, CRF, CCT for the healthy and OAG groups.

Discussion

In this study, OR and corneal biomechanical properties including CH, CRF and CCT were not found to be correlated in healthy eyes, while only CRF was found to be positively, albeit weakly correlated with OR after adjusting for age, sex, ethnicity, IOP and CCT in glaucomatous eyes as seen in Table 9. The covariates were chosen according to the correlations presented in this paper and the literature (521, 522). These results demonstrate limited associations between corneal biomechanical factors and the rigidity of the overall corneoscleral shell. This also demonstrates that corneal biomechanical factors do not appear to be a surrogate for OR. This is corroborated by similar findings from a previous study investigating the link between OR and acute IOP elevation following intravitreal injections. IOP spikes were strongly correlated with OR, whereas they were not significantly associated with CCT, CH and CRF (523) (as shown in the following chapter).

It is speculated that corneal biomechanical parameters could reflect glaucoma susceptibility in a given eye through similar properties of the extracellular matrix of the cornea, lamina cribrosa and peripapillary sclera. In other words, this would mean that an eye with a more deformable cornea, or low CH, CRF and CCT, may also be more vulnerable to IOP-induced ONH damage. Several experiments were carried out to better understand the link between CH, CRF and CCT and posterior structures of the eye in glaucoma. However, the relationship between the biomechanics of the cornea and the globe remains unclear. Our study further indicates that the link between corneal and corneoscleral biomechanical properties are indeed limited. Since CRF is akin to the elasticity of the corneal tissue, and OR reflects the elastic properties of the corneoscleral shell, this may explain our correlation between CRF and OR, more so than CH or CCT. The presence of such a relationship in glaucomatous eyes but not in healthy eyes is in line with similar findings in the literature. For example, previous studies have reported that low CH is associated with larger cup-to-disc ratio, deeper cup and smaller rim area in eyes with glaucoma (376, 377), while neither CH nor CCT were correlated with measures of optic disc cupping in a large, non-glaucomatous cohort (378). Similarly, CCT and optic nerve surface displacement (onsd) were correlated in OAG and OHT eyes undergoing therapeutic IOP reduction (349), while CH and onsd were correlated in glaucomatous eyes subjected to an acute IOP elevation, but not in healthy controls (366). In fact,

there is conflicting data regarding corneal biomechanical parameters and optic nerve parameters in healthy eyes. The discrepancy between findings is suggested to be due, at least partially, to sample size, study population and methodology (501).

In this case, the methodology used may indeed provide some explanation for discrepancies between our findings and published reports. The development of a direct, non-invasive and reliable method to measure OR has long posed a challenge to the investigation of this important biomechanical property *in vivo*. While anterior chamber manometry is the main technique to directly measure OR (351, 411-413), it involves the intraoperative cannulation of the anterior chamber to inject fluid in the eye (351). Its invasive nature limits the technique's applicability. One of the first non-invasive methods to measure OR involved the Schiötz tonometer. It has been shown to be inaccurate due to its dependence on the biomechanical properties of the eye (406-409). The most significant source of this variability in OR coefficients originates from the use of weights in Schiötz tonometry, which compress the ocular wall and displace a significant amount of intraocular fluid (406, 409), but also through the erroneous assumption that the OR of all eyes is standard in the applicability of the conversion table which provides the IOP reading in mmHg (39, 51, 406). A recently developed non-invasive technique to measure OR, based on choroidal laser Doppler flowmetry gave only relative values because choroidal blood flow was measured in arbitrary units (23). Our group has since developed the first non-invasive and direct method to measure OR in living human eyes (27). The novelty of the method consists mainly in its ability to measure the pulsatile ocular volume change, or amount of blood pumped into the eye with each heartbeat, directly from OCT videos coupled with automated choroidal segmentation. The approach also uses Pascal DCT to measure the pulsatile IOP change. It has been validated against an invasive method and shown to be well correlated and reliable (494). As aforementioned, the current findings using this method are consistent with those obtained with the manometric technique regarding OR and CCT (351).

The results of this study also confirm previous reported findings. CH and CRF are positively correlated with each other, and also with CCT (to a lesser extent with CH than CRF) (365, 522, 524). CRF and age are negatively correlated (382, 524). This is shown in glaucomatous subjects but not in controls in our study. A negative correlation with AL and OR was confirmed in both

groups (23, 422). CH, CRF and CCT values were found to be lower in glaucomatous eyes compared with controls, similarly to previous reports (365-368). There was a tendency for lower OR in the glaucoma group, however this difference did not attain significance (p=0.124). This may be explained by the heterogeneity of the glaucoma group in this study. Indeed, while our group has previously reported lower OR in OAG (23), OR is thought to be altered throughout the course of the disease, and may increase with advanced glaucoma (17, 23, 399, 400).

A potential limitation of this study is that, while both OR and corneal properties may be altered by topical hypotensive medications routinely prescribed for the treatment of glaucoma (18, 357-359, 419, 420), this was not accounted for in our analysis. Our data shows that 67 out of 79 glaucomatous patients in our study were treated with an average of 2±1 pressure-lowering agents. Of those, 59 were on prostaglandin analogs, 49 on beta-blockers, 12 on alpha-2 adrenergic receptor agonists, 37 on topical carbonic anhydrase inhibitors (CAI), 3 on pilocarpine and 7 on oral CAIs. The agents could have been administered alone or as part of a combination. However, post-hoc analysis showed no significant correlation between OR and CH, CRF and CCT in the 12 non-treated eyes (p=0.866, p=0.150 and p=0.662 respectively).

Finally, this study demonstrates no association between corneal biomechanical parameters and OR, except for a weak correlation between OR and CRF in glaucomatous eyes. This shows that there is limited association between the biomechanical properties of the cornea and those of the entire ocular globe. Corneal biomechanical factors do not appear to be a surrogate for overall OR.

Chapter 8 – Ocular Rigidity as a Predictor of IOP spikes following Therapeutic Intravitreal Injections

Elevated IOP is a risk factor for glaucoma. IOP spikes are known to occur in eyes undergoing intravitreal injections (IVI) of bevacizumab, a common and effective treatment for various exudative retinal diseases. If we consider a rigid eye as a soccer ball and a compliant eye as a birthday balloon, we expect the rigid eye to have a bigger IOP change after injecting a known volume of fluid into it. When patients at risk of, or with concurrent glaucoma present with exudative retinal diseases requiring therapeutic IVIs, we hypothesized that OR could help us predict the magnitude of IOP spikes prior to initiating therapeutic IVIs. This would help prevent elevated IOP and subsequent ONH damage. This concept motivated the following study titled "Correlation of Ocular Rigidity with Intraocular Pressure Spike After Intravitreal Injection of Bevacizumab in Exudative Retinal Disease".

This work was published in the British Journal of Ophthalmology in 2020 (523). The authors are Diane N. Sayah, Andrei A. Szigiato, Javier Mazzaferri, Denise Descovich, Renaud Duval, Flavio Rezende, Santiago Costantino and Mark R. Lesk.

Clinical science

Correlation of ocular rigidity with intraocular pressure spike after intravitreal injection of bevacizumab in exudative retinal disease

Diane N Sayah ,[1,2] Andrei-Alexandru Szigiato ,[2] Javier Mazzaferri,[1] Denise Descovich,[1] Renaud Duval,[1,2] Flavio A Rezende,[1,2] Santiago Costantino,[1,2] Mark R Lesk[1,2]

[1]Ophthalmology, Maisonneuve-Rosemont Hospital Research Centre, Montreal, Quebec, Canada
[2]Ophthalmology, University of Montreal, Montreal, Quebec, Canada

Correspondence to
Dr Mark R Lesk, Ophthalmology, Maisonneuve-Rosemont Hospital Research Centre, Montreal, QC H1T 2M4, Canada

Received 22 November 2019
Revised 3 April 2020
Accepted 7 April 2020

To cite: Sayah DN, Szigiato A-A, Mazzaferri J, *et al*. *Br J Ophthalmol* Epub ahead of print: [*please include* Day Month Year]. doi:10.1136/bjophthalmol-2019-315595

ABSTRACT

Background/aims To evaluate the non-invasive measurement of ocular rigidity (OR), an important biomechanical property of the eye, as a predictor of intraocular pressure (IOP) elevation after anti-vascular endothelial growth factor (anti-VEGF) intravitreal injection (IVI).

Methods Subjects requiring IVI of anti-VEGF for a pre-existing retinal condition were enrolled in this prospective cross-sectional study. OR was assessed in 18 eyes of 18 participants by measurement of pulsatile choroidal volume change using video-rate optical coherence tomography, and pulsatile IOP change using dynamic contour tonometry. IOP was measured using Tono-Pen XL before and immediately following the injection and was correlated with OR.

Results The average increase in IOP following IVI was 19±9 mm Hg, with a range of 7–33 mm Hg. The Spearman correlation coefficient between OR and IOP elevation following IVI was 0.796 ($p<0.001$), showing higher IOP elevation in more rigid eyes. A regression line was also calculated to predict the IOP spike based on the OR coefficient, such that IOP spike=664.17 mm Hg·µL×OR + 4.59 mm Hg.

Conclusion This study shows a strong positive correlation between OR and acute IOP elevation following IVI. These findings indicate that the non-invasive measurement of OR could be an effective tool in identifying patients at risk of IOP spikes following IVI.

INTRODUCTION

Intravitreal injections (IVI) with anti-vascular endothelial growth factor (anti-VEGF) agents are a common and effective treatment for a multitude of retinal diseases. Given that a relatively large volume of fluid is added into the eye, IVI can cause a significant acute intraocular pressure (IOP) elevation. In fact, up to a third of patients may experience an IOP of over 50 mm Hg immediately after anti-VEGF injection.[1–3] Based on clinical studies, it is currently unknown whether IOP spikes following IVI contribute to the development of glaucoma or affect disease progression in patients with established glaucoma. However, experimental studies suggest that brief but rapid IOP elevation can result in retinal ganglion cell injury.[4] Ocular rigidity (OR) was previously shown to decrease with longer axial length (AL), increase with age and increase with advanced glaucoma and exudative age-related macular degeneration (AMD).[5–8] Furthermore, according to finite element modelling, the most influential factor determining mechanical strain in the optic nerve head is the stiffness of the sclera.[9] To our knowledge, although increased scleral thickness was shown to be associated with higher IOP spikes following IVI,[10] the relationship between OR and IOP spikes following IVI has never been investigated in living human eyes.

Despite the potential relevance of OR, traditional techniques used for its measurement were either invasive or unreliable,[6] and limited its assessment in a clinical setting. Our group has developed a non-invasive and direct method to measure OR in living human eyes.[7 11] This method is based on the measurement of the pulsatile ocular volume change from video-rate optical coherence tomography (OCT) imaging by automated choroidal segmentation, and the pulsatile IOP change using Pascal tonometry, to compute the OR coefficient using Friedenwald's equation.[12]

In the current study, we applied this method to investigate the role of OR as a risk factor and predictor of acute IOP spikes in eyes that undergo therapeutic IVI. We hypothesise that patients with a higher OR measured with this technique will have higher IOP elevation following a fixed increase in ocular volume delivered by IVI.

MATERIAL AND METHODS

Eighteen adult subjects who were to receive a therapeutic IVI of anti-VEGF for a pre-existing retinal condition such as exudative AMD, vascular occlusion or proliferative diabetic retinopathy were enrolled. Subjects were excluded if they had corneal, lens, or media opacities that resulted in poor retinal OCT quality, had unsteady fixation, were unable to fixate a target with the contralateral eye, or if segmentation algorithms did not yield usable data. Subjects were also excluded if they had prior incisional glaucoma surgery, including trabeculectomy or a tube shunt, vitrectomy as well as recent laser treatment or ocular surgery within the past 3 months.

During the first part of the visit, subjects underwent a review of their medical history including ocular and surgical history. A complete ocular examination was performed, followed by measurements of blood pressure, OR and additional corneal

biomechanical properties such as corneal ultrasound pachymetry, corneal hysteresis (CH) and corneal resistance factor (CRF) (Ocular Response Analyzer, Reichert Technologies, Buffalo, New York, USA).

Our method for measuring OR is based on the Friedenwald equation[12] :

$$\ln \frac{IOP}{IOP_0} = OR\ (V - V_0)$$

where $V - V_0$ is the change in ocular volume and (IOP/IOP_0) represents the change in IOP. Our approach[7] uses video-rate spectral domain OCT (Spectralis SD-OCT, Heidelberg Engineering GmbH, Heidelberg, Germany) with enhanced depth imaging coupled with an automated segmentation algorithm[13] to measure the pulsatile ocular volume change ($V - V_0$) as well as dynamic contour tonometry (DCT) to measure the pulsatile IOP change (IOP/IOP_0).[7] More specifically, our custom segmentation algorithm enables the precise measurement of the fluctuations in submacular choroidal thickness associated with the heart rate throughout the time-series. Our scan covers 8 mm of the central macula. Considering that the choroid represents approximately 90% of the blood flow in the eye,[14] the pulsatile ocular volume change is extrapolated from the measured pulsatile submacular choroidal thickness change. This is done using a mathematical model of the eye which accounts for AL (IOL Master, Carl Zeiss Meditec, Dublin, California, USA).[11] The ocular pulse amplitude, corresponding to the change in IOP between the systole and diastole, is measured with the Pascal tonometer (Ziemer Ophthalmic Systems AG, Port, Switzerland). This non-invasive methodology has been previously validated.[11] The method's repeatability, both intrasession and intersession, was found to be good, with an intraclass correlation coefficient of 0.925, 95% CI (0.881 to 0.953) and 0.950, 95% CI (0.763 to 0.990), respectively.[11]

The second part of the visit took place within the same session and involved assessment of IOP spikes due to IVI. The pre-IVI IOP was measured immediately prior to asepsis and speculum placement with the patient in the semi-supine position using a portable tonometer, the Tono-Pen XL (Reichert Technologies). Following this, 50 µL of bevacizumab (1.25 mg) was delivered off-label by IVI through a 30G needle following standard clinical protocol by a retinal specialist. Immediately after the removal of the speculum, post-IVI IOP was measured with the patient remaining in the semi-supine position. The presence or absence of fluid reflux was recorded and estimated by the retinal specialist.

Descriptive statistical analysis of the participants' baseline demographics, as well as the correlation between OR and the magnitude of the IOP spike following IVI were assessed using SPSS (V.23). A priori sample size of 13 was calculated to achieve 80% power to detect a correlation of 0.7 using a two-sided hypothesis test with a significance level of 0.05 (G*Power V.3.1.9.2)[15] based on prior findings.[11 16]

A linear regression analysis was carried out to evaluate the association between OR and IOP spikes and enable the prediction of IOP spikes following IVI from the OR coefficient for a given eye. The correlation coefficients between other variables such as CH, CRF, central corneal thickness (CCT), AL, age, baseline IOP and IOP spikes were also computed.

RESULTS

A description of the baseline characteristics of the 18 participants in this study is presented in table 1, including the measured IOP elevation and OR coefficients.

Table 1 Patient characteristics at baseline

Study eye (OD/OS)		7/11
Sex (female/male)		8/10
Age (years)*		68±10
Ethnicity	African-American	1
	Caucasian	16
	Hispanic	1
Retinal conditions	Retinal vein occlusion	7
	Diabetic macular oedema	3
	Exudative age-related macular degeneration	5
	Chronic central serous chorioretinopathy	2
	Idiopathic juxtapapillary choroidal neovascularisation	1
No. of subjects on glaucoma medications		3
No. of subjects with observed reflux post-IVI		3
No. of previous IVI per subject*		19±15
No. of previous IVI in last 12 months per subject*		8±3
Baseline pre-IVI IOP (mm Hg)*		17±5
Measured IOP spike, <30 s post-IVI (mm Hg)*		19±9
Range of measured IOP spike (mm Hg)		7–33
Measured ocular rigidity coefficients (1/µL)*		0.022±0.010
Range of measured ocular rigidity coefficients (1/µL)		0.006–0.042
Ocular axial length (mm)		23.53±0.90
Central corneal thickness (µm)*		529±47
Corneal hysteresis (mm Hg)*		9.9±1.7
Corneal resistance factor (mm Hg)*		10.6±2.4
Previous ocular surgery (>3 months)	Cataract extraction	5
Previous laser treatment (>3 months)	Panretinal photocoagulation	2
	Verteporfin	1
Systemic blood pressure	Systolic (mm Hg)*	145±24
	Diastolic (mm Hg)*	80±8
Medical history	Diabetes	5
	Hypertension	11
	Cardiovascular disease	5
	Asthma	1
Systemic medications	Insulin	3
	Oral hypoglycemics	5
	Statins	9
	Diuretic	5
	ACE inhibitors	7
	Blood thinners	4
	Beta blockers	5
	Calcium channel blockers	1

*Data is presented as: mean±SD.
ACE, angiotensin-converting enzyme; IOP, intraocular pressure; IVI, intravitreal injection; OD, right eye; OS, left eye.

The Spearman rank correlation coefficient between OR coefficients and IOP spikes measured within 30 s following the IVI of 50 µL of bevacizumab was r_s=0.796 (p<0.001). A scatter plot comparing OR and IOP spikes is presented in figure 1. A significant regression equation was found with an R^2 of 0.53. The equation of the regression line is: IOP spike=664.17 mm Hg·µL×OR + 4.59 mm Hg. These results demonstrate a strong, positive correlation in which eyes with greater OR tend to have significantly greater IOP spikes.

There was no significant correlation between IOP spikes and CCT (r_s=−0.077, p=0.763), CH (r_s=−0.111, p=0.660) and

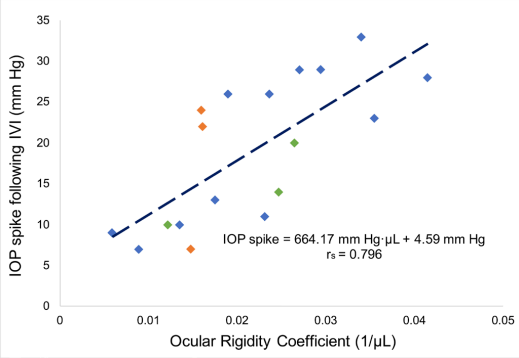

Figure 1 Linear regression plot showing a strong positive correlation (r_s=0.796, p<0.001) between the ocular rigidity (OR) coefficient and the transient elevation of intraocular pressure (IOP) as measured immediately post intravitreal injection (IVI) of bevacizumab in 18 eyes from 18 subjects with pre-existing retinal conditions. A significant regression equation represented by the dotted line was found with an R^2 of 0.53. The equation of the regression line calculated is IOP spike=664.17 mm Hg·µL×OR + 4.59 mm Hg. The green data points represent the three eyes with fluid reflux and the orange data points represent the three eyes with concomitant glaucoma respectively.

CRF (r_s=−0.334, p=0.176), as well as AL (r_s=0.365, p=0.136) and age (r_s=0.039, p=0.878). Similarly, no correlation was found between baseline pre-IVI IOP and IOP spikes (r_s=−0.315, p=0.203).

DISCUSSION

To our knowledge, this is the first study to establish elevated OR as a major risk factor for acute IOP spikes following IVI. This finding is consistent with the relationship described between delta IOP and K (OR) in the Friedenwald equation. This is also in agreement with findings from an experimental ex vivo study performed in porcine eyes showing an increased magnitude of IOP change due to microvolumetric change (15 µL) with increased tangential and radial strains in the superotemporal region of the sclera, suggesting larger IOP elevation in eyes with a stiffer sclera.[16] The present study also indicates that a non-invasive measurement of OR can accurately predict the magnitude of IOP elevation after IVI.

Since scleral stiffness is the major determinant of the ocular globe's rigidity, the Friedenwald equation can be approximated from first principles using the mechanical properties (stress–strain relationship) of its primary constituent (collagen) and shape.[17] Thus, OR values obtained in this study are closely linked to scleral stiffness and are sometimes used as a surrogate.

Twelve subjects from this study were also included in the validation of the method, which showed a strong correlation between OR coefficients obtained using our non-invasive method and those obtained using an invasive procedure involving IVIs.[11] Hence, we could reasonably expect to find a positive correlation between OR and IOP spikes. Furthermore, a rigid eye should lead to higher IOP elevation following IVI compared with a compliant eye, due to the inability of the former to expand. This is consistent with the results reported in our study.

Factors such as medication reflux, history of ocular surgery or glaucoma, as well as the tonometer used could have had an impact on the measured IOP spike. Mild reflux was observed in three subjects. A small bore-needle size (30G) was used in all eyes to minimise reflux through the injection site.[2] The equation of the regression line calculated when these three subjects were excluded is 668.02 mm Hg·µL×OR + 5.29 mm Hg (R^2=0.55). Three subjects were on IOP-lowering topical medications due to glaucoma. The equation of the regression line calculated when these three subjects were excluded is 696.76 mm Hg·µL×OR + 3.30 mm Hg (R^2=0.62). These two scenarios would result in little to no difference in the prediction of IOP spikes, considering its given purpose. The difference in the predicted value of IOP spike would be between 0 and 1.7 mm Hg over the range of OR when compared with the IOP spike predicted by the model that includes all 18 eyes. Although excluded from this study, as vitrectomy could alter the fluid dynamics on injection, we measured OR and IOP spike for one vitrectomised eye. This subject had the highest IOP spike, 42 mm Hg, among all participants, despite an OR coefficient in the mid-range, of 0.0244/µL. We suggest that IOP spikes prediction should be explored further in vitrectomised eyes in an extended study. Finally, we recognise that the TonoPen XL used in this study may underestimate IOP when IOP is very high compared with Goldmann tonometry,[18] however its use has been deemed acceptable and more practical in similar studies.[2 19 20] Despite these potential limitations, the technique used in this study remains reliable as was validated previously.[11]

Various studies report yields of visualisation of the choroidal–sclera interface (CSI). The largest study carried out with the Spectralis SD-OCT to measure subfoveal choroidal thickness reported a success rate of 93% out of 3468 subjects by averaging 100 scans and carrying out manual segmentation at specific locations along the b-scan.[21] Since we carry out dynamic imaging, as opposed to static, and it must be faster than the heart rate frequency, we can average only about five scans per frame. Our segmentation is automated and performed along the width of the b-scan and must detect the subtle thickness change corresponding to choroidal filling. In many cases requiring IVI the choroidal boundaries are less well delineated than in normal eyes. Furthermore, because of maculopathy some patients had inadequate fixation for the longer scan time required. These factors led to a lower yield, which was 35%. We are currently working on several fronts to improve this yield in challenging patients. These strategies include imaging away from the obstruction (lesion/oedema), software improvements to our segmentation algorithms and migrating to OCT devices with longer, better penetrating wavelengths and faster acquisition, for better image averaging. While we use a spectral domain OCT (Spectralis SD-OCT at 40 000 A-scans/s), we are currently adapting our algorithm and imaging protocol to a swept-source (SS)-OCT. Regardless of the relatively low yield we believe that the strong relationship between OR and IOP spike magnitude is valid.

For a diagnostic test to be useful it must detect a problem that has significant morbidity or mortality and has an effective treatment.[22] We hereby present a method to predict large IOP elevations after IVI, which may increase the risk of developing glaucomatous optic nerve damage, one of the most common causes of irreversible blindness worldwide.[23] Preventing loss of peripheral vision is of vital importance to preserve function and independence in patients with poor central vision, as is often the case in patients requiring IVI. Much like patients with established glaucoma, those with high OR could need to be treated more rigorously with acute pre-treatment IOP lowering medications on injection day, chronic IOP therapy, glaucoma surgery to prevent glaucoma development or progression, or half-dose (smaller volume) injections. Post-IVI paracentesis has been

proposed to temper IOP spikes but has been associated with an increased risk of endophthalmitis.[24–26] Slow release devices might also be advantageous because they would require less frequent injections.[27]

A recent case from our clinic illustrates the use of this innovation. A male patient in the seventh decade of life presented to our glaucoma clinic with advanced open-angle glaucoma that had progressed to central islands on visual fields despite IOPs in the high teens. We proposed filtration surgery but found that he also had early proliferative diabetic retinopathy with macular oedema in his right eye. Was it safe to administer anti-VEGF IVI before filtration surgery? A large IOP spike might threaten his fixation. Therefore, we measured his OR and found it to be 0.00958 μL^{-1}. Using the regression equation described in the Results section, this predicted an IOP spike of 11.0 mm Hg, which we considered safe. A retina colleague proceeded with the IVI and measured a change of IOP of 10 mm Hg immediately following injection.

While IOP elevations following IVI are thought to return to normal levels within 30–60 min,[2 3] longer durations of these IOP spikes may occur in some eyes, particularly in those with existing glaucoma.[2 3] In fact, with repeated IVI, subjects can develop chronic IOP elevation.[28–31] The mechanism behind this is poorly understood, with multiple proposed hypotheses including outflow obstruction from protein aggregates and/or silicone oil droplets as contaminants from the syringes used or the anti-VEGF molecules themselves.[3] It remains unknown whether the rigidity of the eye could influence the duration of IOP elevations following IVI.

Despite the absence of prospective trials to show whether transient IOP spikes following IVI contribute to glaucomatous damage or not, various clinical and experimental studies have shown that transient increases in IOP can compress prelaminar tissue,[32 33] alter optic nerve blood flow,[34] cause axonal transport blockage[35] and alter electroretinogram responses.[36] These findings suggest that IOP spikes have the potential to cause optic nerve damage. Recent clinical studies may support this point in demonstrating increased glaucoma surgery procedures in patients with repeated IVI.[37 38]

The advantages of the method we used to measure OR in this study include its non-invasive nature, its ease-of-use and its reliability and safety compared with invasive techniques.[7 11] Based on OCT video-rate imaging to measure the pulsatile ocular volume change, it could be easily implemented in a clinical setting where OCT is widely available. Clinics where IVI are performed usually are equipped with an OCT device. Some limitations to consider regarding this technique is the possible obstruction of the choroid–sclera interface by macular oedema or scarring in subjects with exudative retinal conditions. As discussed, imaging of the CSI can be improved by using an OCT with longer wavelengths which penetrate deeper in tissue, such as SS-OCT. Studies have shown that SS-OCT can minimise light scattering in deeper tissues of the eye, such as the choroid. This technology can permit CSI identification in 100% of cases according to a study by Copete *et al*.[39] Another strategy that can be employed is to image away from the diseased region in the eye, instead of submacularly if the CSI visualisation is hindered or shadowed by disease processes. In our unpublished data, imaging at the posterior pole, away from the macula, yields a similar OR coefficient than imaging at the macula in healthy eyes. We also found that CCT, CH and CRF, other parameters of the corneo-scleral shell, did not predict the magnitude of IOP spikes and therefore do not appear to be a surrogate for OR. The finding regarding CCT is consistent with previous investigations,[10] while a pilot study found lower CH to be associated with elevated IOP following IVI.[40]

Finally, this study shows for the first time a strong and positive correlation between the OR and acute IOP spikes in eyes that undergo therapeutic IVI. Further research could lead the way for future assessment of the clinical impact of OR in a number of ocular diseases, leading to the development of improved screening and treatment protocols.

Contributors DS, SC and ML designed the study. DS, DD, RD and FAR were involved in data collection. DS, A-AS, JM, SC and ML analysed and interpreted the data. DS and A-AS drafted the first manuscript.

Funding This work was supported by the Canadian Institutes of Health Research (grant number 311562, SC and ML); the Natural Sciences and Engineering Research Council of Canada (grant number RGPIN-2016–04227, SC); the Fonds de Recherche en Ophtalmologie de l'Université de Montréal (ML and SC), the Fonds de Recherche du Québec—Santé (SC and DS) and the Glaucoma Research Society of Canada (ML).

Competing interests None declared.

Patient consent for publication Informed consent was obtained from all participants prior to testing.

Ethics approval This study was approved by the Maisonneuve-Rosemont Hospital Institutional Review Board and conformed to the principles of the Declaration of Helsinki.

Provenance and peer review Not commissioned; externally peer reviewed.

Data availability statement All data relevant to the study are included in the article or uploaded as supplementary information.

ORCID iDs
Diane N Sayah http://orcid.org/0000-0002-3734-403X
Andrei-Alexandru Szigiato http://orcid.org/0000-0003-0862-9068

REFERENCES

1 Lemos-Reis R, Moreira-Gonçalves N, Melo AB, *et al*. Immediate effect of intravitreal injection of bevacizumab on intraocular pressure. *Clin Ophthalmol* 2014;8:1383–8.
2 Kim JE, Mantravadi AV, Hur EY, *et al*. Short-term intraocular pressure changes immediately after intravitreal injections of anti-vascular endothelial growth factor agents. *Am J Ophthalmol* 2008;146:930–4.
3 Kampougeris G, Spyropoulos D, Mitropoulou A. Intraocular pressure rise after anti-VEGF treatment: prevalence, possible mechanisms and correlations. *J Curr Glaucoma Pract* 2013;7:19–24.
4 Resta V, Novelli E, Vozzi G, *et al*. Acute retinal ganglion cell injury caused by intraocular pressure spikes is mediated by endogenous extracellular ATP. *Eur J Neurosci* 2007;25:2741–54.
5 Pallikaris IG, Kymionis GD, Ginis HS, *et al*. Ocular rigidity in patients with age-related macular degeneration. *Am J Ophthalmol* 2006;141:611.
6 Pallikaris IG, Kymionis GD, Ginis HS, *et al*. Ocular rigidity in living human eyes. *Invest Ophthalmol Vis Sci* 2005;46:409–14.
7 Beaton L, Mazzaferri J, Lalonde F, *et al*. Non-invasive measurement of choroidal volume change and ocular rigidity through automated segmentation of high-speed OCT imaging. *Biomed Opt Express* 2015;6:1694–706.
8 Wang J, Freeman EE, Descovich D, *et al*. Estimation of ocular rigidity in glaucoma using ocular pulse amplitude and pulsatile choroidal blood flow. *Invest Ophthalmol Vis Sci* 2013;54:1706–11.
9 Sigal IA, Flanagan JG, Ethier CR. Factors influencing optic nerve head biomechanics. *Invest Ophthalmol Vis Sci* 2005;46:4189–99.
10 Fuest M, Kotliar K, Walter P, *et al*. Monitoring intraocular pressure changes after intravitreal ranibizumab injection using rebound tonometry. *Ophthalmic Physiol Opt* 2014;34:438–44.
11 Sayah DN, Mazzaferri J, Ghesquière P, *et al*. Non-invasive in vivo measurement of ocular rigidity: clinical validation, repeatability and method improvement. *Exp Eye Res* 2020;190:107831.
12 Friedenwald JS. Contribution to the theory and practice of Tonometry*. *Am J Ophthalmol* 1937;20:985–1024.
13 Mazzaferri J, Beaton L, Hounye G, *et al*. Open-source algorithm for automatic choroid segmentation of OCT volume reconstructions. *Sci Rep* 2017;7:42112.
14 Alm A, Bill A. Ocular and optic nerve blood flow at normal and increased intraocular pressures in monkeys (Macaca irus): a study with radioactively labelled microspheres including flow determinations in brain and some other tissues. *Exp Eye Res* 1973;15:15–29.
15 Erdfelder E, Faul F, Buchner A. GPOWER: a general power analysis program. *Behav Res Method Instrument Comp* 1996;28:1–11.

16 Morris HJ, Tang J, Cruz Perez B, *et al*. Correlation between biomechanical responses of posterior sclera and IOP elevations during micro intraocular volume change. *Invest Ophthalmol Vis Sci* 2013;54:7215–22.
17 Ethier CR, Johnson M, Ruberti J. Ocular biomechanics and biotransport. *Annu Rev Biomed Eng* 2004;6:249–73.
18 van der Jagt LH, Jansonius NM. Three portable tonometers, the TGDc-01, the ICARE and the Tonopen XL, compared with each other and with Goldmann applanation tonometry*. *Ophthalmic Physiol Opt* 2005;25:429–35.
19 Murray CD, Wood D, Allgar V, *et al*. Short-Term intraocular pressure trends following intravitreal ranibizumab injections for neovascular age-related macular degeneration-the role of oral acetazolamide in protecting glaucoma patients. *Eye* 2014;28:1218–22.
20 Gregori NZ, Weiss MJ, Goldhardt R, *et al*. Ocular decompression with cotton swabs lowers intraocular pressure elevation after intravitreal injection. *J Glaucoma* 2014;23:508–12.
21 Wei WB, Xu L, Jonas JB, *et al*. Subfoveal choroidal thickness: the Beijing eye study. *Ophthalmology* 2013;120:175–80.
22 Herman C. What makes a screening exam "good"? *Virtual Mentor* 2006;8:34–7.
23 Quigley HA, Broman AT. The number of people with glaucoma worldwide in 2010 and 2020. *Br J Ophthalmol* 2006;90:262–7.
24 Avery RL, Bakri SJ, Blumenkranz MS, *et al*. Intravitreal injection technique and monitoring: updated guidelines of an expert panel. *Retina* 2014;34 (Suppl 12):S1-S18–18.
25 Helbig H, Noske W, Kleineidam M, *et al*. Bacterial endophthalmitis after anterior chamber paracentesis. *Br J Ophthalmol* 1995;79:866.
26 Joondeph BC, Joondeph HC. Purulent anterior segment endophthalmitis following paracentesis. *Ophthalmic Surg* 1986;17:91–3.
27 Kang-Mieler JJ, Osswald CR, Mieler WF. Advances in ocular drug delivery: emphasis on the posterior segment. *Expert Opin Drug Deliv* 2014;11:1647–60.
28 Adelman RA, Zheng Q, Mayer HR. Persistent ocular hypertension following intravitreal bevacizumab and ranibizumab injections. *J Ocul Pharmacol Ther* 2010;26:105–10.
29 Good TJ, Kimura AE, Mandava N, *et al*. Sustained elevation of intraocular pressure after intravitreal injections of anti-VEGF agents. *Br J Ophthalmol* 2011;95:1111–4.
30 Hoang QV, Mendonca LS, Della Torre KE, *et al*. Effect on intraocular pressure in patients receiving unilateral intravitreal anti-vascular endothelial growth factor injections. *Ophthalmology* 2012;119:321–6.
31 Hoang QV, Tsuang AJ, Gelman R, *et al*. Clinical predictors of sustained intraocular pressure elevation due to intravitreal anti-vascular endothelial growth factor therapy. *Retina* 2013;33:179–87.
32 Agoumi Y, Sharpe GP, Hutchison DM, *et al*. Laminar and prelaminar tissue displacement during intraocular pressure elevation in glaucoma patients and healthy controls. *Ophthalmology* 2011;118:52–9.
33 Strouthidis NG, Fortune B, Yang H, *et al*. Effect of acute intraocular pressure elevation on the monkey optic nerve head as detected by spectral domain optical coherence tomography. *Invest Ophthalmol Vis Sci* 2011;52:9431–7.
34 Michelson G, Groh MJ, Langhans M. Perfusion of the juxtapapillary retina and optic nerve head in acute ocular hypertension. *Ger J Ophthalmol* 1996;5:315–21.
35 Quigley HA, Anderson DR. Distribution of axonal transport blockade by acute intraocular pressure elevation in the primate optic nerve head. *Invest Ophthalmol Vis Sci* 1977;16:640–4.
36 Choh V, Gurdita A, Tan B, *et al*. Short-Term moderately elevated intraocular pressure is associated with elevated scotopic electroretinogram responses. *Invest Ophthalmol Vis Sci* 2016;57:2140–51.
37 Eadie BD, Etminan M, Carleton BC, *et al*. Association of repeated Intravitreous bevacizumab injections with risk for glaucoma surgery. *JAMA Ophthalmol* 2017;135:363–8.
38 Du J, Patrie JT, Prum BE, *et al*. Effects of intravitreal anti-VEGF therapy on Glaucoma-like progression in susceptible eyes. *J Glaucoma* 2019;28:1035–40.
39 Copete S, Flores-Moreno I, Montero JA, *et al*. Direct comparison of spectral-domain and swept-source OCT in the measurement of choroidal thickness in normal eyes. *Br J Ophthalmol* 2014;98:334–8.
40 Chikun E, Karpilova M, Kuznetsov A, *et al*. Role of biomechanical properties of fibrous coat of the eye in intraocular pressure changes in patients after intravitreal ranibizumab injections. Pilot study. *Invest Ophthalmol Vis Sci* 2013;54:6307.

Chapter 9 – Lower Ocular Rigidity in Myopia

In this chapter, we will briefly present the relationship between OR and myopia. Our motivation is to show that the pathophysiological mechanisms governing axial myopia, a risk factor for glaucoma and sight-threatening disease (525), can be studied using our method. This is particularly relevant due to its reliability, non-invasive nature and ease-of-use, which could be employed to study myopia longitudinally from early childhood to adulthood. In turn, this could lead to novel treatments to prevent myopia progression. (Manuscript in preparation)

Abstract

The biomechanical properties of the sclera are thought to be an important characteristic in axial myopia. Longer eyes are expected to have lower rigidity due to connective tissue alterations. The purpose of this study is to measure ocular rigidity using a novel, non-invasive measurement method and to compare OR values in healthy myopic and non-myopic eyes, as well as in glaucomatous myopic and non-myopic eyes. Based on Friedenwald's equation, this method involves video-rate OCT imaging of the choroid coupled with a novel automated segmentation algorithm to measure the pulsatile ocular volume change, as well as Dynamic Contour Tonometry to determine the ocular pulse amplitude, and thus calculate OR. Fifty-nine adults with healthy eyes (17 myopic eyes with axial length ≥ 25.00mm, and 42 non-myopic eyes), and 53 adults diagnosed with open-angle glaucoma (OAG; 25 axial myopic eyes and 28 non-myopic eyes) were recruited and OR measurement was carried out. A Welch one-way ANOVA with Tukey post hoc test was conducted to compare differences between groups. There was a significant difference ($p<0.001$) in the OR coefficients between healthy myopic eyes (OR= 0.0154 ± 0.007/µL) and healthy non-myopic eyes (OR = 0.0329 ± 0.013/µL). Similarly, OR was significantly lower ($p=0.020$) in glaucomatous myopic eyes (OR = 0.0189 ± 0.007/µL) than in glaucomatous non-myopic eyes (OR = 0.0282 ± 0.014/µL). A negative correlation between OR and AL was also found in all 112 eyes ($r=-0.475$, $p<0.001$). This confirms that eyes with axial myopia have lower OR than non-myopic eyes, both in healthy eyes and eyes with OAG. Future longitudinal investigations of OR

change over time may help elucidate the mechanisms leading to myopia progression, and whether low OR leads to myopia.

Introduction

Axial myopia is characterized by an eye that is too long for its focal length, leading to distance vision impairment if left uncorrected. With a global prevalence predicted to reach 50% by 2050 (526), and an increased risk of developing sight-threatening diseases including open-angle glaucoma (OAG) (426, 527, 528), the pathophysiology of axial myopia warrants further investigation. Ocular biomechanics are thought to be involved in the development and progression of axial myopia. There is evidence for an inverse correlation between OR and axial length (AL) in the literature (23, 422). Previous reports showed thinner peripapillary sclera and lamina cribrosa (423), as well as scleral remodeling in elongated eyes (424). Increased scleral creep, suggestive of lower OR, was associated with ocular growth in induced experimental myopia (529). These changes in the composition of the sclera and lamina cribrosa can lead to alterations in the biomechanical environment in the eye, facilitating the elongation of the eye. These alterations can also contribute to axonal damage and glaucoma via greater IOP-induced strain in longer, more compliant eyes (427).

The objective of this study is to measure OR using our clinical method and evaluate differences in OR values between healthy axial myopic and non-myopic eyes as well as those with concurrent open-angle glaucoma (OAG). Axial myopic eyes are expected to have lower rigidity due to connective tissue alterations.

Methods

This study followed the tenets of the Declaration of Helsinki and was approved by the Maisonneuve-Rosemont Hospital institutional review board. Informed consent was obtained from all participants prior to testing.

Adult subjects with healthy eyes or with OAG were recruited in this study. A complete ocular examination was performed for all participants. Normal subjects had intraocular pressure (IOP) less than 21 mmHg, normal optic nerve appearance on fundus exam, normal visual fields and no

other ocular disease. Subjects with OAG had open (non-occludable) angles on gonioscopy, a glaucomatous optic nerve appearance, as well as repeatable structural and/or functional findings with optical coherence tomography (OCT; Cirrus 5000, Carl Zeiss Meditec AG, Dublin, USA) imaging and Humphrey visual field (VF; Zeiss Humphrey Systems, Dublin, California, USA) testing (SITA standard threshold 24–2 strategy). Participants were required to have clear media, steady fixation, and the ability to fixate a target light with the study or contralateral eye. Patients with a previous history of intraocular surgery (except cataract extraction) including trabeculectomy, tube shunt, and refractive surgery were excluded. Other exclusion criteria included secondary glaucoma, non-glaucomatous optic neuropathy, any retinopathy, and documented systemic collagen disease. OR was measured non-invasively using our previously described method (27, 494).

The cohort was divided into four groups (healthy axial myopic, healthy non-myopic, glaucomatous axial myopic, glaucomatous non-myopic) according to AL measurements and refractive error (RE). The spherical equivalent was considered for RE assessment. We defined the myopic groups as having an AL ≥ 25.00 mm and a myopic RE of ≤-0.50 diopter (D) (526, 530, 531). The RE threshold was set as the most commonly used definition for myopia in published prevalence studies (526, 530). While the cut-off for pathologic axial myopia is generally defined as 26.0 mm or 26.5 mm in most studies, we established a lower cut-off due to recent findings suggesting higher risk of sight-threatening complications, namely myopic maculopathy, at shorter AL values (in the 25mm range) (531). Non-myopic eyes were defined as having an AL < 25.00 mm and RE > -0.50 diopter (D). Finally, the correlation between OR and AL was computed for all subjects.

Statistical analyses were performed using SPSS statistical software (version 23; SPSS, Inc., Chicago, IL). Descriptive analysis of baseline demographics was carried out and presented as the mean ± standard deviation. To compare OR in the four groups, and between the corresponding myopic and non-myopic groups, a one-way ANOVA with Tukey post-hoc test was carried out. If the assumption of equal variances by Levene's Test for Equality of Variances was not respected, a Welch one-way ANOVA test was conducted. The Pearson correlation coefficient was then computed for all subjects. For all statistical tests, a p-value inferior to 0.05 was considered significant.

Results

A total of 112 adult subjects were recruited, 59 with healthy eyes and 53 with OAG. Out of the healthy eyes, 17 were myopic (11 OD; 7 M) and 42 were non myopic (28 OD; 18 M), whereas 25 were myopic (15 OD; 15 M) and 28 were non-myopic (10 OD; 13 M) in the OAG group. One eye per subject was examined. The baseline demographics are presented in Table 10 for all 4 groups. As expected, a statistically significant difference in AL, RE and ocular pulse amplitude (OPA) is reported between the myopic and non-myopic groups in both healthy and glaucomatous eyes. CCT, CH and CRF values were not discriminative between myopic and non-myopic eyes within healthy or glaucomatous eyes respectively.

	Myopia (n=17)	No Myopia (n=42)	p-value	Glaucoma and Myopia (n=25)	Glaucoma, No Myopia (n=28)	p-value	All Groups: p-value
Age (years)	58±21	67±16	0.111	64±9	69±8	0.588	0.076
RE (D)	-4.38±3.53	+1.13±1.06	<0.001	-6.30±3.15	+0.93±1.09	<0.001	<0.001
AL (mm)	25.80±0.65	23.34±0.58	<0.001	26.49±1.26	23.71±0.62	<0.001	<0.001
Pascal-IOP (mmHg)	17.6±2.8	16.8±2.9	0.927	20.4±5.8	18.7±4.5	0.446	0.007
OPA (mmHg)	2.3±0.4	3.2±1.0	0.011	2.6±1.2	3.3±1.2	0.040	0.001
CCT (µm)	544±40	550±33	0.968	544±39	523±41	0.186	0.036
CH (mmHg)	9.6±2.1	10.1±1.5	0.879	8.9±1.8	8.8±2.0	0.991	0.027
CRF (mmHg)	9.9±1.8	10.1±1.6	0.991	10.0±2.0	8.9±1.6	0.124	0.038
OR (μL^{-1})	0.015±0.007	0.033±0.013	<0.001	0.019±0.007	0.028±0.014	0.020	<0.001
MD (dB)	-0.06±0.25	0.04±0.25	0.999	-2.96±3.28	-4.39±4.60	0.282	<0.001
PSD (dB)	0.17±0.70	0.23±0.57	1.000	3.66±3.18	4.45±2.94	0.572	<0.001
Average RNFLt (µm)	90±11	94±12	0.826	76±10	74±10	0.899	<0.001

Data is presented as the mean ± standard deviation where applicable. RE=Refractive error; D=Diopter; AL= Axial length; IOP=Intraocular pressure; OPA=Ocular pulse amplitude; CCT=Central corneal thickness; CH=Corneal hysteresis; CRF=Corneal resistance factor; OR=Ocular rigidity; MD=Mean defect; PSD=Pattern standard deviation; RNFLt= Retinal nerve fiber layer thickness.

Table 10. – Baseline characteristics of participants in the healthy axial myopic group, healthy non-myopic group, glaucomatous myopic group and glaucomatous non-myopic group.

A Welch one-way ANOVA was carried out to compare the four groups, and showed statistically significant differences in OR between all groups ($p<0.001$) as shown in Figure 16. A post hoc Tukey test showed that OR values between healthy axial myopic eyes (OR= 0.0154 ± 0.007/µL) and healthy non-myopic eyes (OR = 0.0329 ± 0.013/µL) were significantly different ($p<0.001$). In the cohort of glaucomatous subjects, OR was also significantly lower ($p=0.020$) in the myopic eyes (OR = 0.0189 ± 0.007/µL) compared to the non-myopic eyes (OR = 0.0282 ± 0.014/µL).

A negative correlation was also found between OR and AL ($r=-0.475$, $p<0.001$) in all 112 eyes, as displayed in Figure 17.

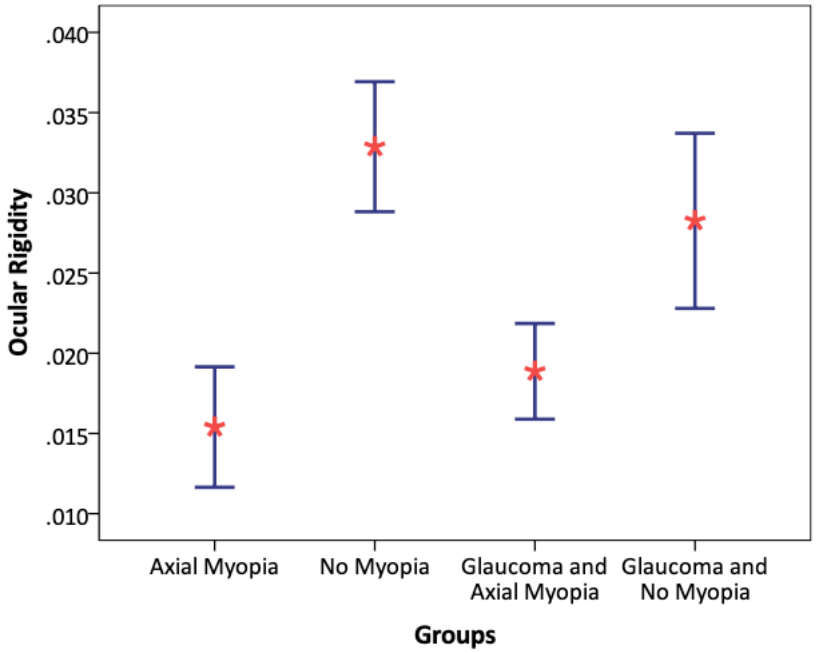

Figure 16. – Ocular rigidity differences between healthy axial myopic (0.015±0.007/µL) and non-myopic (0.033±0.013/µL) eyes ($p<0.001$), as well as glaucomatous axial myopic (0.0189±0.007/µL) and non-myopic eyes (0.0282±0.014/µL) ($p=0.020$). Data is presented as mean of OR coefficients and 95% confidence intervals.

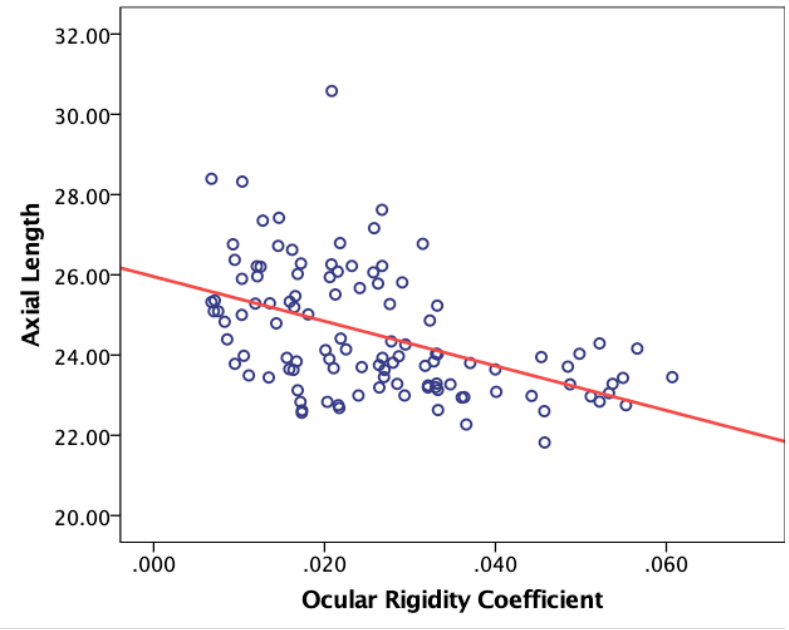

Figure 17. – Linear regression plot showing a moderate positive correlation ($r = -0.475$, $p < 0.001$) between the ocular rigidity (OR) coefficient and ocular axial length (AL) in 112 eyes. A significant regression equation was found: AL = 25.95mm – 55.62mm·µL × OR, $R^2 = 0.23$.

Discussion

This brief report confirms previous findings and shows that OR is lower in axial myopia, both in healthy eyes and those with concurrent OAG. Using a direct, non-invasive and readily usable method, differences between axial myopic and non-myopic eyes can be detected. This is relevant for three reasons: 1) this further confirms the validity of our method, as it can detect OR differences between these two groups, 2) this confirms that the eye is more compliant in axial myopia, which may help explain the increased risk of developing OAG and myopic chorioretinal degeneration (426, 527, 528), and 3) the method used to measure OR is direct, non-invasive, uses readily available equipment, and can thus be used to study OR in myopia in large-scale and longitudinal studies. In an era where efforts are deployed to halt the progression of axial myopia and reduce its potential for vision loss, investigating the role of low OR in the elongation of the eye could be particularly useful, particularly as novel treatments to alter the stiffness of the sclera are being developed (446, 532, 533).

Chapter 10 – Discussion

10.1 Synthesis

In this thesis work, the validity of a novel optical method to measure OR was improved and demonstrated and the relevance of OR in ocular diseases, particularly OAG was investigated.

10.1.1 Method Validation and Improvement

Until recently, there was no reliable, non-invasive clinical method to measure OR directly in living human eyes. Such a method has been developed recently, and published in 2015 (27). Based on the measurements of ΔV from video-rate OCT imaging coupled with automated choroidal segmentation, and of the pulsatile IOP change using Pascal tonometry, the OR coefficient can be computed using Friedenwald's equation. An improved mathematical model was proposed to extrapolate ΔV from submacular ΔCT that would account for the peripheral shape of the choroid, contrary to the previous model that was oversimplified (494). This new model remains simple enough to be used in a clinical setting as it uses easily measurable properties of the eye. The measurement of AL and ACD was initially proposed to be carried out in future iterations to determine the diameter of the spheres used in this model. With the onset of newer biometry devices, it is recommended that an additional parameter, the lens thickness (LT), be measured to further improve this model's accuracy. Thus, the diameter of the inner sphere, or AL_{adj}, would be determined as the difference between the measured AL and the effective lens position (ACD+0.5*LT), rendering this a more robust measurement when phakic status is considered. One caveat of this model remains: it considers the globe to be spherical, and should not be applied in eyes with a staphyloma or other shape irregularities. Despite this limitation, implications for the development of such a method are significant. This non-invasive method was validated by comparing OR coefficients obtained with those obtained using an invasive procedure involving intravitreal injections in the same eyes. The new mathematical model yielded OR values which are closer to those obtained using the invasive procedure and previously reported techniques. A strong correlation between the OR coefficients using both methods was found, with a Spearman coefficient of 0.853 ($p < 0.001$). Both intrasession and intersession repeatability were assessed,

with an intraclass correlation coefficient of 0.925, 95% CI [0.881, 0.953] and 0.950, 95% CI [0.763, 0.990] respectively. This confirmed the validity and good repeatability of OR measurements using our non-invasive clinical method.

By validating the method, a more precise estimation of ΔV was enabled. A question remains: can one estimate the pulsatile ocular volume from the pulsatile choroidal thickness change? Considering that the choroid accounts for about 90% of the total ocular blood flow, it can be assumed to be a fair approximation. Furthermore, if the AH turnover rate and ΔV are considered, we realize that the former is very small in comparison with the latter. Assuming a heart rate of 1Hz, while the AH turnover rate is on average 2.4 µl/min, the ΔV per minute would be 438 µl/min (the average ΔV is 7.3 µl per heartbeat, according to our published findings (494)). We can thus effectively use video-rate OCT imaging coupled with our segmentation algorithm to reliably and directly measure ΔV, a parameter related to choroidal blood flow.

The development of this optical method fills a big gap that once limited the effective study of ocular biomechanics *in vivo*. Previously, the interpretation of OR results with non-invasive measurement techniques had to be done carefully, and invasive methods were not suitable for large scale testing. The development of an accurate and non-invasive instrument to measure OR can now permit large scale and longitudinal studies to be carried out, to effectively determine whether low or high OR predispose to OAG, and how OR changes over the course of the disease. We speculate that ultimately this method could become a new diagnostic tool for assessing and predicting the progression of glaucomatous optic neuropathy, myopia and other diseases.

10.1.2 Relevance of Ocular Rigidity in Disease

We investigated the relevance of OR in healthy and diseased eyes, including OAG and axial myopia, as well as in preventing glaucoma in patients with exudative retinal diseases.

First, it was demonstrated, for the first time, that lower OR is a risk factor for neuro-retinal glaucomatous damage. In a cohort of subjects with healthy eyes, suspect discs or primary open-angle glaucoma, a modest but positive correlation between OR and structural OCT-based parameters was found. More specifically, this means that a more compliant eye is associated with thinner GCC and RNFL. Furthermore, the correlations obtained between OR and structural

damage parameters were comparable to those obtained with recognized risk factors such as Tmax, CH, CRF and CCT. To investigate whether OR plays a greater role in certain subgroups of glaucoma patients, a pilot study looking at differences between vasospastic and atherosclerotic patients was carried out. A strong correlation was reported between low OR and glaucomatous damage in patients with concurrent vasospasticity, compared with those with ischemic vascular disease. Despite some limitations including a small sample size and the use of a questionnaire instead of objective testing to establish the presence of vasospasticity, the results of this pilot study seem to confirm a greater susceptibility to glaucoma due to ocular biomechanical properties in vasospastic patients. This corroborates previous findings (144, 145) and may also translate to an increased benefit for therapeutic IOP-lowering in vasospastic patients, especially those with lower OR, in the clinical management of glaucoma.

Then, we aimed to measure OR and investigate its relationship with corneal biomechanical parameters including CH, CRF and CCT in both healthy and glaucomatous eyes. We showed no significant correlation between OR and CCT, no correlation between CH and OR after adjusting for confounding variables, and a weak adjusted correlation between CRF and OR in glaucomatous eyes. This is important as it indicates that there is limited association between the biomechanical properties of the cornea and those of the entire ocular globe, and that corneal biomechanical parameters are not a surrogate measurement for overall OR.

Always in an effort to prevent glaucomatous damage, we developed a model to predict the magnitude of IOP spikes following therapeutic intravitreal injections of bevacizumab from the OR coefficient in patients with exudative retinal diseases. We showed that IOP spikes = 699.94 mmHg·µL $\times$ OR + 4.92 mmHg, and that IOP spikes and OR are strongly correlated (r_s=0.758, $p<0.001$). For the first time, this study showed that higher IOP elevations occur in more rigid eyes. We show once again that corneal biomechanical parameters do not appear to be a surrogate for OR, as they did not predict the magnitude of IOP spikes. In addition, the findings of our study indicate that the non-invasive measurement of OR could be an effective tool in identifying patients at risk of IOP spikes following IVI in a clinical setting. We discussed various strategies to improve the visualization of the CSI, and thus the yield of our method in eyes with exudative retinal diseases. The largest study carried out with the Spectralis SD-OCT to

measure subfoveal choroidal thickness reported a success rate of 93% out of 3468 subjects by averaging 100 scans and carrying out manual segmentation at specific locations along the b-scan (534). Since our method involves dynamic imaging, as opposed to static, that must be faster than the heart rate frequency, we only average 5 scans per frame. Our segmentation is automated and performed along the width of the b-scan and must detect the subtle thickness change corresponding to choroidal filling. We are currently working on several fronts to improve this yield in challenging patients. These strategies include imaging away from the obstruction (lesion/edema), software improvements to our segmentation algorithms, and migrating to swept-source OCT devices with longer, better penetrating wavelengths and faster acquisition, for better image averaging.

Finally, we were able to confirm OR differences between healthy non-myopic (OR = 0.033 ± 0.013/µL) and axial myopic (OR= 0.015 ± 0.007/µL) eyes, as well as between glaucomatous non-myopic (OR = 0.0282 ± 0.014/µL) and myopic eyes (OR = 0.0189 ± 0.007/µL). A negative correlation between OR and AL ($r=-0.475$, $p<0.001$) was also demonstrated. By its nature and ease of use, this non-invasive methodology could be used to measure OR and investigate its role in myopia and glaucoma progression in large scale, longitudinal studies.

Although much remains to be investigated, our findings bring some light unto the pathophysiology of ocular diseases, particularly glaucoma. The biomechanical paradigm of glaucoma stipulates that IOP produces stress and strain within ocular tissues which ultimately lead to RGC damage (13). While the ONH's response has been found to depend on eye-specific geometrical and material properties, it is interesting that finite element models found the stiffness of the sclera to be the most influential property on the biomechanical response of the ONH to IOP. We now know that low OR is correlated with glaucomatous damage, almost as well as IOP (Tmax). This may favor the theory that OR is lower in early glaucoma, engendering axonal stretching and damage, and that OR increases in the later stages of the disease.

10.2 Future Work

Despite the tremendous progress that has been achieved in understanding how biomechanical properties of the eye are critical in glaucoma, the pathophysiological mechanisms leading to

axonal degeneration in this blinding disease remain unclear. Our reliable, non-invasive OR measurement method will help us to better understand whether having a low or high OR suggests a predisposition for POAG or whether it simply reflects a change caused by the condition. A major obstacle in these studies is that OR seems to become more rigid both with aging and as glaucoma becomes more advanced. These factors can obscure the influence of low ocular rigidity when a heterogeneous population is studied. Overcoming these obstacles would require a long prospective study of early glaucoma patients. We will also need to evaluate the effect of numerous factors on OR, including medication, ethnic origin and cardiovascular disease. The idea that perhaps the rigidity of the eye can modulate the amount of blood pumped into the eye (ΔV), as opposed to their strong correlation being solely based on the use of Friedenwald's equation to compute OR from ΔV, is also intriguing and will need to be assessed.

To provide a complete picture of the optic nerve's biomechanical responses in glaucoma, we will need to evaluate the interplay between scleral and laminar stiffness. Most attempts to study LC compliance *in vivo* measure laminar displacement with IOP change (349, 468, 469, 471, 472, 485, 486, 535) or pulsatility (27, 536, 537). While early studies used scanning laser ophthalmoscopy to measure mean cup depth, IOP-induced deformation of the prelaminar neural tissue was not found to be a good surrogate for the deformation of the LC (401). Improved imaging methods such as OCT are now used for the direct visualization of the LC deeper in the ONH tissue (538). While this remains a challenge, coupling the laminar biomechanical properties with OR measurements in a same eye would be ideal to understand how RGC axonal damage is mediated by scleral and laminar interactions. We think that perhaps glaucoma predisposition occurs from a mismatch between scleral and laminar stiffness. However, this hypothesis remains to be fully assessed.

We think that the integration of measured OR in biomechanical modeling could be useful to evaluate the interaction between scleral and laminar stiffness. While numerical models most often base scleral properties on data obtained *ex vivo*, our method would enable the inclusion of OR into these models. This has the potential to improve not only our understanding of ocular biomechanics' role in glaucoma, but also of permitting the customization of these models for live patients' eyes.

Perhaps the measurement of OR would also help predict the progression of OAG in patients, hence giving clinicians the ability to identify which patients will require more aggressive treatment. Currently, the only evidence-based treatment to prevent the progression of OAG is to lower IOP, regardless of baseline IOP (45-48). This supports the importance of biomechanics in OAG. IOP reduction can be carried out using pharmaceuticals, laser trabeculoplasty, surgical procedures, or a combination of these methods. However, current therapeutic options to lower IOP may also bring forth changes in the biomechanical properties of the corneoscleral shell (18, 357, 419). Commonly used hypotensive drugs may have an impact on OR. On the other hand, while studies unequivocally show the benefit of IOP-lowering therapy in slowing structural and functional loss in glaucoma, this does not always halt the progression of the disease. Hence, the prevention and treatment of glaucoma remain an unsolved problem. This has fueled the development of neuroprotective treatments which do not rely on IOP reduction. Several experiments have shown some promise in protecting RGC following injury (539-545). One of them demonstrated that human recombinant insulin administered as eye drops could regenerate RGCs in experimental glaucoma (546).

Given that the biomechanical properties of the sclera and LC are involved in axonal damage in glaucoma, altering these properties may also protect against the disease. Indeed, the study of OR could lead to new avenues of therapy for glaucoma. We believe that our method could be extended to animal models, and that its use to measure OR in experimental studies could be useful in drug development. Attempts to alter the stiffness of ocular tissues to prevent initial RGC injury have been carried out (547). Potential therapeutic approaches include targeting the matrix metallo-proteinases which modify collagen stiffness, or UV-crosslinking of collagen as is currently performed for corneal ectasias (548) and attempted in the sclera (446, 532, 533). Of course, a central question to this treatment option remains: is a stiffer or a more compliant sclera protective against IOP-induced stress and strain? We believe that this thesis work has brought us closer to answering this question.

References

1. Quigley HA, Broman AT. The number of people with glaucoma worldwide in 2010 and 2020. Br J Ophthalmol. 2006;90(3):262-7.

2. Foster PJ, Buhrmann R, Quigley HA, Johnson GJ. The definition and classification of glaucoma in prevalence surveys. Br J Ophthalmol. 2002;86(2):238-42.

3. Sommer A, Tielsch JM, Katz J, Quigley HA, Gottsch JD, Javitt J, et al. Relationship between intraocular pressure and primary open angle glaucoma among white and black Americans. The Baltimore Eye Survey. Arch Ophthalmol. 1991;109(8):1090-5.

4. Suzuki Y, Iwase A, Araie M, Yamamoto T, Abe H, Shirato S, et al. Risk factors for open-angle glaucoma in a Japanese population: the Tajimi Study. Ophthalmology. 2006;113(9):1613-7.

5. Gordon MO, Beiser JA, Brandt JD, Heuer DK, Higginbotham EJ, Johnson CA, et al. The Ocular Hypertension Treatment Study: baseline factors that predict the onset of primary open-angle glaucoma. Arch Ophthalmol. 2002;120(6):714-20; discussion 829-30.

6. Quigley H, Anderson DR. The dynamics and location of axonal transport blockade by acute intraocular pressure elevation in primate optic nerve. Invest Ophthalmol. 1976;15(8):606-16.

7. Quigley HA, Anderson DR. Distribution of axonal transport blockade by acute intraocular pressure elevation in the primate optic nerve head. Invest Ophthalmol Vis Sci. 1977;16(7):640-4.

8. Quigley HA, Flower RW, Addicks EM, McLeod DS. The mechanism of optic nerve damage in experimental acute intraocular pressure elevation. Invest Ophthalmol Vis Sci. 1980;19(5):505-17.

9. Quigley HA, Addicks EM, Green WR, Maumenee AE. Optic nerve damage in human glaucoma. II. The site of injury and susceptibility to damage. Arch Ophthalmol. 1981;99(4):635-49.

10. Quigley HA, Addicks EM, Green WR. Optic nerve damage in human glaucoma. III. Quantitative correlation of nerve fiber loss and visual field defect in glaucoma, ischemic neuropathy, papilledema, and toxic neuropathy. Arch Ophthalmol. 1982;100(1):135-46.

11. Fechtner RD, Weinreb RN. Mechanisms of optic nerve damage in primary open angle glaucoma. Surv Ophthalmol. 1994;39(1):23-42.

12. Yan DB, Coloma FM, Metheetrairut A, Trope GE, Heathcote JG, Ethier CR. Deformation of the lamina cribrosa by elevated intraocular pressure. Br J Ophthalmol. 1994;78(8):643-8.

13. Sigal IA, Ethier CR. Biomechanics of the optic nerve head. Exp Eye Res. 2009;88(4):799-807.

14. Burgoyne CF, Downs JC, Bellezza AJ, Suh JK, Hart RT. The optic nerve head as a biomechanical structure: a new paradigm for understanding the role of IOP-related stress and strain in the pathophysiology of glaucomatous optic nerve head damage. Prog Retin Eye Res. 2005;24(1):39-73.

15. Sigal IA, Roberts MD, Girard MJA, Burgoyne CF, Downs JC. Chapter 20: Biomechanical Changes of the Optic Disc. In: Levin LA, Albert DM, editors. Ocular Disease: Mechanisms and Management. London: Elsevier; 2010. p. 153-64.

16. Sigal IA, Flanagan JG, Ethier CR. Factors influencing optic nerve head biomechanics. Invest Ophthalmol Vis Sci. 2005;46(11):4189-99.

17. Drance SM. The coefficient of scleral rigidity in normal and glaucomatous eyes. Arch Ophthalmol. 1960;63:668-74.

18. Agrawal KK, Sharma DP, Bhargava G, Sanadhya DK. Scleral rigidity in glaucoma, before and during topical antiglaucoma drug therapy. Indian J Ophthalmol. 1991;39(3):85-6.

19. Hommer A, Fuchsjager-Mayrl G, Resch H, Vass C, Garhofer G, Schmetterer L. Estimation of ocular rigidity based on measurement of pulse amplitude using pneumotonometry and fundus pulse using laser interferometry in glaucoma. Invest Ophthalmol Vis Sci. 2008;49(9):4046-50.

20. Ebneter A, Wagels B, Zinkernagel MS. Non-invasive biometric assessment of ocular rigidity in glaucoma patients and controls. Eye (Lond). 2009;23(3):606-11.

21. Coudrillier B, Tian J, Alexander S, Myers KM, Quigley HA, Nguyen TD. Biomechanics of the human posterior sclera: age- and glaucoma-related changes measured using inflation testing. Invest Ophthalmol Vis Sci. 2012;53(4):1714-28.

22. Dastiridou AI, Tsironi EE, Tsilimbaris MK, Ginis H, Karyotakis N, Cholevas P, et al. Ocular rigidity, outflow facility, ocular pulse amplitude, and pulsatile ocular blood flow in open-angle glaucoma: a manometric study. Invest Ophthalmol Vis Sci. 2013;54(7):4571-7.

23. Wang J, Freeman EE, Descovich D, Harasymowycz PJ, Kamdeu Fansi A, Li G, et al. Estimation of ocular rigidity in glaucoma using ocular pulse amplitude and pulsatile choroidal blood flow. Invest Ophthalmol Vis Sci. 2013;54(3):1706-11.

24. Quigley HA, Cone FE. Development of diagnostic and treatment strategies for glaucoma through understanding and modification of scleral and lamina cribrosa connective tissue. Cell Tissue Res. 2013;353(2):231-44.

25. Pallikaris IG, Dastiridou AI, Tsilimbaris MK, Karyotakis NG, Ginis HS. Ocular Rigidity. Expert Rev Ophthalmol. 2010;5(3):343-51.

26. Friedenwald JS. Contribution to the Theory and Practice of Tonometry. Am J Ophthalmol. 1937;20(10):985-1024.

27. Beaton L, Mazzaferri J, Lalonde F, Hidalgo-Aguirre M, Descovich D, Lesk MR, et al. Non-invasive measurement of choroidal volume change and ocular rigidity through automated segmentation of high-speed OCT imaging. Biomed Opt Express. 2015;6(5):1694-706.

28. Hayreh SS. Posterior Drainage of the Intraocular Fluid from the Vitreous. Exp Eye Res. 1966;5:123-44.

29. Goel M, Picciani RG, Lee RK, Bhattacharya SK. Aqueous humor dynamics: a review. Open Ophthalmol J. 2010;4:52-9.

30. Heys JJ, Barocas VH. A boussinesq model of natural convection in the human eye and the formation of Krukenberg's spindle. Ann Biomed Eng. 2002;30(3):392-401.

31. Tamm ER. The trabecular meshwork outflow pathways: structural and functional aspects. Exp Eye Res. 2009;88(4):648-55.

32. Goldmann H. [Minute volume of the aqueous in the anterior chamber of the human eye in normal state and in primary glaucoma]. Ophthalmologica. 1950;120(1-2):19-21.

33. Ascher KW. [Veins of the aqueous humor in glaucoma]. Boll Ocul. 1954;33(3):129-44.

34. Kaufman PL, Wiedman T, Robinson JR. Cholinergics. In: Sears ML, editor. Pharmacology of the Eye. Berlin, Heidelberg: Springer Berlin Heidelberg; 1984. p. 149-91.

35. Millar C, Kaufman PL. Aqueous humor: secretion and dynamics. In: Tasman W, Jaeger EA, editors. Duane's foundations of clinical ophthalmology. Philadelphia: Lippincott-Raven; 1995.

36. Brubaker RF. Flow of aqueous humor in humans [The Friedenwald Lecture]. Invest Ophthalmol Vis Sci. 1991;32(13):3145-66.

37. Gabelt BT, Kaufman PL. Aqueous humor hydrodynamics. In: Hart WM, editor. Adler's Physiology of the Eye. 9th ed. St. Louis: Mosby; 2003.

38. American Academy of Ophthalmology. Intraocular Pressure and Aqueous Humor Dynamics. In: Girkin CA, editor. Basic and Clinical Science Course: Glaucoma: American Academy of Ophthalmology; 2011. p. 17-32.

39. Grant WM. Clinical measurements of aqueous outflow. AMA Arch Ophthalmol. 1951;46(2):113-31.

40. Kass MA, Hart WM, Jr., Gordon M, Miller JP. Risk factors favoring the development of glaucomatous visual field loss in ocular hypertension. Surv Ophthalmol. 1980;25(3):155-62.

41. Last JA, Pan T, Ding Y, Reilly CM, Keller K, Acott TS, et al. Elastic modulus determination of normal and glaucomatous human trabecular meshwork. Invest Ophthalmol Vis Sci. 2011;52(5):2147-52.

42. Wang K, Johnstone MA, Xin C, Song S, Padilla S, Vranka JA, et al. Estimating Human Trabecular Meshwork Stiffness by Numerical Modeling and Advanced OCT Imaging. Invest Ophthalmol Vis Sci. 2017;58(11):4809-17.

43. Wang K, Read AT, Sulchek T, Ethier CR. Trabecular meshwork stiffness in glaucoma. Exp Eye Res. 2017;158:3-12.

44. Boland MV, Ervin AM, Friedman DS, Jampel HD, Hawkins BS, Vollenweider D, et al. Comparative effectiveness of treatments for open-angle glaucoma: a systematic review for the U.S. Preventive Services Task Force. Ann Intern Med. 2013;158(4):271-9.

45. Morrison JC, Nylander KB, Lauer AK, Cepurna WO, Johnson E. Glaucoma drops control intraocular pressure and protect optic nerves in a rat model of glaucoma. Invest Ophthalmol Vis Sci. 1998;39(3):526-31.

46. Heijl A, Leske MC, Bengtsson B, Hyman L, Bengtsson B, Hussein M, et al. Reduction of intraocular pressure and glaucoma progression: results from the Early Manifest Glaucoma Trial. Arch Ophthalmol. 2002;120(10):1268-79.

47. Kass MA, Heuer DK, Higginbotham EJ, Johnson CA, Keltner JL, Miller JP, et al. The Ocular Hypertension Treatment Study: a randomized trial determines that topical ocular hypotensive medication delays or prevents the onset of primary open-angle glaucoma. Arch Ophthalmol. 2002;120(6):701-13; discussion 829-30.

48. Garway-Heath DF, Crabb DP, Bunce C, Lascaratos G, Amalfitano F, Anand N, et al. Latanoprost for open-angle glaucoma (UKGTS): a randomised, multicentre, placebo-controlled trial. Lancet. 2015;385(9975):1295-304.

49. Stamper RL. A history of intraocular pressure and its measurement. Optom Vis Sci. 2011;88(1):E16-28.

50. Patel H, Gilmartin B, Cubbidge RP, Logan NS. In vivo measurement of regional variation in anterior scleral resistance to Schiotz indentation. Ophthalmic Physiol Opt. 2011;31(5):437-43.

51. Friedenwald JS. Tonometer calibration; an attempt to remove discrepancies found in the 1954 calibration scale for Schiotz tonometers. Trans Am Acad Ophthalmol Otolaryngol. 1957;61(1):108-22.

52. Friedenwald JS. Clinical significance of ocular rigidity in relation to the tonometric measurement. Trans Am Acad Ophthalmol Otolaryngol. 1949;53:262-4.

53. Imbert A. Theories ophthalmotonometres. Arch Ophthalmol. 1885;5:358-63.

54. Ehlers N, Bramsen T, Sperling S. Applanation tonometry and central corneal thickness. Acta Ophthalmol (Copenh). 1975;53(1):34-43.

55. Whitacre MM, Stein RA, Hassanein K. The effect of corneal thickness on applanation tonometry. Am J Ophthalmol. 1993;115(5):592-6.

56. Orssengo GJ, Pye DC. Determination of the true intraocular pressure and modulus of elasticity of the human cornea in vivo. Bull Math Biol. 1999;61(3):551-72.

57. Doughty MJ, Zaman ML. Human corneal thickness and its impact on intraocular pressure measures: a review and meta-analysis approach. Surv Ophthalmol. 2000;44(5):367-408.

58. Kohlhaas M, Boehm AG, Spoerl E, Pursten A, Grein HJ, Pillunat LE. Effect of central corneal thickness, corneal curvature, and axial length on applanation tonometry. Arch Ophthalmol. 2006;124(4):471-6.

59. Gunvant P, Newcomb RD, Kirstein EM, Malinovsky VE, Madonna RJ, Meetz RE. Measuring accurate IOPs: Does correction factor help or hurt? Clin Ophthalmol. 2010;4:611-6.

60. Garway-Heath DF, Kotecha A, Lerner F, Dayanir V, Brandt JD, Pepose J, et al. Measurement of intraocular pressure. In: Weinreb RN, Brandt JD, Garway-Heath DF, Medeiros FA, editors. Intraocular Pressure. Amsterdam: Kugler Publications; 2007. p. 17-58.

61. Luce DA. Determining in vivo biomechanical properties of the cornea with an ocular response analyzer. J Cataract Refract Surg. 2005;31(1):156-62.

62. Hong J, Xu J, Wei A, Deng SX, Cui X, Yu X, et al. A new tonometer--the Corvis ST tonometer: clinical comparison with noncontact and Goldmann applanation tonometers. Invest Ophthalmol Vis Sci. 2013;54(1):659-65.

63. Aziz K, Friedman DS. Tonometers-which one should I use? Eye (Lond). 2018;32(5):931-7.

64. Punjabi OS, Kniestedt C, Stamper RL, Lin SC. Dynamic contour tonometry: principle and use. Clin Exp Ophthalmol. 2006;34(9):837-40.

65. Boehm AG, Weber A, Pillunat LE, Koch R, Spoerl E. Dynamic contour tonometry in comparison to intracameral IOP measurements. Invest Ophthalmol Vis Sci. 2008;49(6):2472-7.

66. Medeiros FA, Weinreb RN. Evaluation of the influence of corneal biomechanical properties on intraocular pressure measurements using the ocular response analyzer. J Glaucoma. 2006;15(5):364-70.

67. Saari JC. Metabolism and photochemistry in the retina. In: Moses RA, Hart WM, editors. Adler's Physiology of the Eye Clinical Application. St Louis: Mosby; 1987. p. 356-73.

68. Buttery RG, Hinrichsen CF, Weller WL, Haight JR. How thick should a retina be? A comparative study of mammalian species with and without intraretinal vasculature. Vision Res. 1991;31(2):169-87.

69. Sugiyama DT, Townsend JC, Bright DC, Ilsen PF. Support for the vasogenic theory of glaucoma: case reports and literature review. J Am Optom Assoc. 1993;64(8):568-82.

70. Luo X, Shen YM, Jiang MN, Lou XF, Shen Y. Ocular Blood Flow Autoregulation Mechanisms and Methods. J Ophthalmol. 2015;2015:864871.

71. Harris A, Jonescu-Cuypers C, Kagemann L, Ciulla T, Kreiglstein G. Ocular Vascular Anatomy. In: Harris A, editor. Atlas of Ocular Blood Flow. Philadelphia 2003. p. 1-19.

72. Mohindroo C, Ichhpujani P, Kumar S. Current Imaging Modalities for assessing Ocular Blood Flow in Glaucoma. J Curr Glaucoma Pract. 2016;10(3):104-12.

73. Bill A. Blood circulation and fluid dynamics in the eye. Physiol Rev. 1975;55(3):383-417.

74. Hogan MJ, Alvarado JA, Weddell JE. Histology of the human eye; an atlas and textbook. Philadelphia,: Saunders; 1971. xiii, 687 p. p.

75. Nickla DL, Wallman J. The multifunctional choroid. Prog Retin Eye Res. 2010;29(2):144-68.

76. Jonas JB, Guggenmoos-Holzmann I, Naumann GO. Cilioretinal arteries in large optic disks. Ophthalmic Res. 1988;20(5):269-74.

77. Anand-Apte B, Hollyfield JG. Developmental Anatomy of the Retinal and Choroidal Vasculature. In: Dartt DA, editor. Encyclopedia of the Eye: Academic Press; 2010. p. 9-15.

78. Iaizzo PA. General features of the cardiovascular system. In: Iaizzo PA, editor. The Handbook of Cardiac Anatomy, Physiology and Devices. Totowa, New Jersey: Humana Press; 2005.

79. Pournaras CJ, Riva CE. Retinal blood flow evaluation. Ophthalmologica. 2013;229(2):61-74.

80. Ethier CR, Johnson M, Ruberti J. Ocular biomechanics and biotransport. Annu Rev Biomed Eng. 2004;6:249-73.

81. Murray CD. The Physiological Principle of Minimum Work: I. The Vascular System and the Cost of Blood Volume. Proc Natl Acad Sci U S A. 1926;12(3):207-14.

82. Pasquale L, Jonas J, Anderson D. Anatomy and Physiology. In: Weinreb RN, Harris A, editors. Ocular Blood Flow in Glaucoma. Amsterdam: Kugler Publications; 2009. p. 3-13.

83. Harris A, Lerner F, Costa V, Martinez A, Siesky B. Autoregulation. Vascular Considerations in Glaucoma. Amsterdam: Kugler Publications; 2012. p. 33-42.

84. Johnson PC. Autoregulation of blood flow. Circ Res. 1986;59(5):483-95.

85. Guyton AC, Hall JE. Textbook of medical physiology. 9 ed. Philadelphia: W.B. Saunders; 1996.

86. Delaey C, Van de Voorde J. Pressure-induced myogenic responses in isolated bovine retinal arteries. Invest Ophthalmol Vis Sci. 2000;41(7):1871-5.

87. Delaey C, Van De Voorde J. Regulatory mechanisms in the retinal and choroidal circulation. Ophthalmic Res. 2000;32(6):249-56.

88. Laties AM. Central retinal artery innervation. Absence of adrenergic innervation to the intraocular branches. Arch Ophthalmol. 1967;77(3):405-9.

89. Marmorstein AD. The polarity of the retinal pigment epithelium. Traffic. 2001;2(12):867-72.

90. Kur J, Newman EA, Chan-Ling T. Cellular and physiological mechanisms underlying blood flow regulation in the retina and choroid in health and disease. Prog Retin Eye Res. 2012;31(5):377-406.

91. Chan-Ling T, Koina ME, McColm JR, Dahlstrom JE, Bean E, Adamson S, et al. Role of CD44+ stem cells in mural cell formation in the human choroid: evidence of vascular instability due to limited pericyte ensheathment. Invest Ophthalmol Vis Sci. 2011;52(1):399-410.

92. Robinson F, Riva CE, Grunwald JE, Petrig BL, Sinclair SH. Retinal blood flow autoregulation in response to an acute increase in blood pressure. Invest Ophthalmol Vis Sci. 1986;27(5):722-6.

93. Riva CE, Grunwald JE, Petrig BL. Autoregulation of human retinal blood flow. An investigation with laser Doppler velocimetry. Invest Ophthalmol Vis Sci. 1986;27(12):1706-12.

94. Weinstein JM, Funsch D, Page RB, Brennan RW. Optic nerve blood flow and its regulation. Invest Ophthalmol Vis Sci. 1982;23(5):640-5.

95. Tachibana H, Gotoh F, Ishikawa Y. Retinal vascular autoregulation in normal subjects. Stroke. 1982;13(2):149-55.

96. Kiel JW, Shepherd AP. Autoregulation of choroidal blood flow in the rabbit. Invest Ophthalmol Vis Sci. 1992;33(8):2399-410.

97. Kiel JW, van Heuven WA. Ocular perfusion pressure and choroidal blood flow in the rabbit. Invest Ophthalmol Vis Sci. 1995;36(3):579-85.

98. Garhofer G, Huemer KH, Zawinka C, Schmetterer L, Dorner GT. Influence of diffuse luminance flicker on choroidal and optic nerve head blood flow. Curr Eye Res. 2002;24(2):109-13.

99. Bill A, Sperber GO. Control of retinal and choroidal blood flow. Eye (Lond). 1990;4 (Pt 2):319-25.

100. Riva CE, Cranstoun SD, Grunwald JE, Petrig BL. Choroidal blood flow in the foveal region of the human ocular fundus. Invest Ophthalmol Vis Sci. 1994;35(13):4273-81.

101. Riva CE, Titze P, Hero M, Movaffaghy A, Petrig BL. Choroidal blood flow during isometric exercises. Invest Ophthalmol Vis Sci. 1997;38(11):2338-43.

102. Wilson TM, Strang R, Wallace J, Horton PW, Johnson NF. The measurement of the choroidal blood flow in the rabbit using 85-krypton. Exp Eye Res. 1973;16(6):421-5.

103. Kiss B, Dallinger S, Polak K, Findl O, Eichler HG, Schmetterer L. Ocular hemodynamics during isometric exercise. Microvasc Res. 2001;61(1):1-13.

104. Riva CE, Titze P, Hero M, Petrig BL. Effect of acute decreases of perfusion pressure on choroidal blood flow in humans. Invest Ophthalmol Vis Sci. 1997;38(9):1752-60.

105. Lovasik JV, Kergoat H, Riva CE, Petrig BL, Geiser M. Choroidal blood flow during exercise-induced changes in the ocular perfusion pressure. Invest Ophthalmol Vis Sci. 2003;44(5):2126-32.

106. Costa VP, Harris A, Anderson D, Stodtmeister R, Cremasco F, Kergoat H, et al. Ocular perfusion pressure in glaucoma. Acta Ophthalmol. 2014;92(4):e252-66.

107. Mottet B, Aptel F, Geiser M, Romanet JP, Chiquet C. [Vascular factors in glaucoma]. J Fr Ophtalmol. 2015;38(10):983-95.

108. Nakazawa T. Ocular Blood Flow and Influencing Factors for Glaucoma. Asia Pac J Ophthalmol (Phila). 2016;5(1):38-44.

109. Pemp B, Georgopoulos M, Vass C, Fuchsjager-Mayrl G, Luksch A, Rainer G, et al. Diurnal fluctuation of ocular blood flow parameters in patients with primary open-angle glaucoma and healthy subjects. Br J Ophthalmol. 2009;93(4):486-91.

110. Feke GT, Pasquale LR. Retinal blood flow response to posture change in glaucoma patients compared with healthy subjects. Ophthalmology. 2008;115(2):246-52.

111. Nagel E, Vilser W, Lanzl IM. Retinal vessel reaction to short-term IOP elevation in ocular hypertensive and glaucoma patients. Eur J Ophthalmol. 2001;11(4):338-44.

112. Hafez AS, Bizzarro RL, Rivard M, Lesk MR. Changes in optic nerve head blood flow after therapeutic intraocular pressure reduction in glaucoma patients and ocular hypertensives. Ophthalmology. 2003;110(1):201-10.

113. Ulrich A, Ulrich C, Barth T, Ulrich WD. Detection of disturbed autoregulation of the peripapillary choroid in primary open angle glaucoma. Ophthalmic Surg Lasers. 1996;27(9):746-57.

114. Gugleta K, Orgul S, Hasler PW, Picornell T, Gherghel D, Flammer J. Choroidal vascular reaction to hand-grip stress in subjects with vasospasm and its relevance in glaucoma. Invest Ophthalmol Vis Sci. 2003;44(4):1573-80.

115. James CB. Effect of trabeculectomy on pulsatile ocular blood flow. Br J Ophthalmol. 1994;78(11):818-22.

116. Quill B, Henry E, Simon E, O'Brien CJ. Evaluation of the Effect of Hypercapnia on Vascular Function in Normal Tension Glaucoma. Biomed Res Int. 2015;2015:418159.

117. Evans DW, Harris A, Garrett M, Chung HS, Kagemann L. Glaucoma patients demonstrate faulty autoregulation of ocular blood flow during posture change. Br J Ophthalmol. 1999;83(7):809-13.

118. Trible JR, Sergott RC, Spaeth GL, Wilson RP, Katz LJ, Moster MR, et al. Trabeculectomy is associated with retrobulbar hemodynamic changes. A color Doppler analysis. Ophthalmology. 1994;101(2):340-51.

119. Sines D, Harris A, Siesky B, Januleviciene I, Haine CL, Yung CW, et al. The response of retrobulbar vasculature to hypercapnia in primary open-angle glaucoma and ocular hypertension. Ophthalmic Res. 2007;39(2):76-80.

120. Harris A, Januleviciene I. Clinical Measurement of Ocular Blood Flow. In: Weinreb RN, Harris A, editors. Ocular Blood Flow in Glaucoma. Amsterdam: Kugler Publications; 2009. p. 19-56.

121. Jonas JB, Harazny J, Budde WM, Mardin CY, Papastathopoulos KI, Michelson G. Optic disc morphometry correlated with confocal laser scanning Doppler flowmetry measurements in normal-pressure glaucoma. J Glaucoma. 2003;12(3):260-5.

122. Chung HS, Harris A, Kagemann L, Martin B. Peripapillary retinal blood flow in normal tension glaucoma. Br J Ophthalmol. 1999;83(4):466-9.

123. Hafez AS, Bizzarro RL, Lesk MR. Evaluation of optic nerve head and peripapillary retinal blood flow in glaucoma patients, ocular hypertensives, and normal subjects. Am J Ophthalmol. 2003;136(6):1022-31.

124. Wang Y, Tan O, Huang D. Investigation of retinal blood flow in normal and glaucoma subjects by Doppler Fourier-domain optical coherence tomography. SPIE Proceedings 7168. 2009.

125. Leveque PM, Zeboulon P, Brasnu E, Baudouin C, Labbe A. Optic Disc Vascularization in Glaucoma: Value of Spectral-Domain Optical Coherence Tomography Angiography. J Ophthalmol. 2016;2016:6956717.

126. Spaide RF, Klancnik JM, Jr., Cooney MJ. Retinal vascular layers imaged by fluorescein angiography and optical coherence tomography angiography. JAMA Ophthalmol. 2015;133(1):45-50.

127. Hollo G. Vessel density calculated from OCT angiography in 3 peripapillary sectors in normal, ocular hypertensive, and glaucoma eyes. Eur J Ophthalmol. 2016;26(3):e42-5.

128. Yarmohammadi A, Zangwill LM, Diniz-Filho A, Suh MH, Yousefi S, Saunders LJ, et al. Relationship between Optical Coherence Tomography Angiography Vessel Density and Severity of Visual Field Loss in Glaucoma. Ophthalmology. 2016;123(12):2498-508.

129. Liu L, Jia Y, Takusagawa HL, Pechauer AD, Edmunds B, Lombardi L, et al. Optical Coherence Tomography Angiography of the Peripapillary Retina in Glaucoma. JAMA Ophthalmol. 2015;133(9):1045-52.

130. Galassi F, Sodi A, Ucci F, Renieri G, Pieri B, Baccini M. Ocular hemodynamics and glaucoma prognosis: a color Doppler imaging study. Arch Ophthalmol. 2003;121(12):1711-5.

131. Flammer J, Mozaffarieh M. Autoregulation, a balancing act between supply and demand. Can J Ophthalmol. 2008;43(3):317-21.

132. Mozaffarieh M, Grieshaber MC, Flammer J. Oxygen and blood flow: players in the pathogenesis of glaucoma. Mol Vis. 2008;14:224-33.

133. Sacca SC, Izzotti A, Rossi P, Traverso C. Glaucomatous outflow pathway and oxidative stress. Exp Eye Res. 2007;84(3):389-99.

134. Hernandez MR. The optic nerve head in glaucoma: role of astrocytes in tissue remodeling. Prog Retin Eye Res. 2000;19(3):297-321.

135. Sasaki S, Yasuda K. Vasospastic Syndrome. In: Chang JB, editor. Textbook of Angiology. New York, NY: Springer; 2000.

136. Smith CR, Rodeheffer RJ. Treatment of Raynaud's phenomenon with calcium channel blockers. Am J Med. 1985;78(2B):39-42.

137. Lesk MR, Wajszilber M, Deschenes MC. The effects of systemic medications on ocular blood flow. Can J Ophthalmol. 2008;43(3):351-5.

138. Nicolela MT. Clinical clues of vascular dysregulation and its association with glaucoma. Can J Ophthalmol. 2008;43(3):337-41.

139. Flammer J, Konieczka K, Flammer AJ. The primary vascular dysregulation syndrome: implications for eye diseases. EPMA J. 2013;4(1):14.

140. Broadway DC, Drance SM. Glaucoma and vasospasm. Br J Ophthalmol. 1998;82(8):862-70.

141. Nicolela MT, Drance SM. Various glaucomatous optic nerve appearances: clinical correlations. Ophthalmology. 1996;103(4):640-9.

142. Flammer J, Pache M, Resink T. Vasospasm, its role in the pathogenesis of diseases with particular reference to the eye. Prog Retin Eye Res. 2001;20(3):319-49.

143. Gasser P, Flammer J. Blood-cell velocity in the nailfold capillaries of patients with normal-tension and high-tension glaucoma. Am J Ophthalmol. 1991;111(5):585-8.

144. Schulzer M, Drance SM, Carter CJ, Brooks DE, Douglas GR, Lau W. Biostatistical evidence for two distinct chronic open angle glaucoma populations. Br J Ophthalmol. 1990;74(4):196-200.

145. Hafez AS, Bizzarro R, Descovich D, Lesk MR. Correlation between finger blood flow and changes in optic nerve head blood flow following therapeutic intraocular pressure reduction. J Glaucoma. 2005;14(6):448-54.

146. Satilmis M, Orgul S, Doubler B, Flammer J. Rate of progression of glaucoma correlates with retrobulbar circulation and intraocular pressure. Am J Ophthalmol. 2003;135(5):664-9.

147. Liang Y, Downs JC, Fortune B, Cull G, Cioffi GA, Wang L. Impact of systemic blood pressure on the relationship between intraocular pressure and blood flow in the optic nerve head of nonhuman primates. Invest Ophthalmol Vis Sci. 2009;50(5):2154-60.

148. Harris A, Lerner F, Costa V, Martinez A, Siesky B. Topical Medications and Ocular Blood Flow. Vascular Considerations in Glaucoma. Amsterdam: Kugler Publications; 2012. p. 115-23.

149. Quaid P, Simpson T, Freddo T. Relationship between diastolic perfusion pressure and progressive optic neuropathy as determined by Heidelberg retinal tomography topographic change analysis. Invest Ophthalmol Vis Sci. 2013;54(1):789-98.

150. Geyer O, Man O, Weintraub M, Silver DM. Acute effect of latanoprost on pulsatile ocular blood flow in normal eyes. Am J Ophthalmol. 2001;131(2):198-202.

151. Sponsel WE, Paris G, Trigo Y, Pena M. Comparative effects of latanoprost (Xalatan) and unoprostone (Rescula) in patients with open-angle glaucoma and suspected glaucoma. Am J Ophthalmol. 2002;134(4):552-9.

152. Sponsel WE, Mensah J, Kiel JW, Remky A, Trigo Y, Baca W, et al. Effects of latanoprost and timolol-XE on hydrodynamics in the normal eye. Am J Ophthalmol. 2000;130(2):151-9.

153. Sponsel WE, Paris G, Trigo Y, Pena M, Weber A, Sanford K, et al. Latanoprost and brimonidine: therapeutic and physiologic assessment before and after oral nonsteroidal anti-inflammatory therapy. Am J Ophthalmol. 2002;133(1):11-8.

154. Georgopoulos GT, Diestelhorst M, Fisher R, Ruokonen P, Krieglstein GK. The short-term effect of latanoprost on intraocular pressure and pulsatile ocular blood flow. Acta Ophthalmol Scand. 2002;80(1):54-8.

155. Vetrugno M, Cantatore F, Gigante G, Cardia L. Latanoprost 0.005% in POAG: effects on IOP and ocular blood flow. Acta Ophthalmol Scand Suppl. 1998(227):40-1.

156. McKibbin M, Menage MJ. The effect of once-daily latanoprost on intraocular pressure and pulsatile ocular blood flow in normal tension glaucoma. Eye (Lond). 1999;13 (Pt 1):31-4.

157. Izumi N, Nagaoka T, Sato E, Mori F, Takahashi A, Sogawa K, et al. Short-term effects of topical tafluprost on retinal blood flow in cats. J Ocul Pharmacol Ther. 2008;24(5):521-6.

158. Ishii K, Tomidokoro A, Nagahara M, Tamaki Y, Kanno M, Fukaya Y, et al. Effects of topical latanoprost on optic nerve head circulation in rabbits, monkeys, and humans. Invest Ophthalmol Vis Sci. 2001;42(12):2957-63.

159. Tamaki Y, Nagahara M, Araie M, Tomita K, Sandoh S, Tomidokoro A. Topical latanoprost and optic nerve head and retinal circulation in humans. J Ocul Pharmacol Ther. 2001;17(5):403-11.

160. Liu CJ, Ko YC, Cheng CY, Chiu AW, Chou JC, Hsu WM, et al. Changes in intraocular pressure and ocular perfusion pressure after latanoprost 0.005% or brimonidine tartrate 0.2% in normal-tension glaucoma patients. Ophthalmology. 2002;109(12):2241-7.

161. Sugiyama T, Azuma I. Effect of UF-021 on optic nerve head circulation in rabbits. Jpn J Ophthalmol. 1995;39(2):124-9.

162. Ohashi M, Mayama C, Ishii K, Araie M. Effects of topical travoprost and unoprostone on optic nerve head circulation in normal rabbits. Curr Eye Res. 2007;32(9):743-9.

163. Kimura I, Shinoda K, Tanino T, Ohtake Y, Mashima Y. Effect of topical unoprostone isopropyl on optic nerve head circulation in controls and in normal-tension glaucoma patients. Jpn J Ophthalmol. 2005;49(4):287-93.

164. Makimoto Y, Sugiyama T, Kojima S, Azuma I. Long-term effect of topically applied isopropyl unoprostone on microcirculation in the human ocular fundus. Jpn J Ophthalmol. 2002;46(1):31-5.

165. Tamaki Y, Araie M, Tomita K, Nagahara M, Sandoh S, Tomidokoro A. Effect of topical unoprostone on circulation of human optic nerve head and retina. J Ocul Pharmacol Ther. 2001;17(6):517-27.

166. Beano F, Orgul S, Stumpfig D, Gugleta K, Flammer J. An evaluation of the effect of unoprostone isopropyl 0.15% on ocular hemodynamics in normal-tension glaucoma patients. Graefes Arch Clin Exp Ophthalmol. 2001;239(2):81-6.

167. Costa VP, Harris A, Stefansson E, Flammer J, Krieglstein GK, Orzalesi N, et al. The effects of antiglaucoma and systemic medications on ocular blood flow. Prog Retin Eye Res. 2003;22(6):769-805.

168. Polska E, Doelemeyer A, Luksch A, Ehrlich P, Kaehler N, Percicot CL, et al. Partial antagonism of endothelin 1-induced vasoconstriction in the human choroid by topical unoprostone isopropyl. Arch Ophthalmol. 2002;120(3):348-52.

169. Allemann R, Flammer J, Haefliger IO. Vasoactive properties of bimatoprost in isolated porcine ciliary arteries. Klin Monbl Augenheilkd. 2003;220(3):161-4.

170. Dong Y, Watabe H, Su G, Ishikawa H, Sato N, Yoshitomi T. Relaxing effect and mechanism of tafluprost on isolated rabbit ciliary arteries. Exp Eye Res. 2008;87(3):251-6.

171. Allemann R, Flammer J, Haefliger IO. Absence of vasoactive properties of travoprost in isolated porcine ciliary arteries. Klin Monbl Augenheilkd. 2003;220(3):152-5.

172. Zeitz O, Matthiessen ET, Reuss J, Wiermann A, Wagenfeld L, Galambos P, et al. Effects of glaucoma drugs on ocular hemodynamics in normal tension glaucoma: a randomized trial comparing bimatoprost and latanoprost with dorzolamide [ISRCTN18873428]. BMC Ophthalmol. 2005;5:6.

173. Koz OG, Ozsoy A, Yarangumeli A, Kose SK, Kural G. Comparison of the effects of travoprost, latanoprost and bimatoprost on ocular circulation: a 6-month clinical trial. Acta Ophthalmol Scand. 2007;85(8):838-43.

174. Akarsu C, Yilmaz S, Taner P, Ergin A. Effect of bimatoprost on ocular circulation in patients with open-angle glaucoma or ocular hypertension. Graefes Arch Clin Exp Ophthalmol. 2004;242(10):814-8.

175. Chen MJ, Cheng CY, Chen YC, Chou CK, Hsu WM. Effects of bimatoprost 0.03% on ocular hemodynamics in normal tension glaucoma. J Ocul Pharmacol Ther. 2006;22(3):188-93.

176. Alagoz G, Gurel K, Bayer A, Serin D, Celebi S, Kukner S. A comparative study of bimatoprost and travoprost: effect on intraocular pressure and ocular circulation in newly diagnosed glaucoma patients. Ophthalmologica. 2008;222(2):88-95.

177. Inan UU, Ermis SS, Orman A, Onrat E, Yucel A, Ozturk F, et al. The comparative cardiovascular, pulmonary, ocular blood flow, and ocular hypotensive effects of topical travoprost, bimatoprost, brimonidine, and betaxolol. J Ocul Pharmacol Ther. 2004;20(4):293-310.

178. Ciro C, Francesco P, Marco C, Emanuele D'O Leonardo M, Adolfo S. Ocular perfusion pressure and visual field indice modifications induced by alpha-agonist compound (Clonidine 0.125%, apraclonidine 1.0% and brimonidine 0.2%) topical administration. Ophthalmologica. 2003;217:39-44.

179. Vetrugno M, Maino A, Cantatore F, Ruggeri G, Cardia L. Acute and chronic effects of brimonidine 0.2% on intraocular pressure and pulsatile ocular blood flow in patients with primary open-angle glaucoma: an open-label, uncontrolled, prospective study. Clin Ther. 2001;23(9):1519-28.

180. Liu CJ, Ko YC, Cheng CY, Chou JC, Hsu WM, Liu JH. Effect of latanoprost 0.005% and brimonidine tartrate 0.2% on pulsatile ocular blood flow in normal tension glaucoma. Br J Ophthalmol. 2002;86(11):1236-9.

181. Quaranta L, Gandolfo F, Turano R, Rovida F, Pizzolante T, Musig A, et al. Effects of topical hypotensive drugs on circadian IOP, blood pressure, and calculated diastolic ocular perfusion pressure in patients with glaucoma. Invest Ophthalmol Vis Sci. 2006;47(7):2917-23.

182. Netland PA, Schwartz B, Feke GT, Takamoto T, Konno S, Goger DG. Diversity of response of optic nerve head circulation to timolol maleate in gel-forming solution. J Glaucoma. 1999;8(3):164-71.

183. Wang TH, Hung PT, Huang JK, Shih YF. The effect of 0.5% timolol maleate on the ocular perfusion of ocular hypertensive patients by scanning laser flowmetry. J Ocul Pharmacol Ther. 1997;13(3):225-33.

184. Lubeck P, Orgul S, Gugleta K, Gherghel D, Gekkieva M, Flammer J. Effect of timolol on anterior optic nerve blood flow in patients with primary open-angle glaucoma as assessed by the Heidelberg retina flowmeter. J Glaucoma. 2001;10(1):13-7.

185. Morsman CD, Bosem ME, Lusky M, Weinreb RN. The effect of topical beta-adrenoceptor blocking agents on pulsatile ocular blood flow. Eye (Lond). 1995;9 (Pt 3):344-7.

186. Fuchsjager-Mayrl G, Wally B, Rainer G, Buehl W, Aggermann T, Kolodjaschna J, et al. Effect of dorzolamide and timolol on ocular blood flow in patients with primary open angle glaucoma and ocular hypertension. Br J Ophthalmol. 2005;89(10):1293-7.

187. Haefliger IO, Lietz A, Griesser SM, Ulrich A, Schotzau A, Hendrickson P, et al. Modulation of Heidelberg Retinal Flowmeter parameter flow at the papilla of healthy subjects: effect of carbogen, oxygen, high intraocular pressure, and beta-blockers. Surv Ophthalmol. 1999;43 Suppl 1:S59-65.

188. Yoshida A, Ogasawara H, Fujio N, Konno S, Ishiko S, Kitaya N, et al. Comparison of short- and long-term effects of betaxolol and timolol on human retinal circulation. Eye (Lond). 1998;12 (Pt 5):848-53.

189. Yoshida A, Feke GT, Ogasawara H, Goger DG, Murray DL, McMeel JW. Effect of timolol on human retinal, choroidal and optic nerve head circulation. Ophthalmic Res. 1991;23(3):162-70.

190. Carenini AB, Sibour G, Boles Carenini B. Differences in the longterm effect of timolol and betaxolol on the pulsatile ocular blood flow. Surv Ophthalmol. 1994;38 Suppl:S118-24.

191. Sato T, Muto T, Ishibashi Y, Roy S. Short-term effect of beta-adrenoreceptor blocking agents on ocular blood flow. Curr Eye Res. 2001;23(4):298-306.

192. Orgul S, Mansberger S, Bacon DR, Van Buskirk EM, Cioffi GA. Optic nerve vasomotor effects of topical beta-adrenergic antagonists in rabbits. Am J Ophthalmol. 1995;120(4):441-7.

193. Araie M, Muta K. Effect of long-term topical betaxolol on tissue circulation in the iris and optic nerve head. Exp Eye Res. 1997;64(2):167-72.

194. Kim JH, Kim DM, Park WC. Effect of betaxolol on impaired choroidal blood flow after intravitreal injection of endothelin-1 in albino rabbits. J Ocul Pharmacol Ther. 2002;18(3):203-9.

195. Barnes GE, Li B, Dean T, Chandler ML. Increased optic nerve head blood flow after 1 week of twice daily topical brinzolamide treatment in Dutch-belted rabbits. Surv Ophthalmol. 2000;44 Suppl 2:S131-40.

196. Iester M, Altieri M, Michelson G, Vittone P, Traverso CE, Calabria G. Retinal peripapillary blood flow before and after topical brinzolamide. Ophthalmologica. 2004;218(6):390-6.

197. Chiou GC, Yan HY. Effects of antiglaucoma drugs on the blood flow in rabbit eyes. Ophthalmic Res. 1986;18(5):265-9.

198. Claridge KG. The effect of topical pilocarpine on pulsatile ocular blood flow. Eye (Lond). 1993;7 (Pt 4):507-10.

199. Green K, Hatchett TL. Regional ocular blood flow after chronic topical glaucoma drug treatment. Acta Ophthalmol (Copenh). 1987;65(4):503-6.

200. Schmetterer L, Strenn K, Findl O, Breiteneder H, Graselli U, Agneter E, et al. Effects of antiglaucoma drugs on ocular hemodynamics in healthy volunteers. Clin Pharmacol Ther. 1997;61(5):583-95.

201. Germano RA, Finzi S, Challa P, Susanna Junior R. Rho kinase inhibitors for glaucoma treatment - Review. Arq Bras Oftalmol. 2015;78(6):388-91.

202. Rao VP, Epstein DL. Rho GTPase/Rho kinase inhibition as a novel target for the treatment of glaucoma. BioDrugs. 2007;21(3):167-77.

203. Chiou GC, Chen YJ. Effects of antiglaucoma drugs on ocular blood flow in ocular hypertensive rabbits. J Ocul Pharmacol. 1993;9(1):13-24.

204. Petropoulos IK, Pournaras JA, Munoz JL, Pournaras CJ. Effect of acetazolamide on the optic disc oxygenation in miniature pigs. Klin Monbl Augenheilkd. 2004;221(5):367-70.

205. Pedersen DB, Koch Jensen P, la Cour M, Kiilgaard JF, Eysteinsson T, Bang K, et al. Carbonic anhydrase inhibition increases retinal oxygen tension and dilates retinal vessels. Graefes Arch Clin Exp Ophthalmol. 2005;243(2):163-8.

206. Haustein M, Spoerl E, Boehm AG. The effect of acetazolamide on different ocular vascular beds. Graefes Arch Clin Exp Ophthalmol. 2013;251(5):1389-98.

207. Reber F, Gersch U, Funk RW. Blockers of carbonic anhydrase can cause increase of retinal capillary diameter, decrease of extracellular and increase of intracellular pH in rat retinal organ culture. Graefes Arch Clin Exp Ophthalmol. 2003;241(2):140-8.

208. Muntwyler J, Follath F. Calcium channel blockers in treatment of hypertension. Prog Cardiovasc Dis. 2001;44(3):207-16.

209. Katz AM. Pharmacology and mechanisms of action of calcium-channel blockers. J Clin Hypertens. 1986;2(3 Suppl):28S-37S.

210. Braunwald E. Mechanism of action of calcium-channel-blocking agents. N Engl J Med. 1982;307(26):1618-27.

211. Abernethy DR, Schwartz JB. Calcium-antagonist drugs. N Engl J Med. 1999;341(19):1447-57.

212. Araie M, Crowston J. Clinical Relevance of Ocular Blood Flow (OBF) Measurements Including Effects of General Medications or Specific Glaucoma Treatment. In: Weinreb RN, Harris A, editors. Ocular Blood Flow in Glaucoma. Amsterdam: Kugler Publications; 2009. p. 59-128.

213. Luksch A, Rainer G, Koyuncu D, Ehrlich P, Maca T, Gschwandtner ME, et al. Effect of nimodipine on ocular blood flow and colour contrast sensitivity in patients with normal tension glaucoma. Br J Ophthalmol. 2005;89(1):21-5.

214. Nyborg NC, Prieto D, Benedito S, Nielsen PJ. Endothelin-1-induced contraction of bovine retinal small arteries is reversible and abolished by nitrendipine. Invest Ophthalmol Vis Sci. 1991;32(1):27-31.

215. Lang MG, Zhu P, Meyer P, Noll G, Haefliger IO, Flammer J, et al. Amlodipine and benazeprilat differently affect the responses to endothelin-1 and bradykinin in porcine ciliary arteries: effects of a low and high dose combination. Curr Eye Res. 1997;16(3):208-13.

216. Meyer P, Lang MG, Flammer J, Luscher TF. Effects of calcium channel blockers on the response to endothelin-1, bradykinin and sodium nitroprusside in porcine ciliary arteries. Exp Eye Res. 1995;60(5):505-10.

217. Harino S, Riva CE, Petrig BL. Intravenous nicardipine in cats increases optic nerve head but not retinal blood flow. Invest Ophthalmol Vis Sci. 1992;33(10):2885-90.

218. Shimazawa M, Sugiyama T, Azuma I, Araie M, Iwakura Y, Watari M, et al. Effect of lomerizine, a new Ca(2+)channel blocker, on the microcirculation in the optic nerve head in conscious rabbits: a study using a laser speckle technique. Exp Eye Res. 1999;69(2):185-93.

219. Tamaki Y, Araie M, Tomita K, Urashima H. Effects of pranidipine, a new calcium antagonist, on circulation in the choroid, retina and optic nerve head. Curr Eye Res. 1999;19(3):241-7.

220. Tomita K, Tomidokoro A, Tamaki Y, Araie M, Matsubara M, Fukaya Y. Effects of semotiadil, a novel calcium antagonist, on the retina and optic nerve head circulation. J Ocul Pharmacol Ther. 2000;16(3):231-9.

221. Tamaki Y, Araie M, Tomita K, Tomidokoro A. Time change of nicardipine effect on choroidal circulation in rabbit eyes. Curr Eye Res. 1996;15(5):543-8.

222. Tamaki Y, Araie M, Tomita K, Tomidokoro A. Time-course of changes in nicardipine effects on microcirculation in retina and optic nerve head in living rabbit eyes. Jpn J Ophthalmol. 1996;40(2):202-11.

223. Tamaki Y, Araie M, Fukaya Y, Nagahara M, Imamura A, Honda M, et al. Effects of lomerizine, a calcium channel antagonist, on retinal and optic nerve head circulation in rabbits and humans. Invest Ophthalmol Vis Sci. 2003;44(11):4864-71.

224. Tomita K, Araie M, Tamaki Y, Nagahara M, Sugiyama T. Effects of nilvadipine, a calcium antagonist, on rabbit ocular circulation and optic nerve head circulation in NTG subjects. Invest Ophthalmol Vis Sci. 1999;40(6):1144-51.

225. Ishii K, Fukaya Y, Araie M, Tomita G. Topical administration of iganidipine, a new water-soluble Ca2+ antagonist, increases ipsilateral optic nerve head circulation in rabbits and cynomolgus monkeys. Curr Eye Res. 2004;29(1):67-73.

226. Waki M, Sugiyama T, Watanabe N, Ogawa T, Shirahase H, Azuma I. Effect of topically applied iganidipine dihydrochloride, a novel calcium antagonist, on optic nerve head circulation in rabbits. Jpn J Ophthalmol. 2001;45(1):76-83.

227. Koseki N, Araie M, Tomidokoro A, Nagahara M, Hasegawa T, Tamaki Y, et al. A placebo-controlled 3-year study of a calcium blocker on visual field and ocular circulation in glaucoma with low-normal pressure. Ophthalmology. 2008;115(11):2049-57.

228. Netland PA, Feke GT, Konno S, Goger DG, Fujio N. Optic nerve head circulation after topical calcium channel blocker. J Glaucoma. 1996;5(3):200-6.

229. Michalk F, Michelson G, Harazny J, Werner U, Daniel WG, Werner D. Single-dose nimodipine normalizes impaired retinal circulation in normal tension glaucoma. J Glaucoma. 2004;13(2):158-62.

230. Hirooka K, Shiraga F. Potential role for angiotensin-converting enzyme inhibitors in the treatment of glaucoma. Clin Ophthalmol. 2007;1(3):217-23.

231. Steigerwalt RD, Jr., Belcaro GV, Laurora G, Cesarone MR, De Sanctis MT, Incandela L. Ocular and orbital blood flow in patients with essential hypertension treated with trandolapril. Retina. 1998;18(6):539-45.

232. Matulla B, Streit G, Pieh S, Findl O, Entlicher J, Graselli U, et al. Effects of losartan on cerebral and ocular circulation in healthy subjects. Br J Clin Pharmacol. 1997;44(4):369-75.

233. Spicher T, Orgul S, Gugleta K, Teuchner B, Flammer J. The effect of losartan potassium on choroidal hemodynamics in healthy subjects. J Glaucoma. 2002;11(3):177-82.

234. Goldstein IM, Ostwald P, Roth S. Nitric oxide: a review of its role in retinal function and disease. Vision Res. 1996;36(18):2979-94.

235. Palmer RM, Ferrige AG, Moncada S. Nitric oxide release accounts for the biological activity of endothelium-derived relaxing factor. Nature. 1987;327(6122):524-6.

236. Furchgott RF, Zawadzki JV. The obligatory role of endothelial cells in the relaxation of arterial smooth muscle by acetylcholine. Nature. 1980;288(5789):373-6.

237. Nagaoka T, Takahashi A, Sato E, Izumi N, Hein TW, Kuo L, et al. Effect of systemic administration of simvastatin on retinal circulation. Arch Ophthalmol. 2006;124(5):665-70.

238. Tomida I, Pertwee RG, Azuara-Blanco A. Cannabinoids and glaucoma. Br J Ophthalmol. 2004;88(5):708-13.

239. Marsicano G, Moosmann B, Hermann H, Lutz B, Behl C. Neuroprotective properties of cannabinoids against oxidative stress: role of the cannabinoid receptor CB1. J Neurochem. 2002;80(3):448-56.

240. Novack GD. Cannabinoids for treatment of glaucoma. Curr Opin Ophthalmol. 2016;27(2):146-50.

241. Chung HS, Harris A, Kristinsson JK, Ciulla TA, Kagemann C, Ritch R. Ginkgo biloba extract increases ocular blood flow velocity. J Ocul Pharmacol Ther. 1999;15(3):233-40.

242. Park JW, Kwon HJ, Chung WS, Kim CY, Seong GJ. Short-term effects of Ginkgo biloba extract on peripapillary retinal blood flow in normal tension glaucoma. Korean J Ophthalmol. 2011;25(5):323-8.

243. Ritch R. Natural compounds: evidence for a protective role in eye disease. Can J Ophthalmol. 2007;42(3):425-38.

244. Hirooka K, Tokuda M, Miyamoto O, Itano T, Baba T, Shiraga F. The Ginkgo biloba extract (EGb 761) provides a neuroprotective effect on retinal ganglion cells in a rat model of chronic glaucoma. Curr Eye Res. 2004;28(3):153-7.

245. Quaranta L, Bettelli S, Uva MG, Semeraro F, Turano R, Gandolfo E. Effect of Ginkgo biloba extract on preexisting visual field damage in normal tension glaucoma. Ophthalmology. 2003;110(2):359-62; discussion 62-4.

246. Shim SH, Kim JM, Choi CY, Kim CY, Park KH. Ginkgo biloba extract and bilberry anthocyanins improve visual function in patients with normal tension glaucoma. J Med Food. 2012;15(9):818-23.

247. Lee SJ, McEwen BS. Neurotrophic and neuroprotective actions of estrogens and their therapeutic implications. Annu Rev Pharmacol Toxicol. 2001;41:569-91.

248. Whitsett TL, Manion CV, Christensen HD. Cardiovascular effects of coffee and caffeine. Am J Cardiol. 1984;53(7):918-22.

249. Smits P, Thien T, Van 't Laar A. The cardiovascular effects of regular and decaffeinated coffee. Br J Clin Pharmacol. 1985;19(6):852-4.

250. Lotfi K, Grunwald JE. The effect of caffeine on the human macular circulation. Invest Ophthalmol Vis Sci. 1991;32(12):3028-32.

251. Terai N, Spoerl E, Pillunat LE, Stodtmeister R. The effect of caffeine on retinal vessel diameter in young healthy subjects. Acta Ophthalmol. 2012;90(7):e524-8.

252. Okuno T, Sugiyama T, Tominaga M, Kojima S, Ikeda T. Effects of caffeine on microcirculation of the human ocular fundus. Jpn J Ophthalmol. 2002;46(2):170-6.

253. Higginbotham EJ, Kilimanjaro HA, Wilensky JT, Batenhorst RL, Hermann D. The effect of caffeine on intraocular pressure in glaucoma patients. Ophthalmology. 1989;96(5):624-6.

254. Avisar R, Avisar E, Weinberger D. Effect of coffee consumption on intraocular pressure. Ann Pharmacother. 2002;36(6):992-5.

255. Jiwani AZ, Rhee DJ, Brauner SC, Gardiner MF, Chen TC, Shen LQ, et al. Effects of caffeinated coffee consumption on intraocular pressure, ocular perfusion pressure, and ocular pulse amplitude: a randomized controlled trial. Eye (Lond). 2012;26(8):1122-30.

256. Chandrasekaran S, Rochtchina E, Mitchell P. Effects of caffeine on intraocular pressure: the Blue Mountains Eye Study. J Glaucoma. 2005;14(6):504-7.

257. Kurata K, Fujimoto H, Tsukuda R, Suzuki T, Ando T, Tokuriki M. Aqueous humor dynamics in beagle dogs with caffeine-induced ocular hypertension. J Vet Med Sci. 1998;60(6):737-9.

258. Kurata K, Maeda M, Nishida E, Tsukuda R, Suzuki T, Ando T, et al. Relationship between caffeine-induced ocular hypertension and ultrastructure changes of non-pigmented ciliary epithelial cells in rats. J Toxicol Sci. 1997;22(5):447-54.

259. Kang JH, Willett WC, Rosner BA, Hankinson SE, Pasquale LR. Caffeine consumption and the risk of primary open-angle glaucoma: a prospective cohort study. Invest Ophthalmol Vis Sci. 2008;49(5):1924-31.

260. Wu CM, Wu AM, Tseng VL, Yu F, Coleman AL. Frequency of a diagnosis of glaucoma in individuals who consume coffee, tea and/or soft drinks. Br J Ophthalmol. 2018;102(8):1127-33.

261. Kojima S, Sugiyama T, Kojima M, Azuma II, Ito S. Effect of the consumption of ethanol on the microcirculation of the human optic nerve head in the acute phase. Jpn J Ophthalmol. 2000;44(3):318-9.

262. Harris A, Swartz D, Engen D, Beck D, Evans D, Caldemeyer K, et al. Ocular hemodynamic effects of acute ethanol ingestion. Ophthalmic Res. 1996;28(3):193-200.

263. Houle RE, Grant WM. Alcohol, vasopressin, and intraocular pressure. Invest Ophthalmol. 1967;6(2):145-54.

264. Kang JH, Willett WC, Rosner BA, Hankinson SE, Pasquale LR. Prospective study of alcohol consumption and the risk of primary open-angle glaucoma. Ophthalmic Epidemiol. 2007;14(3):141-7.

265. Solberg Y, Rosner M, Belkin M. The association between cigarette smoking and ocular diseases. Surv Ophthalmol. 1998;42(6):535-47.

266. Langhans M, Michelson G, Groh MJ. Effect of breathing 100% oxygen on retinal and optic nerve head capillary blood flow in smokers and non-smokers. Br J Ophthalmol. 1997;81(5):365-9.

267. Robinson F, Petrig BL, Riva CE. The acute effect of cigarette smoking on macular capillary blood flow in humans. Invest Ophthalmol Vis Sci. 1985;26(5):609-13.

268. Rojanapongpun P, Drance SM. The effects of nicotine on the blood flow of the ophthalmic artery and the finger circulation. Graefes Arch Clin Exp Ophthalmol. 1993;231(7):371-4.

269. Tamaki Y, Araie M, Nagahara M, Tomita K. Acute effects of cigarette smoking on tissue circulation in human optic nerve head and choroid-retina. Ophthalmology. 1999;106(3):564-9.

270. Wennmalm A. Effect of cigarette smoking on basal and carbon dioxide stimulated cerebral blood flow in man. Clin Physiol. 1982;2(6):529-35.

271. Kang JH, Pasquale LR, Rosner BA, Willett WC, Egan KM, Faberowski N, et al. Prospective study of cigarette smoking and the risk of primary open-angle glaucoma. Arch Ophthalmol. 2003;121(12):1762-8.

272. Cekic B, Dogan B, Toslak IE, Dogan U, Saglik S, Erol MK. The effect of bariatric surgery on the retrobulbar flow hemodynamic parameters in patients with obesity: color Doppler evaluation. Int Ophthalmol. 2018;38(5):1845-50.

273. Cekic B, Toslak IE, Dogan B, Cakir T, Erol MK, Bulbuller N. Effects of obesity on retrobulbar flow hemodynamics: color Doppler ultrasound evaluation. Arq Bras Oftalmol. 2017;80(3):143-7.
274. Karadag R, Arslanyilmaz Z, Aydin B, Hepsen IF. Effects of body mass index on intraocular pressure and ocular pulse amplitude. Int J Ophthalmol. 2012;5(5):605-8.
275. Kim YK, Choi HJ, Jeoung JW, Park KH, Kim DM. Five-year incidence of primary open-angle glaucoma and rate of progression in health center-based Korean population: the Gangnam Eye Study. PLoS One. 2014;9(12):e114058.
276. Ramdas WD, Wolfs RC, Hofman A, de Jong PT, Vingerling JR, Jansonius NM. Lifestyle and risk of developing open-angle glaucoma: the Rotterdam study. Arch Ophthalmol. 2011;129(6):767-72.
277. Pasquale LR, Willett WC, Rosner BA, Kang JH. Anthropometric measures and their relation to incident primary open-angle glaucoma. Ophthalmology. 2010;117(8):1521-9.
278. Leske MC, Connell AM, Wu SY, Hyman LG, Schachat AP. Risk factors for open-angle glaucoma. The Barbados Eye Study. Arch Ophthalmol. 1995;113(7):918-24.
279. Le A, Mukesh BN, McCarty CA, Taylor HR. Risk factors associated with the incidence of open-angle glaucoma: the visual impairment project. Invest Ophthalmol Vis Sci. 2003;44(9):3783-9.
280. Jiang X, Varma R, Wu S, Torres M, Azen SP, Francis BA, et al. Baseline risk factors that predict the development of open-angle glaucoma in a population: the Los Angeles Latino Eye Study. Ophthalmology. 2012;119(11):2245-53.
281. Chiang CL, Chen YT, Wang KL, Su VY, Wu LA, Perng DW, et al. Comorbidities and risk of mortality in patients with sleep apnea. Ann Med. 2017:1-7.
282. Young T, Peppard PE, Taheri S. Excess weight and sleep-disordered breathing. J Appl Physiol (1985). 2005;99(4):1592-9.
283. Young T, Skatrud J, Peppard PE. Risk factors for obstructive sleep apnea in adults. JAMA. 2004;291(16):2013-6.
284. Isono S. Obesity and obstructive sleep apnoea: mechanisms for increased collapsibility of the passive pharyngeal airway. Respirology. 2012;17(1):32-42.

285. Bilgin G. Normal-tension glaucoma and obstructive sleep apnea syndrome: a prospective study. BMC Ophthalmol. 2014;14:27.

286. Hashim SP, Al Mansouri FA, Farouk M, Al Hashemi AA, Singh R. Prevalence of glaucoma in patients with moderate to severe obstructive sleep apnea: ocular morbidity and outcomes in a 3 year follow-up study. Eye (Lond). 2014;28(11):1304-9.

287. Batisse JL, Vix J, Swalduz B, Chave N, Mage F. [Sleep-related breathing disorders and normal or high-tension glaucoma: 35 patients with polysomnographic records]. J Fr Ophtalmol. 2004;27(6 Pt 1):605-12.

288. Fan YY, Su WW, Liu CH, Chen HS, Wu SC, Chang SHL, et al. Correlation between structural progression in glaucoma and obstructive sleep apnea. Eye (Lond). 2019;33(9):1459-65.

289. Mojon DS, Hess CW, Goldblum D, Boehnke M, Koerner F, Gugger M, et al. Normal-tension glaucoma is associated with sleep apnea syndrome. Ophthalmologica. 2002;216(3):180-4.

290. Sergi M, Salerno DE, Rizzi M, Blini M, Andreoli A, Messenio D, et al. Prevalence of normal tension glaucoma in obstructive sleep apnea syndrome patients. J Glaucoma. 2007;16(1):42-6.

291. Mojon DS, Hess CW, Goldblum D, Fleischhauer J, Koerner F, Bassetti C, et al. High prevalence of glaucoma in patients with sleep apnea syndrome. Ophthalmology. 1999;106(5):1009-12.

292. Bendel RE, Kaplan J, Heckman M, Fredrickson PA, Lin SC. Prevalence of glaucoma in patients with obstructive sleep apnoea--a cross-sectional case-series. Eye (Lond). 2008;22(9):1105-9.

293. Marcus DM, Costarides AP, Gokhale P, Papastergiou G, Miller JJ, Johnson MH, et al. Sleep disorders: a risk factor for normal-tension glaucoma? J Glaucoma. 2001;10(3):177-83.

294. Tsang CS, Chong SL, Ho CK, Li MF. Moderate to severe obstructive sleep apnoea patients is associated with a higher incidence of visual field defect. Eye (Lond). 2006;20(1):38-42.

295. Kargi SH, Altin R, Koksal M, Kart L, Cinar F, Ugurbas SH, et al. Retinal nerve fibre layer measurements are reduced in patients with obstructive sleep apnoea syndrome. Eye (Lond). 2005;19(5):575-9.

296. Dunet V, Rey-Bataillard V, Allenbach G, Beysard N, Lovis A, Prior JO, et al. Effects of continuous positive airway pressure treatment on coronary vasoreactivity measured by (82)Rb cardiac PET/CT in obstructive sleep apnea patients. Sleep Breath. 2016;20(2):673-9.

297. Urbano F, Roux F, Schindler J, Mohsenin V. Impaired cerebral autoregulation in obstructive sleep apnea. J Appl Physiol (1985). 2008;105(6):1852-7.

298. Oz O, Tasdemir S, Akgun H, Erdem M, Balikci A, Cetiz A, et al. Decreased cerebral vasomotor reactivity in patients with obstructive sleep apnea syndrome. Sleep Med. 2017;30:88-92.

299. Yadav SK, Kumar R, Macey PM, Richardson HL, Wang DJ, Woo MA, et al. Regional cerebral blood flow alterations in obstructive sleep apnea. Neurosci Lett. 2013;555:159-64.

300. Nie S, Peng DC, Gong HH, Li HJ, Chen LT, Ye CL. Resting cerebral blood flow alteration in severe obstructive sleep apnoea: an arterial spin labelling perfusion fMRI study. Sleep Breath. 2017.

301. Joo EY, Tae WS, Han SJ, Cho JW, Hong SB. Reduced cerebral blood flow during wakefulness in obstructive sleep apnea-hypopnea syndrome. Sleep. 2007;30(11):1515-20.

302. Waltz X, Beaudin AE, Hanly PJ, Mitsis GD, Poulin MJ. Effects of continuous positive airway pressure and isocapnic-hypoxia on cerebral autoregulation in patients with obstructive sleep apnoea. J Physiol. 2016;594(23):7089-104.

303. Karakucuk S, Goktas S, Aksu M, Erdogan N, Demirci S, Oner A, et al. Ocular blood flow in patients with obstructive sleep apnea syndrome (OSAS). Graefes Arch Clin Exp Ophthalmol. 2008;246(1):129-34.

304. Tonini M, Khayi H, Pepin JL, Renard E, Baguet JP, Levy P, et al. Choroidal blood-flow responses to hyperoxia and hypercapnia in men with obstructive sleep apnea. Sleep. 2010;33(6):811-8.

305. Khayi H, Pepin JL, Geiser MH, Tonini M, Tamisier R, Renard E, et al. Choroidal blood flow regulation after posture change or isometric exercise in men with obstructive sleep apnea syndrome. Invest Ophthalmol Vis Sci. 2011;52(13):9489-96.

306. Nowak MS, Jurowski P, Gos R, Prost ME, Smigielski J. Pulsatile ocular blood flow in subjects with sleep apnoea syndrome. Arch Med Sci. 2011;7(2):332-6.

307. Zhang LL, Song L, Fan YF, Wang B, Liu ZL. [Changes of ophthalmic blood flow in obstructive sleep apnea-hypopnea syndrome]. Zhonghua Yan Ke Za Zhi. 2012;48(7):631-6.

308. Topouzis F, Coleman AL, Harris A, Jonescu-Cuypers C, Yu F, Mavroudis L, et al. Association of blood pressure status with the optic disk structure in non-glaucoma subjects: the Thessaloniki eye study. Am J Ophthalmol. 2006;142(1):60-7.

309. Bonomi L, Marchini G, Marraffa M, Bernardi P, Morbio R, Varotto A. Vascular risk factors for primary open angle glaucoma: the Egna-Neumarkt Study. Ophthalmology. 2000;107(7):1287-93.

310. Leske MC, Wu SY, Hennis A, Honkanen R, Nemesure B, Group BES. Risk factors for incident open-angle glaucoma: the Barbados Eye Studies. Ophthalmology. 2008;115(1):85-93.

311. Tielsch JM, Katz J, Sommer A, Quigley HA, Javitt JC. Hypertension, perfusion pressure, and primary open-angle glaucoma. A population-based assessment. Arch Ophthalmol. 1995;113(2):216-21.

312. Kaiser HJ, Flammer J. Systemic hypotension: a risk factor for glaucomatous damage? Ophthalmologica. 1991;203(3):105-8.

313. Kaiser HJ, Flammer J, Graf T, Stumpfig D. Systemic blood pressure in glaucoma patients. Graefes Arch Clin Exp Ophthalmol. 1993;231(12):677-80.

314. Hayreh SS, Zimmerman MB, Podhajsky P, Alward WL. Nocturnal arterial hypotension and its role in optic nerve head and ocular ischemic disorders. Am J Ophthalmol. 1994;117(5):603-24.

315. Graham SL, Drance SM, Wijsman K, Douglas GR, Mikelberg FS. Ambulatory blood pressure monitoring in glaucoma. The nocturnal dip. Ophthalmology. 1995;102(1):61-9.

316. Mitchell P, Lee AJ, Wang JJ, Rochtchina E. Intraocular pressure over the clinical range of blood pressure: blue mountains eye study findings. Am J Ophthalmol. 2005;140(1):131-2.

317. Zhao D, Cho J, Kim MH, Guallar E. The association of blood pressure and primary open-angle glaucoma: a meta-analysis. Am J Ophthalmol. 2014;158(3):615-27 e9.

318. Wu SY, Leske MC. Associations with intraocular pressure in the Barbados Eye Study. Arch Ophthalmol. 1997;115(12):1572-6.

319. Klein BE, Klein R, Knudtson MD. Intraocular pressure and systemic blood pressure: longitudinal perspective: the Beaver Dam Eye Study. Br J Ophthalmol. 2005;89(3):284-7.

320. Dielemans I, Vingerling JR, Algra D, Hofman A, Grobbee DE, de Jong PT. Primary open-angle glaucoma, intraocular pressure, and systemic blood pressure in the general elderly population. The Rotterdam Study. Ophthalmology. 1995;102(1):54-60.

321. Yip JL, Aung T, Wong TY, Machin D, Khaw PT, Khaw KT, et al. Socioeconomic status, systolic blood pressure and intraocular pressure: the Tanjong Pagar Study. Br J Ophthalmol. 2007;91(1):56-61.

322. Kiel JW. The effect of arterial pressure on the ocular pressure-volume relationship in the rabbit. Exp Eye Res. 1995;60(3):267-78.

323. Dastiridou AI, Ginis HS, De Brouwere D, Tsilimbaris MK, Pallikaris IG. Ocular rigidity, ocular pulse amplitude, and pulsatile ocular blood flow: the effect of intraocular pressure. Invest Ophthalmol Vis Sci. 2009;50(12):5718-22.

324. Pemp B, Schmetterer L. Ocular blood flow in diabetes and age-related macular degeneration. Can J Ophthalmol. 2008;43(3):295-301.

325. Nagaoka T, Kitaya N, Sugawara R, Yokota H, Mori F, Hikichi T, et al. Alteration of choroidal circulation in the foveal region in patients with type 2 diabetes. Br J Ophthalmol. 2004;88(8):1060-3.

326. Schocket LS, Brucker AJ, Niknam RM, Grunwald JE, DuPont J, Brucker AJ. Foveolar choroidal hemodynamics in proliferative diabetic retinopathy. Int Ophthalmol. 2004;25(2):89-94.

327. Movaffaghy A, Chamot SR, Dosso A, Pournaras CJ, Sommerhalder JR, Riva CE. Effect of isometric exercise on choroidal blood flow in type I diabetic patients. Klin Monbl Augenheilkd. 2002;219(4):299-301.

328. Becker B. Diabetes mellitus and primary open-angle glaucoma. The XXVII Edward Jackson Memorial Lecture. Am J Ophthalmol. 1971;71(1 Pt 1):1-16.

329. Pasquale LR, Kang JH, Manson JE, Willett WC, Rosner BA, Hankinson SE. Prospective study of type 2 diabetes mellitus and risk of primary open-angle glaucoma in women. Ophthalmology. 2006;113(7):1081-6.

330. Mitchell P, Smith W, Chey T, Healey PR. Open-angle glaucoma and diabetes: the Blue Mountains eye study, Australia. Ophthalmology. 1997;104(4):712-8.

331. Chopra V, Varma R, Francis BA, Wu J, Torres M, Azen SP, et al. Type 2 diabetes mellitus and the risk of open-angle glaucoma the Los Angeles Latino Eye Study. Ophthalmology. 2008;115(2):227-32 e1.

332. Bonovas S, Peponis V, Filioussi K. Diabetes mellitus as a risk factor for primary open-angle glaucoma: a meta-analysis. Diabet Med. 2004;21(6):609-14.

333. Quigley HA, Enger C, Katz J, Sommer A, Scott R, Gilbert D. Risk factors for the development of glaucomatous visual field loss in ocular hypertension. Arch Ophthalmol. 1994;112(5):644-9.

334. Jonas JB, Grundler AE. Prevalence of diabetes mellitus and arterial hypertension in primary and secondary open-angle glaucomas. Graefes Arch Clin Exp Ophthalmol. 1998;236(3):202-6.

335. Ellis JD, Evans JM, Ruta DA, Baines PS, Leese G, MacDonald TM, et al. Glaucoma incidence in an unselected cohort of diabetic patients: is diabetes mellitus a risk factor for glaucoma? DARTS/MEMO collaboration. Diabetes Audit and Research in Tayside Study. Medicines Monitoring Unit. Br J Ophthalmol. 2000;84(11):1218-24.

336. Tielsch JM, Katz J, Quigley HA, Javitt JC, Sommer A. Diabetes, intraocular pressure, and primary open-angle glaucoma in the Baltimore Eye Survey. Ophthalmology. 1995;102(1):48-53.

337. Quigley HA, West SK, Rodriguez J, Munoz B, Klein R, Snyder R. The prevalence of glaucoma in a population-based study of Hispanic subjects: Proyecto VER. Arch Ophthalmol. 2001;119(12):1819-26.

338. de Voogd S, Ikram MK, Wolfs RC, Jansonius NM, Witteman JC, Hofman A, et al. Is diabetes mellitus a risk factor for open-angle glaucoma? The Rotterdam Study. Ophthalmology. 2006;113(10):1827-31.

339. Sayah DN, Lesk MR. Ocular Rigidity and Glaucoma. In: Pallikaris I, Dastiridou AI, editors. Ocular Rigidity, Biomechanics and Hydrodynamics of the Eye. unpublished: Springer Nature; n.d.

340. Downs JC, Roberts MD, Burgoyne CF. Mechanical environment of the optic nerve head in glaucoma. Optom Vis Sci. 2008;85(6):425-35.

341. Downs JC, Girkin CA. Lamina cribrosa in glaucoma. Curr Opin Ophthalmol. 2017;28(2):113-9.

342. Wolffsohn JS, Davies LN. Advances in anterior segment imaging. Curr Opin Ophthalmol. 2007;18(1):32-8.

343. Copt RP, Thomas R, Mermoud A. Corneal thickness in ocular hypertension, primary open-angle glaucoma, and normal tension glaucoma. Arch Ophthalmol. 1999;117(1):14-6.

344. Herndon LW. Measuring intraocular pressure-adjustments for corneal thickness and new technologies. Curr Opin Ophthalmol. 2006;17(2):115-9.

345. Medeiros FA, Weinreb RN, Sample PA, Gomi CF, Bowd C, Crowston JG, et al. Validation of a predictive model to estimate the risk of conversion from ocular hypertension to glaucoma. Arch Ophthalmol. 2005;123(10):1351-60.

346. Medeiros FA, Sample PA, Zangwill LM, Bowd C, Aihara M, Weinreb RN. Corneal thickness as a risk factor for visual field loss in patients with preperimetric glaucomatous optic neuropathy. Am J Ophthalmol. 2003;136(5):805-13.

347. Jonas JB, Holbach L. Central corneal thickness and thickness of the lamina cribrosa in human eyes. Invest Ophthalmol Vis Sci. 2005;46(4):1275-9.

348. Oliveira C, Tello C, Liebmann J, Ritch R. Central corneal thickness is not related to anterior scleral thickness or axial length. J Glaucoma. 2006;15(3):190-4.

349. Lesk MR, Hafez AS, Descovich D. Relationship between central corneal thickness and changes of optic nerve head topography and blood flow after intraocular pressure reduction in open-angle glaucoma and ocular hypertension. Arch Ophthalmol. 2006;124(11):1568-72.

350. Pakravan M, Parsa A, Sanagou M, Parsa CF. Central corneal thickness and correlation to optic disc size: a potential link for susceptibility to glaucoma. Br J Ophthalmol. 2007;91(1):26-8.

351. Pallikaris IG, Kymionis GD, Ginis HS, Kounis GA, Tsilimbaris MK. Ocular rigidity in living human eyes. Invest Ophthalmol Vis Sci. 2005;46(2):409-14.

352. Brandt JD, Beiser JA, Kass MA, Gordon MO. Central corneal thickness in the Ocular Hypertension Treatment Study (OHTS). Ophthalmology. 2001;108(10):1779-88.

353. Hahn S, Azen S, Ying-Lai M, Varma R, Los Angeles Latino Eye Study G. Central corneal thickness in Latinos. Invest Ophthalmol Vis Sci. 2003;44(4):1508-12.

354. Nemesure B, Wu SY, Hennis A, Leske MC, Barbados Eye Study G. Corneal thickness and intraocular pressure in the Barbados eye studies. Arch Ophthalmol. 2003;121(2):240-4.

355. Shimmyo M, Ross AJ, Moy A, Mostafavi R. Intraocular pressure, Goldmann applanation tension, corneal thickness, and corneal curvature in Caucasians, Asians, Hispanics, and African Americans. Am J Ophthalmol. 2003;136(4):603-13.

356. Haseltine SJ, Pae J, Ehrlich JR, Shammas M, Radcliffe NM. Variation in corneal hysteresis and central corneal thickness among black, hispanic and white subjects. Acta Ophthalmol. 2012;90(8):e626-31.

357. Meda R, Wang Q, Paoloni D, Harasymowycz P, Brunette I. The impact of chronic use of prostaglandin analogues on the biomechanical properties of the cornea in patients with primary open-angle glaucoma. Br J Ophthalmol. 2017;101(2):120-5.

358. Tsikripis P, Papaconstantinou D, Koutsandrea C, Apostolopoulos M, Georgalas I. The effect of prostaglandin analogs on the biomechanical properties and central thickness of the cornea of patients with open-angle glaucoma: a 3-year study on 108 eyes. Drug Des Devel Ther. 2013;7:1149-56.

359. Brandt JD, Gordon MO, Beiser JA, Lin SC, Alexander MY, Kass MA, et al. Changes in central corneal thickness over time: the ocular hypertension treatment study. Ophthalmology. 2008;115(9):1550-6, 6 e1.

360. Chauhan BC, Hutchison DM, LeBlanc RP, Artes PH, Nicolela MT. Central corneal thickness and progression of the visual field and optic disc in glaucoma. Br J Ophthalmol. 2005;89(8):1008-12.

361. Matsuura M, Hirasawa K, Murata H, Yanagisawa M, Nakao Y, Nakakura S, et al. The Relationship between Corvis ST Tonometry and Ocular Response Analyzer Measurements in Eyes with Glaucoma. PLoS One. 2016;11(8):e0161742.

362. Kotecha A. What biomechanical properties of the cornea are relevant for the clinician? Surv Ophthalmol. 2007;52 Suppl 2:S109-14.

363. Shah S, Laiquzzaman M, Bhojwani R, Mantry S, Cunliffe I. Assessment of the biomechanical properties of the cornea with the ocular response analyzer in normal and keratoconic eyes. Invest Ophthalmol Vis Sci. 2007;48(7):3026-31.

364. Carbonaro F, Andrew T, Mackey DA, Spector TD, Hammond CJ. The heritability of corneal hysteresis and ocular pulse amplitude: a twin study. Ophthalmology. 2008;115(9):1545-9.

365. Mangouritsas G, Morphis G, Mourtzoukos S, Feretis E. Association between corneal hysteresis and central corneal thickness in glaucomatous and non-glaucomatous eyes. Acta Ophthalmol. 2009;87(8):901-5.

366. Wells AP, Garway-Heath DF, Poostchi A, Wong T, Chan KC, Sachdev N. Corneal hysteresis but not corneal thickness correlates with optic nerve surface compliance in glaucoma patients. Invest Ophthalmol Vis Sci. 2008;49(8):3262-8.

367. Abitbol O, Bouden J, Doan S, Hoang-Xuan T, Gatinel D. Corneal hysteresis measured with the Ocular Response Analyzer in normal and glaucomatous eyes. Acta Ophthalmol. 2010;88(1):116-9.

368. Sullivan-Mee M, Katiyar S, Pensyl D, Halverson KD, Qualls C. Relative importance of factors affecting corneal hysteresis measurement. Optom Vis Sci. 2012;89(5):E803-11.

369. Shah S, Laiquzzaman M, Mantry S, Cunliffe I. Ocular response analyser to assess hysteresis and corneal resistance factor in low tension, open angle glaucoma and ocular hypertension. Clin Exp Ophthalmol. 2008;36(6):508-13.

370. Sullivan-Mee M, Billingsley SC, Patel AD, Halverson KD, Alldredge BR, Qualls C. Ocular Response Analyzer in subjects with and without glaucoma. Optom Vis Sci. 2008;85(6):463-70.

371. Medeiros FA, Meira-Freitas D, Lisboa R, Kuang TM, Zangwill LM, Weinreb RN. Corneal hysteresis as a risk factor for glaucoma progression: a prospective longitudinal study. Ophthalmology. 2013;120(8):1533-40.

372. Congdon NG, Broman AT, Bandeen-Roche K, Grover D, Quigley HA. Central corneal thickness and corneal hysteresis associated with glaucoma damage. Am J Ophthalmol. 2006;141(5):868-75.

373. De Moraes CV, Hill V, Tello C, Liebmann JM, Ritch R. Lower corneal hysteresis is associated with more rapid glaucomatous visual field progression. J Glaucoma. 2012;21(4):209-13.

374. Zhang C, Tatham AJ, Abe RY, Diniz-Filho A, Zangwill LM, Weinreb RN, et al. Corneal Hysteresis and Progressive Retinal Nerve Fiber Layer Loss in Glaucoma. Am J Ophthalmol. 2016;166:29-36.

375. Anand A, De Moraes CG, Teng CC, Tello C, Liebmann JM, Ritch R. Corneal hysteresis and visual field asymmetry in open angle glaucoma. Invest Ophthalmol Vis Sci. 2010;51(12):6514-8.

376. Prata TS, Lima VC, Guedes LM, Biteli LG, Teixeira SH, de Moraes CG, et al. Association between corneal biomechanical properties and optic nerve head morphology in newly diagnosed glaucoma patients. Clin Exp Ophthalmol. 2012;40(7):682-8.

377. Khawaja AP, Chan MP, Broadway DC, Garway-Heath DF, Luben R, Yip JL, et al. Corneal biomechanical properties and glaucoma-related quantitative traits in the EPIC-Norfolk Eye Study. Invest Ophthalmol Vis Sci. 2014;55(1):117-24.

378. Carbonaro F, Hysi PG, Fahy SJ, Nag A, Hammond CJ. Optic disc planimetry, corneal hysteresis, central corneal thickness, and intraocular pressure as risk factors for glaucoma. Am J Ophthalmol. 2014;157(2):441-6.

379. Prata TS, Lima VC, de Moraes CG, Guedes LM, Magalhaes FP, Teixeira SH, et al. Factors associated with topographic changes of the optic nerve head induced by acute intraocular pressure reduction in glaucoma patients. Eye (Lond). 2011;25(2):201-7.

380. Mansouri K, Leite MT, Weinreb RN, Tafreshi A, Zangwill LM, Medeiros FA. Association between corneal biomechanical properties and glaucoma severity. Am J Ophthalmol. 2012;153(3):419-27 e1.

381. Vu DM, Silva FQ, Haseltine SJ, Ehrlich JR, Radcliffe NM. Relationship between corneal hysteresis and optic nerve parameters measured with spectral domain optical coherence tomography. Graefes Arch Clin Exp Ophthalmol. 2013;251(7):1777-83.

382. Fontes BM, Ambrosio R, Jr., Alonso RS, Jardim D, Velarde GC, Nose W. Corneal biomechanical metrics in eyes with refraction of -19.00 to +9.00 D in healthy Brazilian patients. J Refract Surg. 2008;24(9):941-5.

383. Ang GS, Bochmann F, Townend J, Azuara-Blanco A. Corneal biomechanical properties in primary open angle glaucoma and normal tension glaucoma. J Glaucoma. 2008;17(4):259-62.

384. Sun L, Shen M, Wang J, Fang A, Xu A, Fang H, et al. Recovery of corneal hysteresis after reduction of intraocular pressure in chronic primary angle-closure glaucoma. Am J Ophthalmol. 2009;147(6):1061-6, 6 e1-2.

385. Pakravan M, Afroozifar M, Yazdani S. Corneal Biomechanical Changes Following Trabeculectomy, Phaco-trabeculectomy, Ahmed Glaucoma Valve Implantation and Phacoemulsification. J Ophthalmic Vis Res. 2014;9(1):7-13.

386. Agarwal DR, Ehrlich JR, Shimmyo M, Radcliffe NM. The relationship between corneal hysteresis and the magnitude of intraocular pressure reduction with topical prostaglandin therapy. Br J Ophthalmol. 2012;96(2):254-7.

387. Hirneiss C, Sekura K, Brandlhuber U, Kampik A, Kernt M. Corneal biomechanics predict the outcome of selective laser trabeculoplasty in medically uncontrolled glaucoma. Graefes Arch Clin Exp Ophthalmol. 2013;251(10):2383-8.

388. Detry-Morel M, Jamart J, Hautenauven F, Pourjavan S. Comparison of the corneal biomechanical properties with the Ocular Response Analyzer(R) (ORA) in African and Caucasian normal subjects and patients with glaucoma. Acta Ophthalmol. 2012;90(2):e118-24.

389. Deol M, Taylor DA, Radcliffe NM. Corneal hysteresis and its relevance to glaucoma. Curr Opin Ophthalmol. 2015;26(2):96-102.

390. Greene PR. Closed-form ametropic pressure-volume and ocular rigidity solutions. Am J Optom Physiol Opt. 1985;62(12):870-8.

391. Fung YC. Elasticity of soft tissues in simple elongation. Am J Physiol. 1967;213(6):1532-44.

392. Woo SL, Kobayashi AS, Lawrence C, Schlegel WA. Mathematical model of the corneo-scleral shell as applied to intraocular pressure-volume relations and applanation tonometry. Ann Biomed Eng. 1972;1(1):87-98.

393. Graebel WP, van Alphen GW. The elasticity of sclera and choroid of the human eye, and its implications on scleral rigidity and accommodation. J Biomech Eng. 1977;99(4):203-8.

394. Woo SL, Kobayashi AS, Schlegel WA, Lawrence C. Nonlinear material properties of intact cornea and sclera. Exp Eye Res. 1972;14(1):29-39.

395. Jue B, Maurice DM. The mechanical properties of the rabbit and human cornea. J Biomech. 1986;19(10):847-53.

396. Hjortdal JO. Regional elastic performance of the human cornea. J Biomech. 1996;29(7):931-42.

397. Sigal IA, Flanagan JG, Tertinegg I, Ethier CR. Modeling individual-specific human optic nerve head biomechanics. Part II: influence of material properties. Biomech Model Mechanobiol. 2009;8(2):99-109.

398. Friedman E. A hemodynamic model of the pathogenesis of age-related macular degeneration. Am J Ophthalmol. 1997;124(5):677-82.

399. Friedman E, Ivry M, Ebert E, Glynn R, Gragoudas E, Seddon J. Increased scleral rigidity and age-related macular degeneration. Ophthalmology. 1989;96(1):104-8.

400. Pallikaris IG, Kymionis GD, Ginis HS, Kounis GA, Christodoulakis E, Tsilimbaris MK. Ocular rigidity in patients with age-related macular degeneration. Am J Ophthalmol. 2006;141(4):611-5.

401. Sigal IA, Flanagan JG, Tertinegg I, Ethier CR. Finite element modeling of optic nerve head biomechanics. Invest Ophthalmol Vis Sci. 2004;45(12):4378-87.

402. Bellezza AJ, Hart RT, Burgoyne CF. The optic nerve head as a biomechanical structure: initial finite element modeling. Invest Ophthalmol Vis Sci. 2000;41(10):2991-3000.

403. Levy NS, Crapps EE. Displacement of optic nerve head in response to short-term intraocular pressure elevation in human eyes. Arch Ophthalmol. 1984;102(5):782-6.

404. Yan DB, Flanagan JG, Farra T, Trope GE, Ethier CR. Study of regional deformation of the optic nerve head using scanning laser tomography. Curr Eye Res. 1998;17(9):903-16.

405. Albon J, Purslow PP, Karwatowski WS, Easty DL. Age related compliance of the lamina cribrosa in human eyes. Br J Ophthalmol. 2000;84(3):318-23.

406. Jackson CR. Schiotz tonometers. An assessment of their usefulness. Br J Ophthalmol. 1965;49(9):478-84.

407. Gloster J, Perkins ES. Ocular rigidity and tonometry. Proc R Soc Med. 1957;50(9):667-74.

408. Perkins ES, Gloster J. Further studies on the distensibility of the eye. Br J Ophthalmol. 1957;41(8):475-86.

409. Moses RA, Grodzki WJ. Ocular rigidity in tonography. Doc Ophthalmol. 1969;26:118-29.

410. Silver DM, Farrell RA, Langham ME, O'Brien V, Schilder P. Estimation of pulsatile ocular blood flow from intraocular pressure. Acta Ophthalmol Suppl. 1989;191:25-9.

411. Ytteborg J. The effect of intraocular pressure on rigidity coefficient in the human eye. Acta Ophthalmol (Copenh). 1960;38:548-61.

412. Ytteborg J. Further investigations of factors influencing size of rigidity coefficient. Acta Ophthalmol (Copenh). 1960;38:643-57.

413. Eisenlohr JE, Langham ME, Maumenee AE. Manometric Studies of the Pressure-Volume Relationship in Living and Enucleated Eyes of Individual Human Subjects. Br J Ophthalmol. 1962;46(9):536-48.

414. Eisenlohr JE, Langham ME. The relationship between pressure and volume changes in living and dead rabbit eyes. Invest Ophthalmol. 1962;1:63-77.

415. Ytteborg J. The role of intraocular blood volume in rigidity measurements on human eyes. Acta Ophthalmol (Copenh). 1960;38:410-36.

416. Kerrigan-Baumrind LA, Quigley HA, Pease ME, Kerrigan DF, Mitchell RS. Number of ganglion cells in glaucoma eyes compared with threshold visual field tests in the same persons. Invest Ophthalmol Vis Sci. 2000;41(3):741-8.

417. Harwerth RS, Carter-Dawson L, Shen F, Smith EL, 3rd, Crawford ML. Ganglion cell losses underlying visual field defects from experimental glaucoma. Invest Ophthalmol Vis Sci. 1999;40(10):2242-50.

418. Medeiros FA, Lisboa R, Weinreb RN, Liebmann JM, Girkin C, Zangwill LM. Retinal ganglion cell count estimates associated with early development of visual field defects in glaucoma. Ophthalmology. 2013;120(4):736-44.

419. Friedenwald JS. Contribution to the theory and practice of tonometry. Am J Ophthalmol. 1937;20:985-1024.

420. Trier K, Ribel-Madsen SM. Latanoprost eye drops increase concentration of glycosaminoglycans in posterior rabbit sclera. J Ocul Pharmacol Ther. 2004;20(3):185-8.

421. Quigley HA, Pitha IF, Welsbie DS, Nguyen C, Steinhart MR, Nguyen TD, et al. Losartan Treatment Protects Retinal Ganglion Cells and Alters Scleral Remodeling in Experimental Glaucoma. PLoS One. 2015;10(10):e0141137.

422. Dastiridou AI, Ginis H, Tsilimbaris M, Karyotakis N, Detorakis E, Siganos C, et al. Ocular rigidity, ocular pulse amplitude, and pulsatile ocular blood flow: the effect of axial length. Invest Ophthalmol Vis Sci. 2013;54(3):2087-92.

423. Jonas JB, Berenshtein E, Holbach L. Lamina cribrosa thickness and spatial relationships between intraocular space and cerebrospinal fluid space in highly myopic eyes. Invest Ophthalmol Vis Sci. 2004;45(8):2660-5.

424. McBrien NA, Gentle A. Role of the sclera in the development and pathological complications of myopia. Prog Retin Eye Res. 2003;22(3):307-38.

425. Boland MV, Quigley HA. Risk factors and open-angle glaucoma: classification and application. J Glaucoma. 2007;16(4):406-18.

426. Mitchell P, Hourihan F, Sandbach J, Wang JJ. The relationship between glaucoma and myopia: the Blue Mountains Eye Study. Ophthalmology. 1999;106(10):2010-5.

427. Quigley HA. The contribution of the sclera and lamina cribrosa to the pathogenesis of glaucoma: Diagnostic and treatment implications. Prog Brain Res. 2015;220:59-86.

428. Friberg TR, Lace JW. A comparison of the elastic properties of human choroid and sclera. Exp Eye Res. 1988;47(3):429-36.

429. Tezel G, Luo C, Yang X. Accelerated aging in glaucoma: immunohistochemical assessment of advanced glycation end products in the human retina and optic nerve head. Invest Ophthalmol Vis Sci. 2007;48(3):1201-11.

430. Malik NS, Moss SJ, Ahmed N, Furth AJ, Wall RS, Meek KM. Ageing of the human corneal stroma: structural and biochemical changes. Biochim Biophys Acta. 1992;1138(3):222-8.

431. Fazio MA, Grytz R, Morris JS, Bruno L, Gardiner SK, Girkin CA, et al. Age-related changes in human peripapillary scleral strain. Biomech Model Mechanobiol. 2014;13(3):551-63.

432. Girkin CA, Fazio MA, Yang H, Reynaud J, Burgoyne CF, Smith B, et al. Variation in the Three-Dimensional Histomorphometry of the Normal Human Optic Nerve Head With Age and Race: Lamina Cribrosa and Peripapillary Scleral Thickness and Position. Invest Ophthalmol Vis Sci. 2017;58(9):3759-69.

433. Fazio MA, Grytz R, Morris JS, Bruno L, Girkin CA, Downs JC. Human scleral structural stiffness increases more rapidly with age in donors of African descent compared to donors of European descent. Invest Ophthalmol Vis Sci. 2014;55(11):7189-98.

434. Ravalico G, Toffoli G, Pastori G, Croce M, Calderini S. Age-related ocular blood flow changes. Invest Ophthalmol Vis Sci. 1996;37(13):2645-50.

435. Bartholomew RS. Lens displacement associated with pseudocapsular exfoliation. A report on 19 cases in the Southern Bantu. Br J Ophthalmol. 1970;54(11):744-50.

436. Futa R, Furuyoshi N. Phakodonesis in capsular glaucoma: a clinical and electron microscopic study. Jpn J Ophthalmol. 1989;33(3):311-7.

437. Kaiser-Kupfer MI, Podgor MJ, McCain L, Kupfer C, Shapiro JR. Correlation of ocular rigidity and blue sclerae in osteogenesis imperfecta. Trans Ophthalmol Soc U K. 1985;104 (Pt 2):191-5.

438. Edmund C. Corneal elasticity and ocular rigidity in normal and keratoconic eyes. Acta Ophthalmol (Copenh). 1988;66(2):134-40.

439. Tengroth B, Ammitzboll T. Changes in the content and composition of collagen in the glaucomatous eye--basis for a new hypothesis for the genesis of chronic open angle glaucoma--a preliminary report. Acta Ophthalmol (Copenh). 1984;62(6):999-1008.

440. Perkins ES. Ocular volume and ocular rigidity. Exp Eye Res. 1981;33(2):141-5.

441. Anderson DR, Hendrickson A. Effect of intraocular pressure on rapid axoplasmic transport in monkey optic nerve. Invest Ophthalmol. 1974;13(10):771-83.

442. Jonas JB, Ritch R, Panda-Jonas S. Cerebrospinal fluid pressure in the pathogenesis of glaucoma. Prog Brain Res. 2015;221:33-47.

443. Lee DS, Lee EJ, Kim TW, Park YH, Kim J, Lee JW, et al. Influence of translaminar pressure dynamics on the position of the anterior lamina cribrosa surface. Invest Ophthalmol Vis Sci. 2015;56(5):2833-41.

444. Morgan WH, Yu DY, Alder VA, Cringle SJ, Cooper RL, House PH, et al. The correlation between cerebrospinal fluid pressure and retrolaminar tissue pressure. Invest Ophthalmol Vis Sci. 1998;39(8):1419-28.

445. Greene PR. Mechanical considerations in myopia: relative effects of accommodation, convergence, intraocular pressure, and the extraocular muscles. Am J Optom Physiol Opt. 1980;57(12):902-14.

446. Strouthidis NG, Girard MJ. Altering the way the optic nerve head responds to intraocular pressure-a potential approach to glaucoma therapy. Curr Opin Pharmacol. 2013;13(1):83-9.

447. Quigley HA, Brown A, Dorman-Pease ME. Alterations in elastin of the optic nerve head in human and experimental glaucoma. Br J Ophthalmol. 1991;75(9):552-7.

448. Morrison JC, Dorman-Pease ME, Dunkelberger GR, Quigley HA. Optic nerve head extracellular matrix in primary optic atrophy and experimental glaucoma. Arch Ophthalmol. 1990;108(7):1020-4.

449. Pena JD, Netland PA, Vidal I, Dorr DA, Rasky A, Hernandez MR. Elastosis of the lamina cribrosa in glaucomatous optic neuropathy. Exp Eye Res. 1998;67(5):517-24.

450. Gaasterland D, Tanishima T, Kuwabara T. Axoplasmic flow during chronic experimental glaucoma. 1. Light and electron microscopic studies of the monkey optic nervehead during development of glaucomatous cupping. Invest Ophthalmol Vis Sci. 1978;17(9):838-46.

451. Quigley HA, Addicks EM. Chronic experimental glaucoma in primates. II. Effect of extended intraocular pressure elevation on optic nerve head and axonal transport. Invest Ophthalmol Vis Sci. 1980;19(2):137-52.

452. Quigley HA, Guy J, Anderson DR. Blockade of rapid axonal transport. Effect of intraocular pressure elevation in primate optic nerve. Arch Ophthalmol. 1979;97(3):525-31.

453. Minckler DS, Bunt AH, Johanson GW. Orthograde and retrograde axoplasmic transport during acute ocular hypertension in the monkey. Invest Ophthalmol Vis Sci. 1977;16(5):426-41.

454. Zhao DY, Cioffi GA. Anterior optic nerve microvascular changes in human glaucomatous optic neuropathy. Eye (Lond). 2000;14 (Pt 3B):445-9.

455. Qu J, Chen H, Zhu L, Ambalavanan N, Girkin CA, Murphy-Ullrich JE, et al. High-Magnitude and/or High-Frequency Mechanical Strain Promotes Peripapillary Scleral Myofibroblast Differentiation. Invest Ophthalmol Vis Sci. 2015;56(13):7821-30.

456. Schneider M, Fuchshofer R. The role of astrocytes in optic nerve head fibrosis in glaucoma. Exp Eye Res. 2016;142:49-55.

457. Wallace DM, O'Brien CJ. The role of lamina cribrosa cells in optic nerve head fibrosis in glaucoma. Exp Eye Res. 2016;142:102-9.

458. Albon J, Karwatowski WS, Avery N, Easty DL, Duance VC. Changes in the collagenous matrix of the aging human lamina cribrosa. Br J Ophthalmol. 1995;79(4):368-75.

459. Luo H, Yang H, Gardiner SK, Hardin C, Sharpe GP, Caprioli J, et al. Factors Influencing Central Lamina Cribrosa Depth: A Multicenter Study. Invest Ophthalmol Vis Sci. 2018;59(6):2357-70.

460. Behkam R, Kollech HG, Jana A, Hill A, Danford F, Howerton S, et al. Racioethnic differences in the biomechanical response of the lamina cribrosa. Acta Biomater. 2019;88:131-40.

461. Zeimer RC, Ogura Y. The relation between glaucomatous damage and optic nerve head mechanical compliance. Arch Ophthalmol. 1989;107(8):1232-4.

462. Bellezza AJ, Rintalan CJ, Thompson HW, Downs JC, Hart RT, Burgoyne CF. Deformation of the lamina cribrosa and anterior scleral canal wall in early experimental glaucoma. Invest Ophthalmol Vis Sci. 2003;44(2):623-37.

463. Quigley HA, Addicks EM. Regional differences in the structure of the lamina cribrosa and their relation to glaucomatous optic nerve damage. Arch Ophthalmol. 1981;99(1):137-43.

464. Quigley HA, Hohman RM, Addicks EM, Massof RW, Green WR. Morphologic changes in the lamina cribrosa correlated with neural loss in open-angle glaucoma. Am J Ophthalmol. 1983;95(5):673-91.

465. Jonas JB, Berenshtein E, Holbach L. Anatomic relationship between lamina cribrosa, intraocular space, and cerebrospinal fluid space. Invest Ophthalmol Vis Sci. 2003;44(12):5189-95.

466. Burgoyne CF, Quigley HA, Thompson HW, Vitale S, Varma R. Early changes in optic disc compliance and surface position in experimental glaucoma. Ophthalmology. 1995;102(12):1800-9.

467. Heickell AG, Bellezza AJ, Thompson HW, Burgoyne CF. Optic disc surface compliance testing using confocal scanning laser tomography in the normal monkey eye. J Glaucoma. 2001;10(5):369-82.

468. Azuara-Blanco A, Harris A, Cantor LB, Abreu MM, Weinland M. Effects of short term increase of intraocular pressure on optic disc cupping. Br J Ophthalmol. 1998;82(8):880-3.

469. Lesk MR, Spaeth GL, Azuara-Blanco A, Araujo SV, Katz LJ, Terebuh AK, et al. Reversal of optic disc cupping after glaucoma surgery analyzed with a scanning laser tomograph. Ophthalmology. 1999;106(5):1013-8.

470. Bowd C, Weinreb RN, Lee B, Emdadi A, Zangwill LM. Optic disk topography after medical treatment to reduce intraocular pressure. Am J Ophthalmol. 2000;130(3):280-6.

471. Irak I, Zangwill L, Garden V, Shakiba S, Weinreb RN. Change in optic disk topography after trabeculectomy. Am J Ophthalmol. 1996;122(5):690-5.

472. Raitta C, Tomita G, Vesti E, Harju M, Nakao H. Optic disc topography before and after trabeculectomy in advanced glaucoma. Ophthalmic Surg Lasers. 1996;27(5):349-54.

473. Sigal IA, Flanagan JG, Tertinegg I, Ethier CR. Reconstruction of human optic nerve heads for finite element modeling. Technol Health Care. 2005;13(4):313-29.

474. Levy NS, Crapps EE, Bonney RC. Displacement of the optic nerve head. Response to acute intraocular pressure elevation in primate eyes. Arch Ophthalmol. 1981;99(12):2166-74.

475. Sharpe GP, Danthurebandara VM, Vianna JR, Alotaibi N, Hutchison DM, Belliveau AC, et al. Optic Disc Hemorrhages and Laminar Disinsertions in Glaucoma. Ophthalmology. 2016;123(9):1949-56.

476. Lee EJ, Kim TW, Kim M, Girard MJ, Mari JM, Weinreb RN. Recent structural alteration of the peripheral lamina cribrosa near the location of disc hemorrhage in glaucoma. Invest Ophthalmol Vis Sci. 2014;55(4):2805-15.

477. Kim YK, Jeoung JW, Park KH. Effect of Focal Lamina Cribrosa Defect on Disc Hemorrhage Area in Glaucoma. Invest Ophthalmol Vis Sci. 2016;57(3):899-907.

478. Park SC, Hsu AT, Su D, Simonson JL, Al-Jumayli M, Liu Y, et al. Factors associated with focal lamina cribrosa defects in glaucoma. Invest Ophthalmol Vis Sci. 2013;54(13):8401-7.

479. Kim YK, Park KH. Lamina cribrosa defects in eyes with glaucomatous disc haemorrhage. Acta Ophthalmol. 2016;94(6):e468-73.

480. You JY, Park SC, Su D, Teng CC, Liebmann JM, Ritch R. Focal lamina cribrosa defects associated with glaucomatous rim thinning and acquired pits. JAMA Ophthalmol. 2013;131(3):314-20.

481. Kim YW, Jeoung JW, Kim DW, Girard MJ, Mari JM, Park KH, et al. Clinical Assessment of Lamina Cribrosa Curvature in Eyes with Primary Open-Angle Glaucoma. PLoS One. 2016;11(3):e0150260.

482. Li L, Bian A, Cheng G, Zhou Q. Posterior displacement of the lamina cribrosa in normal-tension and high-tension glaucoma. Acta Ophthalmol. 2016;94(6):e492-500.

483. Kim YW, Kim DW, Jeoung JW, Kim DM, Park KH. Peripheral lamina cribrosa depth in primary open-angle glaucoma: a swept-source optical coherence tomography study of lamina cribrosa. Eye (Lond). 2015;29(10):1368-74.

484. Kim DW, Jeoung JW, Kim YW, Girard MJ, Mari JM, Kim YK, et al. Prelamina and Lamina Cribrosa in Glaucoma Patients With Unilateral Visual Field Loss. Invest Ophthalmol Vis Sci. 2016;57(4):1662-70.

485. Quigley H, Arora K, Idrees S, Solano F, Bedrood S, Lee C, et al. Biomechanical Responses of Lamina Cribrosa to Intraocular Pressure Change Assessed by Optical Coherence Tomography in Glaucoma Eyes. Invest Ophthalmol Vis Sci. 2017;58(5):2566-77.

486. Agoumi Y, Sharpe GP, Hutchison DM, Nicolela MT, Artes PH, Chauhan BC. Laminar and prelaminar tissue displacement during intraocular pressure elevation in glaucoma patients and healthy controls. Ophthalmology. 2011;118(1):52-9.

487. Huang D, Swanson EA, Lin CP, Schuman JS, Stinson WG, Chang W, et al. Optical coherence tomography. Science. 1991;254(5035):1178-81.

488. Mazzaferri J, Beaton L, Hounye G, Sayah DN, Costantino S. Open-source algorithm for automatic choroid segmentation of OCT volume reconstructions. Sci Rep. 2017;7:42112.

489. Andreanos K, Koutsandrea C, Papaconstantinou D, Diagourtas A, Kotoulas A, Dimitrakas P, et al. Comparison of Goldmann applanation tonometry and Pascal dynamic contour tonometry in relation to central corneal thickness and corneal curvature. Clin Ophthalmol. 2016;10:2477-84.

490. Schneider E, Grehn F. Intraocular pressure measurement-comparison of dynamic contour tonometry and goldmann applanation tonometry. J Glaucoma. 2006;15(1):2-6.

491. Ceruti P, Morbio R, Marraffa M, Marchini G. Comparison of Goldmann applanation tonometry and dynamic contour tonometry in healthy and glaucomatous eyes. Eye (Lond). 2009;23(2):262-9.

492. Ziemer Group Company. Pascal Dynamic Contour Tonometry: User Manual. Port, Switzerland2012.

493. De Moraes C, Prata T, Liebmann J, Ritch R. Modalities of Tonometry and their Accuracy with Respect to Corneal Thickness and Irregularities. J Optom. 2008;1(2):43-9.

494. Sayah DN, Mazzaferri J, Ghesquiere P, Duval R, Rezende F, Costantino S, et al. Non-invasive in vivo measurement of ocular rigidity: Clinical validation, repeatability and method improvement. Exp Eye Res. 2020;190:107831.

495. Jefferson AL, Cambronero FE, Liu D, Moore EE, Neal JE, Terry JG, et al. Higher Aortic Stiffness Is Related to Lower Cerebral Blood Flow and Preserved Cerebrovascular Reactivity in Older Adults. Circulation. 2018;138(18):1951-62.

496. Tarumi T, Shah F, Tanaka H, Haley AP. Association between central elastic artery stiffness and cerebral perfusion in deep subcortical gray and white matter. Am J Hypertens. 2011;24(10):1108-13.

497. Herndon LW, Weizer JS, Stinnett SS. Central corneal thickness as a risk factor for advanced glaucoma damage. Arch Ophthalmol. 2004;122(1):17-21.

498. Kim JM, Park KH, Kim SH, Kang JH, Cho SW. The relationship between the cornea and the optic disc. Eye (Lond). 2010;24(11):1653-7.

499. Park K, Shin J, Lee J. Relationship between corneal biomechanical properties and structural biomarkers in patients with normal-tension glaucoma: a retrospective study. BMC Ophthalmol. 2018;18(1):7.

500. Wu RY, Zheng YF, Wong TY, Cheung CY, Loon SC, Chauhan BC, et al. Relationship of central corneal thickness with optic disc parameters: the Singapore Malay Eye Study. Invest Ophthalmol Vis Sci. 2011;52(3):1320-4.

501. Qiu K, Lu X, Zhang R, Wang G, Zhang M. Relationship of corneal hysteresis and optic nerve parameters in healthy myopic subjects. Sci Rep. 2017;7(1):17538.

502. Chauhan BC, O'Leary N, AlMobarak FA, Reis ASC, Yang H, Sharpe GP, et al. Enhanced detection of open-angle glaucoma with an anatomically accurate optical coherence tomography-derived neuroretinal rim parameter. Ophthalmology. 2013;120(3):535-43.

503. Curcio CA, Allen KA. Topography of ganglion cells in human retina. J Comp Neurol. 1990;300(1):5-25.

504. Leung CK, Choi N, Weinreb RN, Liu S, Ye C, Liu L, et al. Retinal nerve fiber layer imaging with spectral-domain optical coherence tomography: pattern of RNFL defects in glaucoma. Ophthalmology. 2010;117(12):2337-44.

505. Mwanza JC, Oakley JD, Budenz DL, Anderson DR, Cirrus Optical Coherence Tomography Normative Database Study G. Ability of cirrus HD-OCT optic nerve head parameters to discriminate normal from glaucomatous eyes. Ophthalmology. 2011;118(2):241-8 e1.

506. Quigley HA. Neuronal death in glaucoma. Prog Retin Eye Res. 1999;18(1):39-57.

507. Hayreh SS. The role of age and cardiovascular disease in glaucomatous optic neuropathy. Surv Ophthalmol. 1999;43 Suppl 1:S27-42.

508. Hayreh SS, Revie IH, Edwards J. Vasogenic origin of visual field defects and optic nerve changes in glaucoma. Br J Ophthalmol. 1970;54(7):461-72.

509. Flammer J, Haefliger IO, Orgul S, Resink T. Vascular dysregulation: a principal risk factor for glaucomatous damage? J Glaucoma. 1999;8(3):212-9.

510. Phelps CD, Corbett JJ. Migraine and low-tension glaucoma. A case-control study. Invest Ophthalmol Vis Sci. 1985;26(8):1105-8.

511. Drance SM, Douglas GR, Wijsman K, Schulzer M, Britton RJ. Response of blood flow to warm and cold in normal and low-tension glaucoma patients. Am J Ophthalmol. 1988;105(1):35-9.

512. Wang JJ, Mitchell P, Smith W. Is there an association between migraine headache and open-angle glaucoma? Findings from the Blue Mountains Eye Study. Ophthalmology. 1997;104(10):1714-9.

513. Konieczka K, Choi HJ, Koch S, Fankhauser F, Schoetzau A, Kim DM. Relationship between normal tension glaucoma and Flammer syndrome. EPMA J. 2017;8(2):111-7.

514. International Headache Society. Migraine diagnostic criteria 2019 [Available from: https://ichd-3.org/1-migraine/1-1-migraine-without-aura/.

515. Chung F, Abdullah HR, Liao P. STOP-Bang Questionnaire: A Practical Approach to Screen for Obstructive Sleep Apnea. Chest. 2016;149(3):631-8.

516. Drance S, Anderson DR, Schulzer M, Collaborative Normal-Tension Glaucoma Study G. Risk factors for progression of visual field abnormalities in normal-tension glaucoma. Am J Ophthalmol. 2001;131(6):699-708.

517. Gramer G, Weber BH, Gramer E. Migraine and Vasospasm in Glaucoma: Age-Related Evaluation of 2027 Patients With Glaucoma or Ocular Hypertension. Invest Ophthalmol Vis Sci. 2015;56(13):7999-8007.

518. Gasser P, Meienberg O. Finger microcirculation in classical migraine. A video-microscopic study of nailfold capillaries. Eur Neurol. 1991;31(3):168-71.

519. Hegyalijai T, Meienberg O, Dubler B, Gasser P. Cold-induced acral vasospasm in migraine as assessed by nailfold video-microscopy: prevalence and response to migraine prophylaxis. Angiology. 1997;48(4):345-9.

520. Lin S-C, Kazemi A, McLaren JW, Moroi SE, Toris CB, Sit AJ. Relationship between Ocular Rigidity, Corneal Hysteresis, and Corneal Resistance Factor. The Association for Research in Vision and Ophthalmology: Investigative Ophthalmology & Visual Science; 2015. p. 6137-.

521. Kotecha A, Elsheikh A, Roberts CR, Zhu H, Garway-Heath DF. Corneal thickness- and age-related biomechanical properties of the cornea measured with the ocular response analyzer. Invest Ophthalmol Vis Sci. 2006;47(12):5337-47.

522. Leite MT, Alencar LM, Gore C, Weinreb RN, Sample PA, Zangwill LM, et al. Comparison of corneal biomechanical properties between healthy blacks and whites using the Ocular Response Analyzer. Am J Ophthalmol. 2010;150(2):163-8 e1.

523. Sayah DN, Szigiato AA, Mazzaferri J, Descovich D, Duval R, Rezende FA, et al. Correlation of ocular rigidity with intraocular pressure spike after intravitreal injection of bevacizumab in exudative retinal disease. Br J Ophthalmol. 2020.

524. Kotecha A, Russell RA, Sinapis A, Pourjavan S, Sinapis D, Garway-Heath DF. Biomechanical parameters of the cornea measured with the Ocular Response Analyzer in normal eyes. BMC Ophthalmol. 2014;14:11.

525. Holden BA, Wilson DA, Jong M, Sankaridurg P, Fricke TR, Smith EL, III, et al. Myopia: a growing global problem with sight-threatening complications. Community Eye Health. 2015;28(90):35.

526. Holden BA, Fricke TR, Wilson DA, Jong M, Naidoo KS, Sankaridurg P, et al. Global Prevalence of Myopia and High Myopia and Temporal Trends from 2000 through 2050. Ophthalmology. 2016;123(5):1036-42.

527. Saw SM, Gazzard G, Shih-Yen EC, Chua WH. Myopia and associated pathological complications. Ophthalmic Physiol Opt. 2005;25(5):381-91.

528. Marcus MW, de Vries MM, Junoy Montolio FG, Jansonius NM. Myopia as a risk factor for open-angle glaucoma: a systematic review and meta-analysis. Ophthalmology. 2011;118(10):1989-94 e2.

529. Phillips JR, Khalaj M, McBrien NA. Induced myopia associated with increased scleral creep in chick and tree shrew eyes. Invest Ophthalmol Vis Sci. 2000;41(8):2028-34.

530. Flitcroft DI, He M, Jonas JB, Jong M, Naidoo K, Ohno-Matsui K, et al. IMI - Defining and Classifying Myopia: A Proposed Set of Standards for Clinical and Epidemiologic Studies. Invest Ophthalmol Vis Sci. 2019;60(3):M20-M30.

531. Hashimoto S, Yasuda M, Fujiwara K, Ueda E, Hata J, Hirakawa Y, et al. Association between Axial Length and Myopic Maculopathy: The Hisayama Study. Ophthalmol Retina. 2019;3(10):867-73.

532. Wollensak G, Spoerl E. Collagen crosslinking of human and porcine sclera. J Cataract Refract Surg. 2004;30(3):689-95.

533. Spoerl E, Boehm AG, Pillunat LE. The influence of various substances on the biomechanical behavior of lamina cribrosa and peripapillary sclera. Invest Ophthalmol Vis Sci. 2005;46(4):1286-90.

534. Wei WB, Xu L, Jonas JB, Shao L, Du KF, Wang S, et al. Subfoveal choroidal thickness: the Beijing Eye Study. Ophthalmology. 2013;120(1):175-80.

535. Kadziauskiene A, Jasinskiene E, Asoklis R, Lesinskas E, Rekasius T, Chua J, et al. Long-Term Shape, Curvature, and Depth Changes of the Lamina Cribrosa after Trabeculectomy. Ophthalmology. 2018;125(11):1729-40.

536. Hidalgo-Aguirre M, Costantino S, Lesk MR. Pilot study of the pulsatile neuro-peripapillary retinal deformation in glaucoma and its relationship with glaucoma risk factors. Curr Eye Res. 2017;42(12):1620-7.

537. Singh K, Dion C, Godin AG, Lorghaba F, Descovich D, Wajszilber M, et al. Pulsatile movement of the optic nerve head and the peripapillary retina in normal subjects and in glaucoma. Invest Ophthalmol Vis Sci. 2012;53(12):7819-24.

538. Lee EJ, Kim TW, Weinreb RN, Park KH, Kim SH, Kim DM. Visualization of the lamina cribrosa using enhanced depth imaging spectral-domain optical coherence tomography. Am J Ophthalmol. 2011;152(1):87-95 e1.

539. Huang W, Fileta JB, Dobberfuhl A, Filippopolous T, Guo Y, Kwon G, et al. Calcineurin cleavage is triggered by elevated intraocular pressure, and calcineurin inhibition blocks retinal ganglion cell death in experimental glaucoma. Proc Natl Acad Sci U S A. 2005;102(34):12242-7.

540. Ji JZ, Elyaman W, Yip HK, Lee VW, Yick LW, Hugon J, et al. CNTF promotes survival of retinal ganglion cells after induction of ocular hypertension in rats: the possible involvement of STAT3 pathway. Eur J Neurosci. 2004;19(2):265-72.

541. Martin KR, Quigley HA, Zack DJ, Levkovitch-Verbin H, Kielczewski J, Valenta D, et al. Gene therapy with brain-derived neurotrophic factor as a protection: retinal ganglion cells in a rat glaucoma model. Invest Ophthalmol Vis Sci. 2003;44(10):4357-65.

542. McKinnon SJ, Lehman DM, Tahzib NG, Ransom NL, Reitsamer HA, Liston P, et al. Baculoviral IAP repeat-containing-4 protects optic nerve axons in a rat glaucoma model. Mol Ther. 2002;5(6):780-7.

543. Nakazawa T, Nakazawa C, Matsubara A, Noda K, Hisatomi T, She H, et al. Tumor necrosis factor-alpha mediates oligodendrocyte death and delayed retinal ganglion cell loss in a mouse model of glaucoma. J Neurosci. 2006;26(49):12633-41.

544. Neufeld AH, Das S, Vora S, Gachie E, Kawai S, Manning PT, et al. A prodrug of a selective inhibitor of inducible nitric oxide synthase is neuroprotective in the rat model of glaucoma. J Glaucoma. 2002;11(3):221-5.

545. Schwartz M. Neurodegeneration and neuroprotection in glaucoma: development of a therapeutic neuroprotective vaccine: the Friedenwald lecture. Invest Ophthalmol Vis Sci. 2003;44(4):1407-11.

546. Agostinone J, Alarcon-Martinez L, Gamlin C, Yu WQ, Wong ROL, Di Polo A. Insulin signalling promotes dendrite and synapse regeneration and restores circuit function after axonal injury. Brain. 2018;141(7):1963-80.

547. Steinhart MR, Cone FE, Nguyen C, Nguyen TD, Pease ME, Puk O, et al. Mice with an induced mutation in collagen 8A2 develop larger eyes and are resistant to retinal ganglion cell damage in an experimental glaucoma model. Mol Vis. 2012;18:1093-106.

548. Mohammadpour M, Masoumi A, Mirghorbani M, Shahraki K, Hashemi H. Updates on corneal collagen cross-linking: Indications, techniques and clinical outcomes. J Curr Ophthalmol. 2017;29(4):235-47.

Appendix

BOOK CHAPTER:

Diane N Sayah, Mark R Lesk. (2020, expected) 'Ocular Rigidity and Glaucoma'. In Pallikaris I, Dastiridou A (Ed.), *Ocular Rigidity, Biomechanics and Hydrodynamics of the Eye*. Springer Nature.

PUBLICATIONS (INCLUDED IN THE THESIS):

Diane N Sayah, Andrei A Szigiato, Javier Mazzaferri, Denise Descovich, Renaud Duval, Flavio Rezende, Santiago Costantino, Mark R Lesk. Correlation between Ocular Rigidity and Intraocular Pressure Spikes After Intravitreal Injection. *British Journal of Ophthalmology*, 2020 Apr

Diane N Sayah, Javier Mazzaferri, Pierre Ghesquière, Renaud Duval, Flavio Rezende, Santiago Costantino, Mark R Lesk. Non-invasive in vivo measurement of ocular rigidity: Clinical validation, repeatability and method improvement. *Experimental Eye Research*. 2020;190:107831.

PUBLICATIONS (NOT INCLUDED IN THE THESIS):

Diane N Sayah*, Tianwei (Ellen) Zhou*, Samy Omri, Javier Mazzaferri, Christiane Quiniou, Maëlle Wirth, France Côté, Rabah Dabouz, Michel Desjarlais, Santiago Costantino, Sylvain Chemtob. Novel anti-Interleukin-1β therapy rescues retinal integrity: a longitudinal investigation using OCT imaging and automated retinal segmentation in small rodents. *Frontiers in Pharmacology*, 2020;11:296.

Javier Mazzaferri, Luke Beaton, Gisèle Hounye, **Diane N Sayah**, Santiago Costantino. Open-source algorithm for automatic choroid segmentation of OCT volume reconstructions. *Nature Scientific Reports*. 2017 Feb; 7: 42112.

Tianwei (Ellen) Zhou, **Diane N Sayah**, Baraa Noueihed, Javier Mazzaferri, Santiago Costantino, Isabelle Brunette, Sylvain Chemtob. Preventing corneal calcification associated with xylazine for longitudinal Optical Coherence Tomography in young rodents. *Investigative Ophthalmology and Visual Science.* 2017 Jan; 58(1): 461-469.